



Technische Universität München
TUM School of Life Sciences

CD4 T cell help sustains distinct subpopulations in functional and dysfunctional CD8 T cell responses

Kristiyan Kanev

Vollständiger Abdruck der von der TUM School of Life Sciences der Technischen Universität München zur Erlangung eines

Doktors der Naturwissenschaften (Dr. rer. nat)

genehmigten Dissertation.

Vorsitz: Prof. Dr. Angelika Schnieke

Prüfer*innen der Dissertation:

1. Prof. Dr. Dietmar Zehn
2. Prof. Dr. Percy A. Knolle
3. Prof. Dr. Robert Thimme

Die Dissertation wurde am 15.11.2021 bei der Technischen Universität München eingereicht und durch die TUM School of Life Sciences am 12.04.2023 angenommen.

CD4 T cell help sustains distinct subpopulations in functional and dysfunctional CD8 T cell responses.

Table of Contents

| | |
|--|----|
| 1. Zusammenfassung..... | 4 |
| 2. Abstract..... | 6 |
| 3. Introduction | 8 |
| 3.1. Composition of the immune system..... | 8 |
| 3.2. T cell development and antigen-recognition | 8 |
| 3.3. CD8 T cell differentiation, function and memory formation in the context of acute infection. | 10 |
| 3.4. CD4 T cell differentiation and its role for CD8 T cell responses in acute infection. | 12 |
| 3.5. CD8 T cell differentiation and function in chronic infection..... | 13 |
| 3.5.1. Long-term maintenance of exhausted T cell responses..... | 15 |
| 3.5.2. Factors inducing, promoting and preventing T cell exhaustion | 16 |
| 3.5.3. Role of CD4 help for CD8 T cell responses in chronic infection. | 18 |
| 3.5.4. CD8 T cells and immunotherapy | 19 |
| 3.5.5. Epigenetic landscape of T cell exhaustion | 21 |
| 3.5.6. Transcriptional landscape of T cell exhaustion | 21 |
| 3.6. Role of single-cell RNA sequencing in investigating the gene expression programs of T cells in health and disease. | 24 |
| 3.7. Mouse infection models and transgenic T cell lines to study T cell responses. | 26 |
| 4. Aim of study | 29 |
| 5. Materials and methods | 31 |
| 6. Results | 45 |
| 6.1. Tailoring the resolution of single-cell RNA sequencing to meet the challenges of primary cytotoxic T cells..... | 45 |

CD4 T cell help sustains distinct subpopulations in functional and dysfunctional CD8 T cell responses.

| | |
|--|-----|
| 6.2. Higher DHODH expression and general capacity for <i>de novo</i> biosynthesis of pyrimidine nucleotides as a potential mechanism of leflunomide resistance in early memory-committed cells. | 58 |
| 6.3. Terminally differentiated but not proliferation competent CD8 T cells require CD4 help in chronic infection. | 64 |
| 7. Discussion..... | 77 |
| 8. Abbreviations | 84 |
| 9. Literature..... | 88 |
| 10. Appendix | 105 |
| 10.1. Supplementary Figure 1 | 105 |
| 10.2. Acknowledgements | 106 |

1. Zusammenfassung

CD8 T-Zellen spielen eine Schlüsselrolle in der adaptiven Immunantwort gegen intrazelluläre Pathogene und Tumore und sind von zentralem Interesse in der Impfstoffforschung und Immuntherapie. Gegenwärtig werden sie selten effektiv zur Infektionskontrolle eingesetzt und ihre Wirksamkeit gegen Tumore muss noch verbessert werden. Dies resultiert aus unserem unvollständigen Verständnis, wie schützende CD8-T-Zell-Antworten gebildet werden, wie Populationsheterogenität in Pathogenkontrolle übersetzt wird und wie definierte molekulare Programme die Differenzierung und Funktion von CD8-T-Zellen steuern. Dies macht die Entwicklung von T-Zell-basierter Therapeutika zu einer Herausforderung. In dieser Arbeit konzentrieren wir uns auf zwei unabhängige, aber für die T-Zell-Biologie grundlegende Fragenstellungen. Ziel war einerseits die Klärung in welcher Form CD4-Helferzellen auf Tcf-1 positive Vorläuferzellen und deren Nachkommen in einem Model der chronischen Infektion wirken. Andererseits haben wir untersucht, wie Teriflunomid – ein Nukleotidininhibitor die Differenzierung von Effektor und Memoryzellen beeinflusst.

Wir sind dabei davon ausgegangen, dass die Verwendung von Einzelzell-Genexpressionsprofilen für das Verständnis der T-Zell-Heterogenität, der Progenitor-Progeny-Beziehungen, der Differenzierungswege und der zugrundeliegenden regulatorischen Netzwerke hilfreich sein werden. Daher haben wir eine Einzelzell-RNA-Sequenzierung (scRNA-seq) in Kombination mit traditionell verwendeten immunologischen Techniken eingesetzt, um bestimmte Aspekte der T-Zell-Differenzierung bei akuten und chronischen Infektionen zu untersuchen.

In der chronischen Infektion hängen die Erhaltung und Funktion der antigenspezifischen CD8 T-Zellen strikt von der Bereitstellung antigenspezifischer CD4 T-Zell-Hilfe ab, deren Fehlen zu einer funktionellen und zahlenmäßigen Verschlechterung der CD8 T-Zell-Antwort führt. In dieser Studie zeigen wir, dass die Vorläuferzellen dysfunktionaler CD8-T-Zellantworten unabhängig von der CD4-Hilfe aufrechterhalten werden, deren Fehlen nur die Anzahl und den Phänotyp des differenzierten Effektor-Kompartiments beeinflusst. Genauer gesagt führt die Abwesenheit von CD4-Hilfe zum Verlust von Cx3cr1+ differenzierten Effektorzellen, denen die klassischen Zeichen der Erschöpfung wie eine hohe Expression von

CD4 T cell help sustains distinct subpopulations in functional and dysfunctional CD8 T cell responses.

inhibitorischen Rezeptoren fehlen, mit gleichzeitiger Akkumulation von Zellen mit ausgeprägterem Phänotyp der Erschöpfung. Der intakte Phänotyp der Vorläuferzellen wird durch die Tatsache belegt, dass sie das differenzierte Effektor-Kompartiment nach Wiederherstellung der antigenspezifischen CD4-T-Zell-Hilfe auffüllen. Im Gegensatz zu dysfunktionalen Antworten ist die Aufrechterhaltung der Vorläuferzellen in funktionellen Antworten bei chronischer Infektion und der nach einer akuten Infektion gebildeten Tcf1+ Erinnerungszellen strikt von der CD4-T-Zell-Hilfe abhängig. Dieser unterschiedliche CD4-Hilfebedarf der Vorläufer funktioneller und erschöpfter CD8-T-Zellantworten kann bei menschlichen Erkrankungen, die mit einem fortschreitenden Verlust von CD4-T-Zellen einhergehen (z. B. AIDS - erworbenes Immundefektsyndrom), kritische Auswirkungen haben.

Der zweite Teil der vorgestellten Studien folgt der Beobachtung, dass der Dihydroorotat-Dehydrogenase (DHODH)-Inhibitor Teriflunomid ein selektiver Suppressor der Bildung von differenzierten Effektor-, aber nicht von Vorläufer- oder Gedächtnis-CD8-T-Zellen ist. Um den Mechanismus einer solchen differentiellen Sensitivität aufzuklären, setzten wir scRNA-seq ein. Hier zeigen wir, dass die Teriflunomid-resistenten Gedächtniszell-ähnlichen Subpopulationen am Tag 4 nach der Infektion eine höhere DHODH-Expression im Vergleich zu den Teriflunomid-sensitiven Effektor-ähnlichen Subpopulationen aufweisen. Darüber hinaus zeigten die Gedächtnis-ähnlichen Subpopulationen eine erhöhte Expression von mehreren Enzymen, die am Weg der *de novo*-Biosynthese von Pyrimidin-Nukleotiden beteiligt sind. Daher favorisieren wir die Hypothese, dass bei dieser Teriflunomid-Konzentration die höhere Kapazität zur Pyrimidin-Produktion der proliferierenden frühen Progenitoren diese unempfindlich gegen die Wirkung des Medikaments macht. Umgekehrt macht die metabolisch reduzierte Fähigkeit zur Produktion von Pyrimidin-Nukleotiden die früh proliferierenden Effektorzellen empfindlich gegenüber der Teriflunomid-Behandlung.

2. Abstract

CD8 T cells play a key role in the adaptive immune responses against intracellular pathogens and tumors, and they are of central interest in vaccine research and immunotherapy. Presently, they are still rarely effectively targeted for infection control and their efficacy against tumors need to be improved. This results from our incomplete understanding of how protective CD8 T cell responses are formed, how population heterogeneity translates into pathogen control, and how defined molecular programs guide the differentiation and function of CD8 T cells. This makes the development of T cell targeted or based therapeutics challenging. In this work, we focus on two independent, but fundamental for T cell biology questions, namely the role of CD4 help for the progenitors and their progeny in functional versus exhausted CD8 T cell responses and the mechanism of teriflunomide-independence of the early memory-like CD8 T cell subpopulations formed in acute infection. We reasoned that the use of single-cell gene expression profiles could be instrumental for understanding T cell heterogeneity, progenitor-progeny relationships, trajectories of differentiation and their underlying regulatory networks. Therefore, we utilized a single-cell RNA sequencing (scRNA-seq) in combination with traditionally used immunological techniques to address certain aspects of T cell differentiation in acute and chronic infection.

In chronic infection, the maintenance and function of the antigen-specific CD8 T cells strictly depend on the provision of cognate CD4 T cell help, which absence results in functional and numerical deterioration of the CD8 T cell response. In this study, we show that the progenitors of dysfunctional CD8 T cell responses are maintained independently of CD4 help, the absence of which only affects the numbers and phenotype of the differentiated effector compartment. More specific, the absence of CD4 help results in loss of Cx3cr1⁺ differentiated effector cells, which lack the classical signs of exhaustion such as high inhibitory receptor expression, at the expense of accumulation of cells with more pronounced phenotype of exhaustion. The intact phenotype of the progenitors is demonstrated by the fact that they repopulate the differentiated effector compartment upon restoration of antigen-specific CD4 T cell help. In contrast to dysfunctional responses, the maintenance of the progenitors of

CD4 T cell help sustains distinct subpopulations in functional and dysfunctional CD8 T cell responses.

functional responses in chronic infection and the Tcf1+ memory cells formed after an acute infection is strictly CD4 T cell help dependent. This differential CD4 help requirement of the precursors of functional and those of exhausted CD8 T cell responses can have critical implications in human conditions associated with progressive loss of CD4 T cells, such as AIDS (acquired immunodeficiency syndrome).

The second part of the presented studies follows up on previously made observations that the dihydroorotate dehydrogenase (DHODH)-inhibitor teriflunomide is a selective suppressor of the formation of differentiated effector, but not precursor or memory CD8 T cells. We were interested in the mechanism of such a differential sensitivity, therefore we deployed scRNA-seq. Here we show that the teriflunomide-resistant memory-like subpopulations found on day 4 post infection display higher DHODH expression in comparison to the teriflunomide-sensitive effector-like subpopulations. Moreover, the memory-like subpopulations showed increased expression of multiple enzymes involved in the pathway of *de novo* biosynthesis of pyrimidine nucleotides. Therefore, we favor the hypothesis that at this teriflunomide concentration the higher capacity for pyrimidine production of the proliferating early progenitors renders them insensitive to the drug's action. Conversely, the metabolically reduced ability to produce pyrimidine nucleotides renders the early proliferating effector cells sensitive to teriflunomide treatment.

3. Introduction

3.1. Composition of the immune system

Our immune system protects us from viruses, bacteria, fungi, parasites, cancer and toxins. The first obstacles an invading pathogen must overcome are the anatomical (skin and mucous) and physiological (e.g. low pH in the stomach; lysozyme in tears and saliva) barriers of the body [17]. The mammalian immune system is composed of innate and adaptive arm. The **innate arm** provides the first line of immune defense against invading pathogens. It becomes activated within minutes of initial pathogen encounter resulting in a protective inflammatory response. The innate immune system has cellular and humoral components scattered across the body, both tasked with danger sensing and effector function [18]. The innate immunity relies on a limited repertoire of germline-encoded pattern recognition receptors (PRRs). This enables immediate response to structures shared between large groups of pathogens – e.g. LPS (lipopolysaccharide), which are called pathogen-associated molecular patterns (PAMPs) [19]. The **adaptive arm** is evolutionary newer and has evolved on top of functioning innate immunity, in order to respond to the immense evolving potential of pathogens [20]. Therefore, the adaptive immune cells (**B and T cells**) rely on an extremely diverse repertoire of antigen-specific B- (BCR) and T cell receptors (TCR) generated via somatic recombination of a large array of gene segments, which are able to specifically recognize virtually any existing antigen. **The biology and specific responses of T cells are the main subject of this monography.**

3.2. T cell development and antigen-recognition

T cells start their **development** from common lymphoid progenitors in the bone marrow, but later migrate to the thymus to complete their maturation. They commit to the T cell lineage (e.g. induction of Notch-1 signaling) [21] and undergo IL7-induced proliferation [22]. During their double-negative (CD8⁻CD4⁻) stage, the developing thymocytes rearrange their β -TCR chain. Subsequently, they progress to a double-

CD4 T cell help sustains distinct subpopulations in functional and dysfunctional CD8 T cell responses.

positive (CD8⁺CD4⁺) stage when they rearrange the α -TCR chains of the T cell receptor. Following this, the newly formed receptor is tested for its capacity to respond to self-peptide MHCs (major histocompatibility complexes) presented in the cortex of the thymus. This process known as positive selection, ensures that only thymocytes with a receptor capable of responding to peptide- MHC stimulation undergo further differentiation, while the irresponsive cells undergo apoptosis. Subsequently or in parallel with the process of positive selection, thymocytes with a strong response to the self-peptide MHCs presented in the thymic cortex or medulla are also enforced to undergo apoptosis. This elimination of potentially autoreactive T cells is known as negative selection. Ultimately, the surviving thymocytes transition into single-positive (CD8⁺CD4⁻ or CD8⁻CD4⁺) stage. Subsequently, they are exported from the thymus and join the peripheral pool of naïve T cells.

As **naïve T cells** are highly mobile, they circulate through secondary lymphoid organs (lymph nodes and spleen) in search of a cognate antigen. There they **survey** **activated, antigen-presenting DCs** (dendritic cells). In order to screen the peptide MHCs presented on the DC's surface with their TCR, the naïve T cells establish a cellular contact with the activated DCs, which then in case of a successful antigen-recognition initiates a T cell response. It is important to note, that CD8 and CD4 T cells recognize peptides presented on two different classes of MHC molecules. CD8 T cells recognize peptides in complex with MHC class I (in humans HLA (human leukocyte antigen)-A, HLA-B or HLA-C) molecules, which are specialized in sampling and presenting intracellular antigens. CD4 T cells recognize peptides in complex with MHC class II (HLA-DR, HLA-DQ and HLA-DP) molecules, which are specialized in sampling and presenting antigens from the extracellular matrix. In addition to antigen-recognition, the successful activation of T cells requires additional signals provided by DCs. These so called co-stimulatory signals are discussed in more details in the context of CD8 T cell activation in the following section. Finally, cytokines and other cues from the inflammatory environment can fine tune the T cell response.

CD4 T cell help sustains distinct subpopulations in functional and dysfunctional CD8 T cell responses.

3.3. CD8 T cell differentiation, function and memory formation in the context of acute infection.

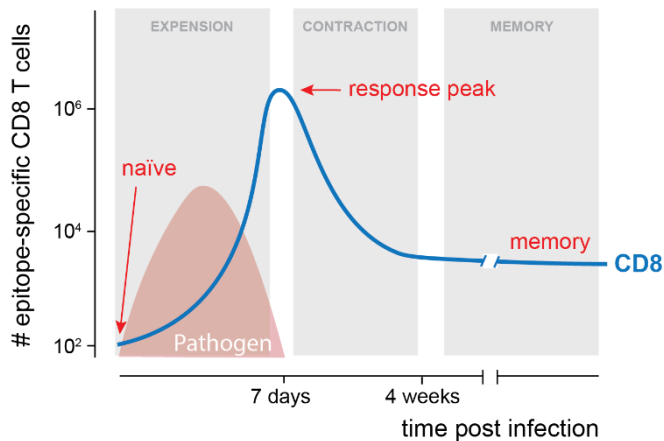


Figure 1. Graphical illustration of CD8 T cell activation and differentiation kinetics in acute infection.

Naïve antigen-specific CD8 T cells get activated by mature dendritic cells, which leads to their massive proliferation and differentiation to cytotoxic effector cells (expansion phase). Following antigen clearance, the majority of the effector CD8 T cells undergo apoptosis (contraction phase). Only 5-10% of the cells survive and form long-lasting memory (memory phase). Adapted from Williams and Bevan [1].

The typical CD8 T cell response in primary acute infection is characterized by three phases – expansion phase upon antigen recognition, contraction phase following pathogen clearance and memory phase ensuring protection in case of secondary infection with the same pathogen (**Figure 1**).

As the number of naïve CD8 T cells specific to any given antigen is small, their response relies on a massive **clonal expansion**. Therefore, upon recognition of its cognate antigen, the naïve CD8 T cell gets activated and undergoes massive expansion, achieved through as many as 20 cycles of proliferation with a division rate of 2-

6 hours [23]. This leads to the formation of sufficient number of **terminally differentiated effector cells** (KLRG-1^{hi}CD127^{lo}) and **memory precursor cells** (KLRG-1^{lo}CD127^{hi}) [24-26], the latter of which express and depend on the transcription factor Tcf1 (T-Cell-Specific Transcription Factor 1) [27, 28]. The process of **CD8 T cell activation and differentiation is under tight regulation**. Apart from CD28, other important co-stimulatory molecules on CD8 T cells include 4-1BB (Tumor Necrosis Factor (TNF) Receptor Superfamily Member 9), CD27 (TNF Receptor Superfamily Member 7), OX40 (TNF Receptor Superfamily Member 4) and GITR (TNF Receptor Superfamily Member 18) [29, 30]. Cytokines like IL-2 and IL-12 promote effector cell differentiation. While IL-12 act primary by inducing T-bet, IL-2 signaling activates

CD4 T cell help sustains distinct subpopulations in functional and dysfunctional CD8 T cell responses.

multiple pathways including STAT5 (Signal Transducer And Activator Of Transcription 5A), PI-3K (Phosphoinositide-3-Kinase) and MAPK (Mitogen-Activated Protein Kinase) [30, 31]. The intensive proliferation mentioned above demands certain metabolic adaptation such as switch from oxidative phosphorylation to aerobic glycolysis as well as enhanced uptake of glucose, amino acids, iron and other nutrients [32]. The metabolic reprogramming of CD8 T cells upon their activation is achieved by TCR- and CD28-induced ERK (Extracellular Signal-Regulated Kinase, also known as MAPK1) and mTOR (Mechanistic Target Of Rapamycin Kinase) signaling among others [32].

In order to exert their **function**, the differentiated effector CD8 T cells upregulate inflammatory cytokine receptors such as Cxcr3 (C-X-C Motif Chemokine Receptor 3), which guide their migration to inflamed tissues [33]. There they ensure pathogen eradication via cytolytic (release of granules containing perforin and granzymes; Fas Ligand-Fas signaling) and non-cytolytic (secretion of Interferon Gamma (INF γ) and TNF) mechanisms [30].

Once the pathogen is eliminated, the terminally differentiated effector cells (representing 90-95% of the T cell response) contract via apoptosis, which leaves only a small number of **long-lived memory** cells behind, which are maintained via IL-7 and IL-15 dependent homeostatic proliferation [34]. In comparison to naïve cells, the memory pool exists in different epigenetic, transcriptional and metabolic state. This allows immediate response in case of Ag re-encounter. Moreover, the memory pool contains cells with heterogeneous phenotype, function and protective capacity [35]. Although not fully reflecting its diversity, the memory pool is formed by central memory (T_{cm}), effector memory (T_{em}) and tissue resident memory (T_{rm}) cells [36]. The T_{cm} (CD127^{hi}CD62L^{hi}CCR7^{hi}Tcf1^{hi}Tbet^{lo}) are circulating cells with pronounced tropism towards the secondary lymphoid organs. The T_{em} (CD127^{hi}CD62L^{lo}CCR7^{lo}Tcf1^{lo}Tbet^{hi}) are circulating cells with pronounced tissue tropism [37]. In line with their tropism, the T_{cm} are better poised for proliferation, while the T_{em} for immediate exertion of effector function. In contrast to the T_{em}, the T_{rm} (CD127^{hi}CD62L^{lo}CCR7^{lo}Tcf1^{lo}CD69^{hi}CD103^{hi}) do not circulate and protect tissues, which could serve as a potential entry point for their cognate pathogen – e.g. skin, salivary glands, lungs, liver and female reproductive tract [38-40].

CD4 T cell help sustains distinct subpopulations in functional and dysfunctional CD8 T cell responses.

3.4. CD4 T cell differentiation and its role for CD8 T cell responses in acute infection.

CD4 T cells have a key role in antiviral immunity by supporting T and B-cell adaptive immune responses as well as by exerting direct antiviral function [41]. Following their activation, CD4 T cells differentiate into helper T cells (**Th**), which are subdivided into subsets (e.g. Th1, Th2, Th17, Th9 and Tfh), based on their function and cytokine secretion profiles [42]. The **Th1** cells differentiate under the influence of IL12, IFN- γ (Interferon Gamma) and the transcription factor T-bet (T-Box Transcription Factor 21). They secrete IFN- γ and IL-2 driving cell-mediated immune responses by mononuclear phagocytes, NK (natural killer) cells and cytotoxic T cells. The **Th2** cells differentiate under the influence of IL-3 and the transcriptional factor GATA-3 (GATA Binding Protein 3). They secrete IL-4, IL-5, IL-10 and IL14 promoting humoral immune responses including antibody production by B cells. The **Th17** cells differentiate under the influence of IL-6, TGF- β (Transforming Growth Factor Beta) and the transcriptional factor ROR γ t (RAR Related Orphan Receptor C). They secrete IL-17 and provide protection against extracellular bacteria and fungi. The Th17 cells were also shown to be involved in autoimmunity and pathological tissue damage. The **Th9** cells differentiate under the influence of IL-4 and TGF- β . They produce IL-9, a potent mediator of mast cell growth and immunity against helminths. The follicular T helper (**Tfh**) cells express the transcriptional factor Bcl6 (B-Cell Lymphoma 6 Protein) and the chemokine receptor Cxcr5 (C-X-C Motif Chemokine Receptor 5). The latter ensures their localization in the B-cell follicles, where via secretion of IL-21 and provision of co-stimulation, the Tfh cells promote B-cell activation and germinal center formation.

In acute infection, the requirement of CD4 help for induction of robust primary CD8 T cell responses depends on the nature of the infecting pathogen [43]. Infections associated with low levels inflammation such as vaccinia virus, strictly require CD4 help for induction of DC maturation [44]. The key mechanism of help in this setting is the licensing of DCs by cognate CD4 T cells via CD40-CD40L interaction [45]. This improves the capacity of DCs to present antigen to cognate CD8 T cells and provide strong co-stimulation. Similar dependence is observed upon immunization, where absence of CD4 help negatively affects the primary CD8 T cell response in terms of

CD4 T cell help sustains distinct subpopulations in functional and dysfunctional CD8 T cell responses.

numbers and function [43]. In contrast, the pathogens inducing strong inflammatory response such as LCMV Armstrong (detailed infection model information in section 3.7. *Mouse infection models and transgenic T cell lines to study T cell responses*) in general can bypass the need of CD4 help for the formation of primary CD8 T cell responses. Nevertheless, in all cases the provision of CD4 help is pivotal for the generation of functional and long-lasting memory cells [46-48].

3.5. CD8 T cell differentiation and function in chronic infection

In the context of acute viral infections like influenza, the naïve antigen-specific CD8 T cells differentiate into highly functional cytotoxic effector and memory cells [30, 49-52]. Those cells produce multiple cytokines (e.g. IL-2, IFN γ , TNF α) and molecules (e.g. Prf1 (Perforin 1), Gzmb (Granzyme B)) which are critical for their function. Therefore they are referred to as “polyfunctional” T cells [53]. Certain viruses like HIV (human immunodeficiency virus) and HCV (hepatitis C virus) in humans, as well as LCMV c13 (detailed infection model information in section 3.7. *Mouse infection models and transgenic T cell lines to study T cell responses*) in mice have developed strategies to escape immune mediated eradication and establish persistent infections [54]. Such infections are characterized with the formation of **CD8 T cells with diminished effector function, a phenomenon known as T cell exhaustion** [54]. The first studies identifying functionally compromised but otherwise maintained CD8 T cell responses date back in the 90s and utilized persistent strains of LCMV (c13 and Docile) [55-57]. Later T cell exhaustion was also observed in human persistent HIV [58-61], HCV [62, 63] and HBV (hepatitis B virus) [64] infections as well as variety of cancers [65-71]. Although exhausted T cells were initially considered a result of failed protection allowing pathogen persistence, it is now widely appreciated that this differentiation path **limits T cell induced immunopathology while providing critical level of long-term viral control** [72, 73]. This view is supported by multiple clinical and experimental observations [72]. The fact that exhausted CD8 T cells exert crucial level of viral control is highlighted by the observation that CD8 T cell depletion in SIV (simian immunodeficiency virus)-infected rhesus macaques leads to strong increase in virus

CD4 T cell help sustains distinct subpopulations in functional and dysfunctional CD8 T cell responses.

titer [74-76]. Moreover, the late appearance of viral variants expressing mutated T cell epitopes in established chronic infections (e.g. HIV, HCV and SIV) is an indicator of an ongoing T cell response exerting viral suppression [77, 78]. In HIV infection, this late emergence of escape variants is also associated with increase in viral load and disease progression [78]. Additionally, in all major types of cancer, the numbers of tumor infiltrating CD8 T cells positively correlate with a favorable prognosis [79]. The ultimate evidence that persistently stimulated CD8 T cells retain the ability to mount potent effector responses is the success of inhibitory receptor blockade (e.g. blocking the PD-1 (Programmed Cell Death 1):PD-L1 (Programmed Cell Death 1 Ligand 1) interaction) in both chronic viral infection and cancer [80-85]. The antigen-specific CD8 T cells were also shown to contribute significantly to the organ damage observed in some viral infections – e.g. HCV [86, 87], which highlights the need for condition-adjusted effector CD8 T cell function. This is **achieved through massive transcriptional and epigenetic reprogramming** [54, 72, 88-94], affecting the expression of variety of genes coding effector molecules, co-stimulatory receptors, inhibitory receptors, factors involved in TCR and cytokine signaling as well as metabolism [95]. Nevertheless, the heterogeneity of CD8 T cell responses in chronic infection is highlighted by the fact that even among cell with the same antigen-specificity a spectrum of effector states can be observed – e.g. cells with functional effector phenotype (TNF⁺; IFN- γ ⁺), intermediate exhaustion (TNF⁻; IFN- γ ⁺) or advanced exhaustion (TNF⁻; IFN- γ ⁻) [96]. This heterogeneity is also pronounced among CD8 T cell clones with different epitope-specificity. Thus, in chronic LCMV c13 infection, the moderate affinity DbGP33- and DbGP276-specific CD8 T cell responses are preserved, while the high affinity D^bNP396- and K^bGP34-specific responses are deleted [96, 97]. The development of T cell exhaustion is also associated with **increased and sustained co-expression of multiple inhibitory receptors** (e.g. PD-1, TIGIT (T Cell Immunoreceptor With Ig And ITIM (Immunoreceptor Tyrosine-based Inhibitory Motif) Domains), Lag-3 (Lymphocyte-Activation Gene 3), Tim-3 (T cell Immunoglobulin Mucin Family Member 3) and CTLA-4 (Cytotoxic T-Lymphocyte Associated Protein 4)), which role is to suppress T cell function in response to environmental stimuli [54, 72, 88-90, 98]. The contribution and effectiveness of this regulatory layer of inhibitory receptors is demonstrated by blocking

CD4 T cell help sustains distinct subpopulations in functional and dysfunctional CD8 T cell responses.

their signaling. *In vivo* blockade of the interaction between PD-1 with its ligand PD-L1 in chronic viral infection [80] and cancer [82, 83, 99, 100] for example, leads to improved T cell proliferation and function. Last but not least, T cell exhaustion involves certain metabolic adaptations. The persistently stimulated CD8 T cells display reduced glucose uptake, as well as suppressed glycolysis and cellular respiration in comparison to their effector counterpart formed in acute infection [101, 102]. Moreover, the interconnection among all aspects of the T cell phenotype observed in persistent stimulation is highlighted by the observation that PD-1 and CTLA-4 inhibitory receptor signaling play a role in metabolic reprogramming of T cells, possibly through suppression of CD28 signaling [101-103].

3.5.1. Long-term maintenance of exhausted T cell responses

In the context of persistent stimulation, the long-term maintenance of antigen-specific CD8 T cell response, with otherwise short-lived terminally differentiated effector cells with limited proliferation capacity and functional plasticity, requires a stem-cell like proliferation competent progenitor population, which is characterized and dependent on the expression of transcription factor Tcf1 [73, 104-111]. The progenitors proliferate and give rise to *de novo* generated short-lived effector cells, thereby sustaining the immune response. This was demonstrated with adoptive transfer experiments in chronic infection and cancer, where the Tcf1⁺ but not the Tcf1⁻ cells were able to repopulate and sustain CD8 T cell response [104, 106, 109, 112]. The progenitors' significance is further highlighted by their crucial role in T cell expansion and enhanced effector function occurring after inhibitory receptor blockade [104, 113]. Moreover, high frequency of Tcf1⁺ CD8 T cells in human tumors positively correlates with favorable clinical outcome [112, 114, 115]. Nevertheless, it is important to note that despite some similarities with the memory-precursor progenitors in acute infection (e.g. both express Tcf1), the progenitors formed in chronic infection show some of the typical for T cell exhaustion signature (e.g. intermediate PD-1 expression, but not Tim3

CD4 T cell help sustains distinct subpopulations in functional and dysfunctional CD8 T cell responses.

(T cell Immunoglobulin And Mucin Domain-Containing Protein 3) expression which is characteristic for short-lived exhausted cells) [104, 106, 109-111].

3.5.2. Factors inducing, promoting and preventing T cell exhaustion

Both **high antigen load** and **prolonged antigen exposure** play a major role in the development of T cell exhaustion [90]. When untreated, the persistent HIV and HCV infections are characterized by high degree of T cell exhaustion due to high viral load [56, 58, 59, 116]. The role of prolonged antigen exposure is demonstrated by adoptive transfer of CD8 T cells primed during chronic viral infection into naïve mice. When those cells are transferred within the first one to two weeks post infection, they recover and develop into memory [104, 117, 118]. In contrast, if transferred at later time point, the state of T cell exhaustion is irreversible.

Certain inflammatory cytokines such as **IL-10** and **TGF- β** can promote T cell exhaustion. IL-10 is a STAT-3 inducing cytokine associated with T cell exhaustion, which is often expressed in chronic infection and cancer [119, 120]. Blocking IL-10 in combination with PD-1 signaling results in robust effector response in chronic LCMV infection [121]. TGF- β is a SMAD (Sma- And Mad-Related Protein)-activating cytokine associated with T cell exhaustion, which has been shown to suppress T-bet expression thus effector function in acute infection [122].

Certain inflammatory cytokines such as **IL-2** and **IL-21** can prevent or diminish T cell exhaustion. IL-2 is a key cytokine required for T cell survival in chronic infection and cells lacking IL-2 receptor are rapidly lost [123]. Although combining IL-2 supplementation with PD-1 blockade has a synergic effect in persistent LCMV infection, IL-2 has a modest effect on the CD8 T cell response in HIV [81, 124]. IL-21 is a BATF (Basic Leucine Zipper ATF-Like Transcription Factor) inducing cytokine, which promotes effector function in chronic infection. The Tfh are the main source of IL-21. Lack of IL-21 signaling in persistently stimulated CD8 T cells further impairs viral control [125, 126].

CD4 T cell help sustains distinct subpopulations in functional and dysfunctional CD8 T cell responses.

The **type I interferons** (IFN- α/β) are cytokines with a complex role in chronic infection. While from one side they can suppress viral replication and promote optimal T cell priming, their prolonged expression in chronic infection is associated with T cell suppression [127].

PD-1 is a member of the CD28 subfamily of Ig receptors and has two ligands - PD-L1 and PD-L2 [84]. While PD-L2 expression is restricted to immune cells (DCs, macrophages, germinal center B cells), PD-L1 is widely expressed and likely evolved as a mechanism to protect tissues from immune mediated tissue damage [84]. PD-L1 expression is regulated by IFN α/β and IFN γ . Certain cancers and infected cells express high levels of PD-L1 to exploit this system [128]. In contrast to acute infection where PD-1 is expressed on CD8 T cells only transiently, in chronic infection and cancer exhausted CD8 T cells sustain high level of PD-1 expression [61, 80, 94, 129]. Upon PD-1 ligation, the SHP-2 (Protein Tyrosine Phosphatase Non-Receptor Type 11) phosphatase gets recruited to the cytoplasmic domain of PD-1, resulting in suppression of key pathways downstream of TCR signaling (PI3K-Akt and Ras-MEK-ERK) and dephosphorylation of the co-stimulatory CD28 [6, 103, 130, 131]. Despite suppressing CD8 T cell function, PD-1 signaling can prevent further exhaustion and potentially clonal deletion. This is demonstrated by the fact that although PD-/- CD8 T cells initially displayed increased functionality, in the long run they developed more severe exhaustion and had poor maintenance [132]. Blocking PD-1:PD-L1 signaling yields higher response rate in cancer with greater mutational burden, likely reflecting the abundance of neoantigen recognized by T cells [133, 134].

TIGIT inhibits T cells function using a dual mechanism [135]. From one side TIGIT has a classical ITIM. From other side, it competes with CD226 for DC provided CD155, thus limiting T cell co-stimulation. Moreover, TIGIT:CD155 ligation induces IL-10 and represses IL-12 production in DCs, which further suppresses T cell function [136].

Lag-3 is a MHC class II binding homolog of CD4, which ligation suppresses multiple T cell functions including cell cycle progression via its intracellular KIEELE motif [137].

CD4 T cell help sustains distinct subpopulations in functional and dysfunctional CD8 T cell responses.

Tim-3 is a large transmembrane inhibitory receptor, which can bind multiple ligands among which Galectin 9 and CEACAM1 [138]. It suppresses T cell function in chronic infection and cancer.

CTLA-4 is a homolog of CD28, which has a higher binding affinity for CD80 and CD86, thus limiting T cell co-stimulation [139].

The conventional **CD4 help** promotes effector CD8 T cell function and viral control in chronic infection (discussed in details in the following section 3.5.3. *Role of CD4 help for CD8 T cell responses in chronic infection*).

Immunosuppressive cells such as **exhausted APCs**, **myeloid-derived suppressor cells**, **CD4 Tregs** and **CD8 Tregs** promote the development of T cell exhaustion. The negative effect of CD4 Tregs over effector CD8 T cell response in chronic infection is mainly attributed to production of IL-10 and TGF- β [140].

3.5.3. Role of CD4 help for CD8 T cell responses in chronic infection.

In the context of chronic infection, the maintenance and function of antigen-specific CD8 T cell responses strictly depends on the provision of cognate CD4 T cell help [41]. In human HIV-1 infection, stronger antigen-specific CD4 responses are associated with lower plasma viral load [141]. In human HCV infection, robust antigen-specific CD4 responses during the early infection phase are associated with subsequent infection control [142]. In mouse LCMV clone-13 infection, the absence of CD4 help is associated with progressive functional and numerical decline of the antigen-specific CD8 T cell response as well as decreased viral control [97, 143, 144]. In contrast to acute infection, the mechanisms of CD4 help in chronic infection are less clear. **Therefore, a central topic of this study is to investigate the role of CD4 help in the formation and maintenance of the Tcf1+ progenitors and their Tcf1-effector progeny in chronic infection.**

3.5.4. CD8 T cells and immunotherapy

Due to their capacity for antigen-directed cytotoxicity, the CD8 T cells are of central interest for immunotherapy. The intensive studies on the T cell biology in the past decades led to the remarkable translation of many basic scientific discoveries to sophisticated clinical applications [145].

One such application is the use of immune checkpoint blockade to unleash protective T cell responses, which was declared “the breakthrough of the year” by Science in 2013 [146]. Later in 2018, Tasuko Honjo and James P. Allison, the pioneers of this approach, were awarded with the Nobel Prize in Physiology and Medicine for their discovery. The two most potent examples of immune checkpoint molecules are CTLA-4 and PD-1. James Allison and colleagues were the first to demonstrate that the use of an antibody to block CTLA-4 signaling boosts anti-tumor responses in mice transplanted with colon carcinoma and fibrosarcoma [147]. Later in 2011, Ipilimumab (a human IgG1k anti-CTLA-4 antibody) was approved for treatment of non-resectable stage III/IV melanoma by FDA (United States Food and Drug Administration). Unfortunately, the use of CTLA-4 blockade did not significantly improved the survival of patients with renal cell carcinoma, non-small cell lung cancer, small cell lung cancer and prostate cancer [145]. In 2014, the use of Pembrolizumab and Nivolumab (both a human IgG4 anti-PD-1 antibodies) were approved for treatment of refractory and non-resectable melanoma by FDA. Later, the use of PD-1:PD-L1 blockade was expended to non-small cell lung carcinoma, renal carcinoma, urothelial carcinoma, hepatocellular carcinoma, head squamous cell carcinoma, neck squamous cell carcinoma, Hodgkin lymphoma, gastric/gastro-oesophageal junction cancer, colorectal cancer with a high degree of microsatellite instability and tissue-agnostic cancers with microsatellite instability [145]. Currently, multiple additional immune checkpoint molecules are being investigated for their effectiveness alone or in combination in variety of cancers (Tim-3, Lag-3, and TIGID among others). As immune checkpoint blockades disrupt the natural mechanisms for self-tolerance, their application is associated with a range of immune-mediated adverse effects in patients. One common feature among all currently used immune checkpoint blockades is the loss of naïve and accumulation of overactivated memory T cells causing inflammatory damage. Interestingly, the pattern

CD4 T cell help sustains distinct subpopulations in functional and dysfunctional CD8 T cell responses.

of immune-mediated toxicity and affected organs is treatment specific. Thus, gastrointestinal and brain toxicity are more common for blocking CTLA-4 signaling, while hypothyroidism, hepatotoxicity and pneumonitis are more common for blocking PD-1 signaling [148]. The management of blockade-mediated toxicity includes administration of glucocorticoids and immunosuppressive agents such as Infliximab (a chimeric monoclonal antibody neutralizing TNF α). Currently in the USA, the average price tag of inhibitory receptor blockade is about 12 500 \$ per month [145].

Another milestone in contemporary immunotherapy is the development of protocols for adoptive transfer of pathogen-specific autologous or allogenic T cells. This type of therapy was pioneered in the late 1980s with the use of *in vitro* expanded tumor-infiltrating lymphocytes (TILs) for the treatment of melanoma [149]. Later this approach was further elaborated with the advent of new technologies for genetic engineering, which resulted in the development of T cells with chimeric antigen receptors (CARs). Importantly, this circumvented the need for availability of tumor-specific patient CD8 T cells. The latest generation of CAR constructs contain an antigen-binding domain (most often the variable region of an antibody) linked to a TCR signaling domain and multiple co-stimulatory molecules [145]. Due to the antigen-binding domain's structure, the CAR T cells are not restricted by MHC, which is often found downregulated by cancer cells [150]. In 2017, the first CAR T cell-based therapy against CD19 was approved for treatment of B-cell malignancies by FDA. Unfortunately, the CAR T cell therapies so far show only modest success in clinical trials for solid tumors. The most common CAR-associated adverse events are cytokine release syndrome (CRS) and neurotoxicity [151]. The management of CRS includes administration of glucocorticoids and Tocilizumab (a humanized anti-IL-6 antibody). Currently in the USA, the average price tag of CAR T cell therapies such as Tisagenlecleucel and Axicabtagene ciloleucel is about 400 000 \$ per patient [145].

The development of the next generation of T cell targeted or T cell-based immunotherapies would greatly benefit from our growing understanding for the transcriptional and epigenetic programs guiding T cell differentiation in chronic infection.

3.5.5. Epigenetic landscape of T cell exhaustion

Unlike the progenitors in acute infection, the PD-1 expressing progenitors in chronic infection are restricted to generating only exhausted progeny via epigenetic mechanism. This was demonstrated in adoptive transfer experiments using the LCMV infection model, where exhausted T cells from chronically infected mice were transferred in naïve hosts and subsequently re-challenged with an acute infection [152]. The expanded progeny retained some of the main hallmarks of T cell exhaustion such as PD-1 expression and impaired cytokine production. The epigenetic regulation of T cell exhaustion is further demonstrated by the approximately 6000 differential accessible chromatin regions between exhausted and polyfunctional effector cells [85, 93], a scale of difference in the epigenetic landscape close to this between distinct hematopoietic lineages [153]. The *Pdcd1* locus is subjected to differential epigenetic regulation during acute and chronic viral infection. In the context of early acute infection, histone acetylation and DNA demethylation of the *Pdcd1* promotor and two proximal enhancers promote temporal PD-1 expression [154]. Following response contraction, the PD-1 expression is repressed through re-methylation. In exhausted CD8 T cells, the expression of the *Pdcd1* locus is continuous [85, 93, 154]. Moreover, PD-1 expression is promoted from an additional enhancer not used in acute infection. It is important to note that the PD-1 blockade does not change the epigenetic state of T cell exhaustion, thus the newly generated effector cells swiftly develop an exhausted phenotype [85]. The reversal of this state would likely require rewiring of the epigenetic landscape. As exhausted CD8 T cells display reduced acetylation of histone H3, one option is to explore the use deacetylase inhibitors. In support of this idea is the observation that *ex vivo* treatment of T cells with deacetylase inhibitors improves their function upon adoptive cell transfer [155].

3.5.6. Transcriptional landscape of T cell exhaustion

In line with the observation that the degree of T cell exhaustion is directly associated with frequency and strength of TCR stimulation [156], multiple TCR-responsive transcriptional factors were reported to contribute to the acquisition of T cell

CD4 T cell help sustains distinct subpopulations in functional and dysfunctional CD8 T cell responses.

exhaustion - e.g. NFATC1 (Nuclear Factor Of Activated T Cells 1), IRF4 (Interferon Regulatory Factor 4), AP-1 (Activator Protein 1) and BATF. However, the engagement of these transcriptional factors is not specific to chronic infection as they also play a key role in acute infection. This context-specific transcriptional factor function might be a result of cofactor availability, differences in the epigenetic landscape, localization or concentration-dependent TF binding. An exception is the transcriptional regulator TOX (Thymocyte Selection Associated High Mobility Group Box), which is a key inducer of T cell exhaustion in chronic infection and cancer, but dispensable for effector cell differentiation and maintenance in acute infection (discussed in details below).

T-bet and **Eomes** (Eomesodermin) are transcriptional factors of the T-box family. In the context of acute infection, T-bet is necessary for the formation of terminally differentiated KLRG1⁺ effector cells, while Eomes for formation of memory cells [157-159]. Loss of T-bet results in loss of KLRG1⁺ but not KLRG1⁻ effector cells and memory cells [157, 160]. Loss of Eomes compromises the formation of memory but does not affect the formation of effector CD8 T cells [157, 161]. In the context of chronic infection, the absence of either of the transcriptional factors compromises the entire CD8 T cell response [162]. Moreover, instead with memory, high Eomes expression in chronic infection is associated with more pronounced level of T cell exhaustion [132, 162]. However, the expression pattern of T-bet and Eomes do not discriminate between the Tcf1⁺ progenitors and their Tcf1⁻ progeny [104, 106, 112].

Although they do not possess DNA binding activity, the transcriptional regulators **ID2** and **ID3** (Inhibitor of Differentiation 2 and 3) are repressors of the E-protein transcription factors. In the context of acute infection, ID2 and ID3 promote the formation of effector and memory CD8 T cells respectively [163]. In chronic infection, ID2 and ID3 preserve similar expression pattern, where ID3 promotes T cell survival and proliferation in chronic LCMV infection [164].

The **NFAT** family of transcriptional factors has a context specific role in acute and chronic infection, which depends on the availability of their AP-1 family binding partner [165]. In the initial stages of acute infection, a balanced NFAT:AP-1 ratio promotes T cell activation and effector function. At the end of the acute response, the ratio increases in favor of NFAT, which attenuates T cell activation. In the context of

CD4 T cell help sustains distinct subpopulations in functional and dysfunctional CD8 T cell responses.

chronic infection, factors like BATF suppress AP-1 levels, thus NFAT promotes the expression of exhaustion associated genes like PD-1, Lag-3 and Tim-3 among others [54, 94, 166, 167].

Similar to acute infection, the expression of **Blimp-1** (B-Lymphocyte-Induced Maturation Protein 1) in chronic infection is limited to the Tcf1- effector compartment [106, 110, 111]. Tcf1 and Blimp-1 are mutually exclusive, as they repress the expression of each other, thus Blimp-1 is not found in the Tcf+ progenitors [110, 111]. Together with T-bet, Blimp-1 promotes the expression of effector and suppresses the expression of memory genes (e.g. IL7ra, Ccr7, Cxcr5 and Sell) [168, 169]. In the setting of persistent stimulation, Blimp-1 was also reported to promote inhibitory receptor expression including this of PD-1 and TIGIT [170].

The expression of **IRF4** is induced by TCR stimulation and is proportional to the epitope affinity. In acute infection, the level of IRF4 determines the extent of clonal expansion and promotes effector differentiation [171]. In comparison to acute infection, IRF4 in chronic infection has elevated expression, which promotes T cell exhaustion [172]. Loss of IRF4 in chronic infection has been reported to restore effector function and promote progenitor development [172].

The transcriptional factor **Foxo1** (Forkhead Box Protein O1) is crucial for the generation of memory T cells in acute infections, but also for the generation and maintenance of the Tcf1+ progenitors in persistent infections [173-175]. Foxo1 directly promotes the expression of multiple memory-associated genes (e.g. Bcl2, Il7ra, Ccr7 and Sell) and is essential for Tcf1 expression in memory, but not in naïve cells [173]. In the context of chronic infection, Foxo1 was also reported to serve as a transcriptional activator of PD-1 [174].

In acute infection, **BATF** promotes the expression of T-bet and Blimp-1, thus promoting effector CD8 T cell development [176]. Paradoxically, BATF also represses the expression of INF- γ and Gzma [176]. In response to PD-1 signaling in chronic infection, increased expression of BATF was demonstrated to suppress T cell proliferation and cytokine production [166].

In recent studies, **TOX** was identified as the first exhaustion specific transcriptional regulator, which is dispensable for CD8 T cell differentiation in acute

infection [177-181]. In chronic infection, TOX induces the transcriptional and epigenetic reprogramming of the progenitors, resulting in the expression of exhaustion specific genes such as Nr4a2 (Nuclear Receptor Subfamily 4 Group A Member 2), Pdcd1 (gene coding PD-1), CD244, Lag-3, ID3, and Havcr2 (gene coding Tim-3) [177]. In absence of TOX, the progenitors do not acquire the transcriptional signature of exhaustion and their progeny display an acute phenotype despite the persistent stimulation. Initially this results in heightened virus control and immunopathology, but at latter stage the TOX-deficient progenitors are lost [177]. This is likely a result of the progenitors lacking mechanisms like inhibitory receptor expression, which protects them from terminal differentiation due to persistent antigen stimulation. Therefore, the complexity of TOX-mediated reprogramming of CD8 T cells makes it an unlikely candidate for direct therapeutic intervention.

3.6. Role of single-cell RNA sequencing in investigating the gene expression programs of T cells in health and disease.

Single-cell genomics offers unique opportunities to expand our knowledge on the regulation of T cell differentiation and function in therapeutically relevant settings. In comparison to bulk population gene expression profiling, the single-cell resolved gene expression profiles (scGEPs) allow to deconvolute heterogeneity within complex cellular populations, to extract gene expression networks and identify their regulators based on truly occurring co-expression within the same cell, to track trajectories of differentiation and to infer progenitor-progeny relationships between cellular subpopulations [182]. Such unbiased analyses are particularly relevant for CD8 T cells, which are known to be heterogeneous with respect to the developmental potential of individual cells, but for which molecular markers identifying distinct subpopulations and differentiation trajectories remain unknown. The available technologies for single-cell gene expression profiling differ by orders of magnitude in terms of throughput (number of cells analyzed and number of genes detected). Methods such as flow cytometry and mass cytometry provide protein expression information rather than gene expression information, and allow the profiling of high number of cells at one time [183, 184]. The

main limitations of flow and mass cytometry are the limited number of proteins detected (about 20 or 40 respectively) and the requirement for prior knowledge or pure guesswork for pre-selection of targets. Moreover, the availability of target-specific antibodies can be another limiting factor. The single-cell quantitative PCR (sc-qPCR), which uses gene-specific primers can overcome the antibody absence [185]. Nevertheless, sc-qPCR is still low throughput and poses the challenge of target pre-selection. These were overcome with the development of technologies for single-cell RNA sequencing (scRNA-seq), which enabled the analysis of thousands of cells in parallel for virtually any gene expressed by them [186, 187]. Since then, scRNA-seq has become the method of choice to obtain an unbiased high-resolution snapshot of the gene expression programs used by individual cells [188]. Moreover, strategies for multiplexed single-cell analysis were developed, combining transcriptome with epigenome, proteome and/or TCR/BCR profiling [189-192]. There are two major groups of protocols currently in use for scRNA-seq. The plate-based protocols rely on fluorescent-activated cell sorting (FACS) to deposit single-cells into individual wells of a PCR plate. These protocols provide several advantages. Following single-cell sorting, the plates can be stored for prolonged periods of time before further processing. Moreover, the plate-based protocols are generally more sensitive and can be used to profile cells with varying sizes [193]. Although the plate-based protocols are amenable to automation, in practice their cell throughput is limited. The microdroplet-based approaches such as Drop-seq [194] and 10xGenomics Chromium, rely on encapsulating single-cells with uniquely barcoded beads into tiny droplets, which represent aqueous compartments formed by precisely combining aqueous and oil flows into a microfluidic device. The microdroplet-based protocols allow for profiling of tens of thousands of cells in parallel. This comes at the cost of reduced sensitivity due to generally lower mRNA capturing efficacy.

In order to advance our study on CD8 T cell differentiation and function, in the first part of this work, we systematically assessed the range of single-cell RNA sequencing solutions available at the conceiving phase of this study (the beginning of 2016). This resulted in the selection of one microdroplet-based

CD4 T cell help sustains distinct subpopulations in functional and dysfunctional CD8 T cell responses.

(DROP-seq) and one plate-based (SCBR-seq) protocol, which we further tailored for profiling of T cells.

3.7. Mouse infection models and transgenic T cell lines to study T cell responses.

To address the questions in this study, we used the following well established mouse infection models and transgenic T cell lines.

Infection models:

LCMV is an enveloped ambisense RNA virus, a member of the arenavirus family, which is well known for its pivotal role in immunobiology research. The LCMV infection model has been used to successfully address key question in viral pathogenesis and immunobiology – e.g. viral-host interaction, T cell function and differentiation, T cell MHC restriction, immune memory and immunologic tolerance [195]. Moreover, LCMV has a central role in understanding T cell function and differentiation in different infection settings due to the availability of strains causing either acutely resolved (Armstrong; low doses of WE) or persistent (clone 13; docile; high doses of WE) systemic infections [196, 197]. LCMV uses a glycoprotein (GP) in its envelope to recognize alpha-dystroglycan (α -DG) on the cell surface and initiate entry. LCMV itself causes little or no-damage to the infected cell, while the observed host pathology is largely caused by the activated immune system. The acute infection caused by LCMV Armstrong induces potent CTL responses, which results in infection resolution within one to two weeks [56]. Although LCMV clone-13 initially induces similarly strong CTL response (~90% of the total CTL repertoire at the peak of infection), eventually the CTL response become exhausted, which coincides with detectable viremia for months post infection and lifelong viral persistence in the kidneys [56]. The differential infection outcome of LCMV Armstrong and LCMV clone-13 is a result of mainly two amino-acid substitutions in their genomes. The substitution of phenylalanine with leucine in position 260 of the viral GP1 proteins and the substitution of lysine with glutamine in position 1079 of the viral polymerase were shown to mediate

CD4 T cell help sustains distinct subpopulations in functional and dysfunctional CD8 T cell responses.

persistence [198-200]. In result to their high genetic similarity, LCMV Armstrong and clone-13 share all known CD4 and CD8 T cell epitopes, which allows side-by-side comparison of the T cell responses formed in acute and chronic infection. Three of the immunodominant CD8 T cell epitopes are H-2Db-restricted NP396-404 (Db/NP396), H-2Db-restricted GP33-41 (Db/GP33) and H-2Kb-restricted GP34-43 (Kb/GP34) [96].

Listeria monocytogenes is a Gram-positive intracellular bacterium, which can be transmitted through contaminated food and causes listeriosis in humans. *Listeria monocytogenes* has long been used as a model infection to study the innate and adaptive immune responses in mice [201, 202]. Following infection, the bacterium is quickly engulfed by macrophages, in the phagosome of which the bacterium uses its pore-forming toxin listeriolysin O (LLO) to gain access into the cytosol and start replication [203]. The innate immune system takes a central role in the early control of bacterial growth and dissemination, thus preventing a systemic infection [202]. The engagement of the adaptive immune system (mainly CD4 and CD8 T cells due to intracellular nature of the pathogen) is necessary for complete bacterial eradication, following which immune memory is formed [202]. As currently we have limited knowledge on the strong MHC I-restricted CD8 T cell epitopes of *Listeria monocytogenes* in C57BL/6 mice, recombinant bacterial strains were generated expressing foreign H-2Kb-restricted epitopes - e.g. derived from chicken ovalbumin (OVA) or LCMV [201].

Transgenic T cell lines:

Tracking endogenous T cell responses can be a challenging task due to the low frequency of antigen-specific precursor cells. Thus, the development of TCR-transgenic mouse models, which can serve as a source of naïve monospecific T cells for adoptive cell transfer, brought a significant advancement in our understanding of adaptive immunity [50]. The transferred TCR-transgenic T cells can be identified into the recipient mouse based on the expression of a congenic marker (e.g. CD45.1 versus CD45.2), which can be recognized by specific antibodies. The TCR-transgenic **P14 CD8 T cells** recognize the H-2Db-restricted gp33-41 (KAVYNFATC) epitope of LCMV. The TCR-transgenic **OT-1 CD8 T cells** recognize the H-2Kb-restricted SIINFEKL

CD4 T cell help sustains distinct subpopulations in functional and dysfunctional CD8 T cell responses.

epitope of chicken ovalbumin (OVA). The TCR-transgenic **SMARTA CD4 T cells** recognize the H-2Ab-restricted gp61–80 epitope of LCMV.

4. Aim of study

(Aim 1) To systematically assess the range of single-cell RNA sequencing solutions and to select a sensitive cost-effective protocol for the subsequent T cell studies.

The utilization of single-cell RNA sequencing data enables unprecedented insights into the molecular programs guiding the differentiative and functional heterogeneity of T cells in variety of clinically relevant settings. Here, a major obstacle is the minute amount of RNA available in a single T cell, which critically impacts sensitivity. At the time this study was conceived in early 2016, there was only one commercially available solution for single-cell RNA sequencing – the Fluidigm C1 System, the running cost of which (~40 EUR/cell) precluded high-throughput single-cell analysis. Therefore, the first aim of this study is to find, assess and potentially develop an alternative cost-effective and sensitive solution for single-cell sequencing of primary T cells, which can be used to achieve **Aim 2** and **Aim 3**.

(Aim 2) To investigate the leflunomide's selective inhibition of effector but not memory T cell differentiation at early timepoint of acute infection using scRNA-seq.

The immunosuppressive drug leflunomide selectively suppresses the formation of effector, but not precursor or memory CD8 T cells when applied early in acute infection. Taking into account that leflunomide was reported to suppress T cell proliferation via reverse inhibition of DHODH, we hypothesized differential requirement for this enzyme between effector and progenitor T cell subpopulations early after activation. To test this hypothesis, we formulated the following sub-aims:

(Sub-aim 1) To explore the range of effector and progenitor CD8 T-subpopulations formed in early acute infection with the use of scRNA-seq.

(Sub-aim 2) To address the differential leflunomide sensitivity of the identified subpopulations based on their gene expression profiles.

CD4 T cell help sustains distinct subpopulations in functional and dysfunctional CD8 T cell responses.

(Aim 3) To examine the CD4 help dependence of the Tcf1+ progenitors and their Tcf1- effector progeny in chronic infection.

In chronic infection, the maintenance and function of the antigen-specific CD8 T cells responses strictly depend on the provision of cognate CD4 help. However, the reason for this dependence remains so far unclear. Despite the exacerbated chronic phenotype and decreased functionality, little is known about CD8 T cell subset differentiation in absence of CD4 help in the context of persistent stimulation. Based on the critical role of CD4 help for the generation of long-lasting and functional memory in acute infection, we hypothesized that absence of CD4 help initially affects the maintenance and function of the progenitors, which later translates in reduced output of newly generated terminally differentiated effector cells and ultimately CD8 T cell response erosion. To test this hypothesis as well as to explore CD8 T cell subset differentiation in presence or absence of CD4 help in chronic infection, we formulated the following sub-aims:

(Sub-aim 1) To explore the CD4 help dependence of the Tcf1+ progenitors and their Tcf- terminally differentiated effector progeny in dysfunctional responses.

(Sub-aim 2) To compare the observations from sub-aim 1 to CD8 T cell responses with acute-like phenotype in otherwise chronic infection using the LCMV c13 MIX model.

(Sub-aim 3) To assess the contribution of CD40-CD40L signaling in providing CD4 help to CD8 T cells in chronic infection.

(Sub-aim 4) To explore the spectrum of CD8 T cell subset differentiation in presence and absence of CD4 help using scRNA-seq.

5. Materials and methods

Mice: C57BL/6 (B6) mice (CD45.2⁺) were obtained from Charles River (Germany or France). The P14 TCR $\alpha\beta$ (CD45.1⁺) and SMARTA TCR $\alpha\beta$ (CD45.1⁺) transgenic mice were kindly provided by A. Oxenius. The OT-1 TCR $\alpha\beta$ (CD45.1⁺) transgenic mice were obtained from Jackson Laboratory. Mice were bred and maintained in modified SPF facilities of the Technical University of Munich. Experiments were performed with at least six-week-old mice in compliance with the institutional guidance of the Technical University of Munich and were legally approved by the regional veterinary authority "Regierung of Oberbayern". Mice were maintained at a temperature 20 – 24°C, humidity 50-70 % and 12 hours light cycle with light phase beginning at 5 am and ending at 5 pm.

Purification of mouse and human lymphocytes: A mouse spleen and human blood were used to isolate mouse and human lymphocytes with Lympholyte M (Cedarlane) and Ficoll-Paque PLUS (GE Healthcare) density gradient media respectively. Cells were washed with supplemented media (RPMI; 10% heat inactivated FCS; 5mM HEPES; 50 μ M 2-Mercaptoethanol; 100U/ml Penicillin / Streptomycin) and sorted on BD FACS Fusion (100-micron nozzle, standard operation settings, single-cell purity), where individual cells meeting the gating strategy were sorted in a tube containing supplemented media and used immediately for the generation of Drop-seq single-cell transcriptomes.

Purification of mouse T cells, adoptive cell transfers: Single cell splenocyte suspensions were obtained by mashing total spleens through a 100 μ m nylon cell strainer (BD Falcon) and red blood cells were lysed with a hypotonic ACK buffer (pH = 7.2 -7.4; 150 mM NH₄Cl; 10 mM KHCO₃; 0.1 mM Na₂EDTA). The mouse CD8⁺ T cell enrichment kit (Miltenyi Biotech, Bergisch-Gladbach, Germany) was used for isolation of transgenic CD8⁺ T cells. The naïve CD45.2⁺ C57BL/6 host mice received 2x10³ CD45.1⁺ P14 TCR $\alpha\beta$ or 2x10⁵ CD45.1⁺ OT-1 TCR $\alpha\beta$ CD8 T cells. The CD4⁺ T cell enrichment kit (Miltenyi Biotech, Bergisch-Gladbach, Germany) was used for isolation of transgenic CD4⁺ T cells. 1x10⁶ CD45.1⁺

CD4 T cell help sustains distinct subpopulations in functional and dysfunctional CD8 T cell responses.

SMARTA TCR $\alpha\beta$ were transferred into LCMV c13 WT infected CD45.2+ C57BL/6 mice 25 days post infection.

Infections:

| | |
|------------------------|---|
| Listeria monocytogenes | 2000 colony-forming units (CFU) of recombinant Listeria stably expressing Ova containing the SIINFEKL (N4) epitope were diluted in PBS and injected intravenously. |
| LCMV Armstrong | 2×10^5 plaque forming units (PFU) of LCMV Armstrong were diluted in PBS and injected intraperitoneally. |
| LCMV clone 13 WT | 5×10^6 plaque forming units (PFU) of wild type (WT) LCMV clone 13 were diluted in PBS and injected intravenously. |
| LCMV clone 13 MIX | The mixed infection was achieved by combining gp33-deprived virus variant (c13 w/o gp33) with wild-type clone-13 virus at a 5:1 ratio [156]. This results in decreased amount of presented gp33 peptide, whereas total virus load, presumably the presentation of any other epitope and the level of inflammation remain unchanged. 5×10^6 plaque forming units (PFU) of the mixed (MIX) LCMV clone 13 were diluted in PBS and injected intravenously. |

CD4 depletion: 300 μ g anti-mouse CD4 antibody (clone GK1.5; Bio X Cell, USA) diluted in PBS was used for in vivo depletion of CD4 lymphocytes. The antibody was administered with intraperitoneal injection on day -2, +1, and thereafter on

CD4 T cell help sustains distinct subpopulations in functional and dysfunctional CD8 T cell responses.

each fifth day up to readout. To avoid depletion of the engrafted cells, the CD4 depletion was interrupted 10 days before SMARTA transgenic cell transfer.

CD40L blockade: 300 µg anti-mouse CD40L antibody (clone MR-1; Bio X Cell, USA) diluted in PBS was used for in vivo CD40L blockade. The antibody was administered with intraperitoneal injection on day -2 and day +1, thereafter on each fifth day up to readout.

Teriflunomide treatment: Teriflunomide was dissolved in 0.5 % Carboxymethylcellulose. Starting 3 days before infection, the animals were treated every second day with 20mg/kg teriflunomide via oral gavage.

Surface and intracellular antibody staining: Single-cell splenocyte suspensions were obtained by mashing total spleens through a 100 µm nylon cell strainer (BD Falcon) and red blood cells were lysed with a hypotonic ACK buffer. Surface staining was performed for 40 min at 4°C in FACS buffer (PBS; 2% heat inactivated FCS; 0.01% sodium azide) using the following antibodies: anti-CD8a (53-6.7, eBioscience), CD4 (RM4-4, Biolegend), CD45.1 (A20, eBioscience), CD45.2 (104, eBioscience), KLGR1 (2F1; eBioscience), CD127 (A7R34, eBioscience), PD-1 (J43, eBioscience), and Cx3cr1 (SA011F11, Biolegend). Cells were washed twice with FACS buffer. The intracellular staining was performed with Foxp3 / Transcription Factor Staining Buffer Set (eBioscience) using the following antibodies: anti-Tcf1 (S33966, BD Pharmingen), T-bet (4B10, eBioscience), EOMES (Dan11mag, eBioscience), Tox (TXRX10, eBioscience), Helios (22F6, eBioscience), and Ki67 (SolA15, eBioscience). The flow cytometry measurements of cells were performed on an LSR-Fortessa flow cytometer (BD). All data were analyzed using FlowJo (TreeStar).

Sorting of naïve P14 T cells: Single-cell splenocyte suspensions were obtained by mashing total spleens through a 100 µm nylon cell strainer (BD Falcon) and lysing red blood cells with a hypotonic ACK buffer. The mouse CD8⁺ T cell enrichment kit (Miltenyi Biotech, Bergisch-Gladbach, Germany) was used for

CD4 T cell help sustains distinct subpopulations in functional and dysfunctional CD8 T cell responses.

isolation of naïve transgenic P14 CD8 T cells. Surface staining was performed for 40 min at 4°C in supplemented media using the following antibodies: anti-CD8a (53-6.7, Biolegend), CD4 (RM4-4, Biolegend), and TCR V alpha 2-PE (V20.1, eBioscience). Cells were washed twice with supplemented media and sorted on BD FACS Fusion (100-micron nozzle, standard operation settings, single-cell purity). Individual cells meeting the gating strategy were sorted in tube containing supplemented media (Drop-seq) and used immediately or directly in lysis buffer into individual wells of a low-binding PCR plate (SCRB-seq), which was subsequently spun down, snap-frozen on dry ice and stored at -80°C until use.

Sorting of P14 and OT-1 T cells recovered from infection: Single-cell splenocyte suspensions were obtained by mashing total spleens through a 100 µm nylon cell strainer (BD Falcon) and red blood cells were lysed with a hypotonic ACK buffer. Activated transgenic P14 or OT-1 CD8 T cells were isolated using anti-CD45.1 biotin/anti-biotin conjugated microbeads and magnetic MACS cell separation (Miltenyi Biotech, Bergisch-Gladbach, Germany). Surface staining was performed for 40 min at 4°C in supplemented media with the following antibodies: anti-CD8a (53-6.7, Biolegend), CD4 (RM4-4, Biolegend), CD45.1 (A20, eBioscience) and CD45.2 (104, eBioscience). Cells were washed twice with supplemented media. For single-cell RNA sequencing the cells were sorted on BD FACS Fusion (100-micron nozzle, standard operation settings, single-cell purity). Individual cells meeting the gating strategy were sorted in a tube containing supplemented media (Drop-seq) and used immediately or directly in lysis buffer into individual wells of a low-binding PCR plate (SCRB-seq), which was subsequently spun down, snap-frozen on dry ice and stored at -80°C until use. For bulk RNA sequencing the cells were sorted on BD FACS Fusion (100-micron nozzle, standard operation settings, 4-way purity). Individual cells meeting the gating strategy were sorted in a tube containing supplemented media.

Generation of single-cell transcriptomes with Drop-seq: The original Drop-seq protocol was performed based on Macosko and colleagues[194]. The hardware

CD4 T cell help sustains distinct subpopulations in functional and dysfunctional CD8 T cell responses.

used included an inverted microscope, three syringe pumps (Legato 100, KD Scientific), a magnetic stirrer (710D2, VP Scientific), a magnetic stirring disc to keep the barcoded beads suspended (772DP-N42-5-2, VP Scientific), a Peqlab PerfectBlot hybridization oven and a thermal cycler. The barcoded Drop-seq oligo-dT beads (MACOSKO-2011-10; ChemGenes Corporation) were washed once with 30 ml pure ethanol, twice with 30 ml TE-TW buffer (10 mM Tris pH 8.0; 1 mM EDTA and 1% Tween-20), resuspended in 20 ml TE-TW buffer, passed through 100 μ m nylon cell strainer (BD Falcon), counted with a Fuchs-Rosenthal hemocytometer and stored at 4°C for up to six months. The needed quantity of beads was aliquoted and resuspended in 2x lysis buffer (6% Ficoll MP-400; 0.2% Sarkosyl; 20 mM EDTA; 200 mM Tris pH 7.5 and 50 mM DTT) at final concentration 120 000 beads/ml. The sorted cells were diluted with PBS supplemented with 1% BSA at final concentration of 100 000 cells/ml. The 20 ml syringe containing droplet generation oil (186-4006, Bio-Rad) was mounted on the oil syringe pump and connected to Drop-seq PDMS (polydimethylsiloxane) device (Nanoshift). The cells were loaded in 3 ml syringe (309657, BD), mounted on the cell syringe pump and connected to Drop-seq PDMS device (Nanoshift). The beads resuspended in 2x lysis buffer were loaded in 3 ml syringe (309657, BD) together with a magnetic stirring disk, mounted on the bead/lysis syringe pump in proximity to the magnetic stirrer and connected to the Drop-seq PDMS device (Nanoshift). The droplet generation was performed at 15 000 μ l/hour oil flow, 3000 μ l/hour cell flow and 3000 μ l/hour bead flow. After removal of the oil, 30 ml 6x SSC (15557-044, Thermo Fisher Scientific) and 1 ml Perfluorooctanol (647-42-7, Sigma-Aldrich) were added and the generated droplets were broken by manual vertical shaking. The beads were washed once with 30 ml 6 x SSC, twice with 1 ml 6 x SSC and once with 300 μ l 5X reverse transcription buffer (EP0753, Thermo Fisher Scientific). The beads were resuspended in 200 μ l of reverse transcription master mix (1 x Maxima H- RT Buffer – EP0753, Thermo Fisher Scientific; 4% Ficoll MP-400; 1mM Advantage UltraPure PCR Deoxynucleotide Mix – 639125, Clontech; 1U/ μ l NxGen RNase Inhibitor - 30281-2, Lucigen; 2,5 μ M Drop-seq Template Switching Oligo – Eurogentec; 10U/ μ l Maxima H Minus Reverse Transcriptase - EP0753, Thermo

Fisher Scientific), incubated in the hybridization oven for 30 minutes at room temperature with rotation and then for 90 minutes at 42°C with rotation. All Drop-seq primer sequences used in this study are available in (**Table 1**, page 42). The beads were washed once with 1 ml TE-SDS (10 mM Tris pH 8.0; 1 mM EDTA; 0.5% SDS), twice with 1 ml TE-TW buffer and once with 1 ml 10 mM Tris pH 8. The beads were resuspended in 200 µl exonuclease reaction mix (1x Exonuclease I Reaction Buffer - B0293S, New England Biolabs; 1U/µl Exonuclease I - M0293S, New England Biolabs) and incubated in the hybridization oven for 45 minutes at 37°C with rotation. The beads were washed once with 1 ml TE-SDS, twice with 1 ml TE-TW buffer, once with 1 ml molecular grade water and resuspended in 1 ml molecular grade water. The beads were counted with a Fuchs-Rosenthal hemocytometer and 2000 beads were apportioned per PCR reaction. The apportioned beads were resuspended in 50 µl PCR master mix (1x Kapa HiFi Hotstart Readymix - KK2602, Kapa Biosystems; 0.8 µM Drop-seq SMART PCR Primer) and incubated in a thermal cycler using the following program – heated lid at 100°C, 3 minutes 95°C, 4 cycles (20 seconds 98°C, 45 seconds 65°C, 3 minutes 72°C), 14 cycles (20 seconds 98°C, 20 seconds 67°C, 3 minutes 72°C), 7 minutes 72°C and hold at 4°C. The barcoded single-cell amplicons were purified with the use of (0.6x) AMPure XP beads (A63881, Beckman Coulter). The quality and quantity of the resulting amplicon was assessed with the use of Agilent High Sensitivity DNA Kit (5067-4626, Agilent). 1 ng of the resulting amplified cDNA was used for library preparation with the Illumina Nextera XT DNA Library reagents (FC-131-1024, Illumina). The Nextera XT N5 index primer was substituted with a Drop-seq custom N5 primer, which was used along with Nextera XT N7 index primer. After PCR amplification of the fragmented libraries, the samples were purified with (0.6x) AMPure XP beads and eluted in 10 µl of molecular grade water. The quality of the resulting library was assessed with the use of Agilent High Sensitivity DNA Kit (5067-4626, Agilent). The library quantification was performed based on the Illumina recommendations (SY-930-1010, Illumina) with the use of KAPA SYBR FAST qPCR Master Mix (KK4600, Kapa Biosystems). The libraries were sequenced on Illumina HiSeq 2500 system at the following conditions - rapid run,

paired-end, 20 bp read 1, 45 bp read 2, single-indexed sequencing resulting in 0.5 million reads per single-cell. Due to the use of Drop-seq custom N5 primer, the Illumina HP10 read 1 primer was replaced with Drop-seq Custom Read 1 Primer following the manufacturer recommendations. In the process of Drop-seq protocol optimization described in this work, the following substitutions were tested. Replacement of the 0.2% Sarkosyl with 0.2% Igepal (I8896-50ML, Sigma-Aldrich; final concentration in the droplet 0.1%). Addition of 0.5 M NaCl (S3014, Sigma-Aldrich) to the lysis buffer. Replacement of the 3' most rG in the template switching oligo (TSO) with a locked nucleic acid base (3'LNA). Replacement of the 10U/μl Maxima H Minus RT for 10U/μl SuperScript IV RT (18090010, ThermoFisher) or 10U/μl SMARTScribe RT (639536, Takara Bio). Addition of 4% Ficoll PM 400 (GE17-0300-10, GE Healthcare) to the PCR master mix as a macromolecular crowding.

Generation of single-cell transcriptomes with SCRB-seq: The original SCRB-seq protocol was performed based on Soumillon and colleagues[204] with some modifications necessary for working with primary T cells. The single-cell RNA was purified with (2.2x) RNAClean XP beads (A63987, Beckman Coulter) before reverse transcription. The RNA was eluted in 2.8 μl of molecular grade water supplemented with 1.42 U/μl NxGen RNase Inhibitor (30281-2, Lucigen). 1.2 μl of unique tSCRB Barcoded Oligo-dT Primer was added to each well of the PCR plate at a final concentration of 2.4 μM during the reverse transcription. The single-cell plates were incubated on a thermal cycler using the following program - heated lid at 105°C, 3 minutes at 72°C, hold at 4°C. The single-cell transcriptomes from the optimization experiments were barcoded with tSCRB Barcoded Oligo-dT Primer Plate v1 (**Table 2**, page 43). All other tSCBR-generated single-cell transcriptomes were barcoded with tSCRB Barcoded Oligo-dT Primer Plate v2 (**Table 3**, page 44). The SCBR-seq primers used in this study are available in (**Table 1**, page 42). 3 μl of reverse transcription master mix (1x Maxima H Minus Buffer - EP0753, Thermo Fisher Scientific; 10 U/μl Maxima H Minus Reverse Transcriptase - EP0753, Thermo Fisher Scientific; 1 mM Advantage dNTPs Mix - 639125, Takara; 1.42 U/μl

CD4 T cell help sustains distinct subpopulations in functional and dysfunctional CD8 T cell responses.

NxGen RNase Inhibitor - 30281-2, Lucigen; and 1.2 μ M SCRB-seq Template Switching Oligo) were added to each well and the plates were incubated on a thermal cycler using the following program - heated lid at 105°C, 90 minutes at 42°C, 15 minutes at 72°C, hold at 4°C. 18 μ l of PCR master mix (1x KAPA HiFi HotStart ReadyMix - 7958935001, KAPA Biosystems; 0.48 μ M SCRB-seq SMART PCR Primer) were added to each well and the plates were incubated on a thermal cycler using the following program - heated lid at 100°C, 3 minutes at 98°C, 20 cycles (20 seconds at 98°C, 30 seconds at 65°C, 6 minutes at 72°C), 5 minutes at 72°C, hold at 4°C. The single-cell amplicons from each plate were pooled together and double purified with the use of (0.6x) AMPure XP beads (A63881, Beckman Coulter). The quality and quantity of the resulting pooled plate amplicon was assessed with the use of Agilent High Sensitivity DNA Kit (5067-4626, Agilent). 1 ng of the resulting amplified cDNA was used for library preparation with the Illumina Nextera XT DNA Library reagents (FC-131-1024, Illumina). The Nextera XT N5 index primer was substituted with a SCRB-seq custom N5 primer, which was used along with Nextera XT N7 index primer. After PCR amplification of the fragmented libraries, the samples were double purified with (0.6x) AMPure XP beads and eluted in 10 μ l of molecular grade water. The quality of the resulting library was assessed with the use of Agilent High Sensitivity DNA Kit (5067-4626, Agilent). The library quantification was performed based on the Illumina recommendations (SY-930-1010, Illumina) with the use of KAPA SYBR FAST qPCR Master Mix (KK4600, Kapa Biosystems). The libraries were sequenced on Illumina HiSeq 2500 system at the following conditions - rapid run, paired-end, 16 bp read 1, 49 bp read 2, single-indexed sequencing resulting in 0.5 (naïve and day 8 acute infection datasets) or 1.0 (all other datasets) million reads per single-cell. Due to the use of SCRB-seq custom N5 primer, the Illumina HP10 read 1 primer was replaced with SCRB-seq Custom Read 1 Primer following the manufacturer recommendations. In the process of SCRB-seq protocol optimization described in this work, the following substitutions were tested. Replacement of the 1:500 dilution of Phusion HF buffer supplemented with Proteinase K for cell lysis with TCL buffer (1031576, Qiagen) supplemented with 1% β -mercaptoethanol (M3148-25ML, Sigma-Aldrich)

or 0.2% Triton X-100 detergent (T9284-100ML, Sigma-Aldrich). Replacement of the 3' most rG in the template switching oligo (TSO) with a locked nucleic acid base (3'LNA). In the experiments comparing unpurified with purified libraries, the purification post reverse transcription was carried using 0.6x AMPure XP beads (A63881, Beckman Coulter). To assess the effect of the unpurified barcoded oligo-dT, the primer was spiked in a final concentration of 0.67 μ M in the PCR master mix.

Single-cell RNA-seq data pre-processing and analysis: DropSeqPipe v0.4 was used for raw data processing [205]. Cutadapt v1.16 was used for trimming [206]. Trimming and filtering were done on both fastq files separately. Reads with a missing pair were discarded using bbmap v38.22. STAR v2.5.3a [207] was used for mapping to annotation release #91 and genome build #38 from *Mus musculus* (Ensembl). Multimapped reads were discarded. Dropseq_tools v1.13 was used for demultiplexing and file manipulation [194]. A whitelist of cells barcodes with minimum distance of 3 bases was used. Cell barcodes and unique molecular identifiers (UMI) with a hamming distance of 1 and 2 respectively were corrected. For the experimental datasets, cells with less than 500 genes and 500 UMIs, number of genes and UMIs higher 3 and 2 times respectively than the median for the library, cells with more than 20% mitochondrial transcripts and more than 50% of transcripts attributed to the top 50 genes were discarded. The subsequent analysis was implemented with Seurat (v 2.3.4) [208]. Gene expression measurements for each cell were column-normalized, multiplied by the scaling factor 10,000 and transformed to log scale. Highly variable genes were detected by estimating the average expression and dispersion of each gene across all cells. Principle component analysis (PCA) was applied for linear dimensional reduction. Top 10 principle components and K=200 were chosen for building K-nearest neighbors graph followed by shared nearest neighbor (SNN) construction [209]. Modularity optimization-based algorithm was applied for cluster identification. T-distributed stochastic neighbor embedding (t-SNE) technique was applied for illustration purpose. Wilcoxon rank-sum test was applied for predicting marker

genes with other default parameters in function FindMarkers. Pheatmap (<https://github.com/raivokolde/pheatmap>) was used for heatmap visualization. Color is encoded by the Z-score of normalized expression values derived from Seurat. Gene set enrichment analysis was performed using clusterProfiler [210] based on the reference datasets downloaded from Molecular Signature Database (MSigDB) V6.2 [211]. The number of splenic P14 or OT-1 T cells predicted to be allocated into each KNN single-cell cluster was calculated by projecting the percentage distribution of the respective cluster over the total number of splenic P14 or OT-1 T cells observed in each animal used for single-cell RNA sequencing.

Bulk population RNA sequencing: The Agencourt RNAdvance Cell v2 kit (A47942, Beckman Coulter) was used for RNA extraction. Following sorting, the cells were spun down, resuspended in lysis buffer supplemented with proteinase K and incubated for 30 minutes at RT. Then cells were snap-frozen on dry ice and stored at -80°C until further processing based on the manufacturer's protocol. The yield and RNA integrity number (RIN) of the RNA isolates were assessed using RNA 6000 Pico Kit (5067-1513, Agilent). Only samples with RIN \geq 8 were used for downstream cDNA synthesis and library preparation. cDNA synthesis and PCR amplification using 1 ng of total RNA from each sample was performed using SMART-Seq v4 Ultra Low Input RNA Kit for Sequencing (634891, Takara/Clontech). After cDNA synthesis, each sample was subjected to 12 cycles of PCR amplification. The concentration of generated amplicons was determined using the Agilent High Sensitivity DNA Kit (5067-4626, Agilent). 150 pg of the resulting amplified cDNA was used for library preparation with the Illumina Nextera XT DNA Library reagents (FC 131-1024, Illumina). After PCR amplification of the fragmented libraries, the samples were purified with (0.6x) Agencourt AMPure XP beads and eluted in 10 μ l of molecular grade water. The quality of the resulting library was assessed using the High Sensitivity DNA Kit (5067-4626, Agilent). The library quantification was performed based on the Illumina recommendations (SY-930-1010, Illumina), with the use of KAPA SYBR FAST qPCR Master Mix (KK4600, Kapa Biosystems). The samples were sequenced on Illumina HiSeq 2500 system

CD4 T cell help sustains distinct subpopulations in functional and dysfunctional CD8 T cell responses.

with rapid run, 100 base pairs single-end read and dual-indexed sequencing resulting in 20 million reads per sample.

Bulk population RNA-seq data analysis: Reads were processed using snakemake pipelines [212] as indicated under (<https://gitlab.lrz.de/ImmunoPhysio/bulkSeqPipe>). Sequencing quality was assessed with FastQC (version 0.11.6; <http://www.bioinformatics.babraham.ac.uk/projects/fastqc>). Filtering was performed using trimmomatic (version 0.36) [213], mapping using STAR (version 2.5.3a) [207] with genome Mus_musculus.GRCm38, counting using htseq (version 0.9.1) [214] with annotation Mus_musculus.GRCm38.91. To supervise STAR and fastqc results multiqc (version 1.2) [215] was used. Genes with a total count <10 were discarded. Differential expression analysis was performed with default parameters using DESeq2 (v 1.24.0) [216]. To compare differential gene expression levels, batch effects were eliminated using the removeBatchEffect function provided by limma (v 3.40.6) [217] in principal component analysis (PCA) [3]. Differences with a Basemean > 50, an absolute log₂ fold change >1 and an adjusted p value <0.05 were considered significant. The ggplot2 (v 3.2.1) [218] was used to generate PCA plots. Heatmaps were generated by pheatmap (v 1.0.12) [219]. Colors are encoded by the Z-score based on log-transformed data obtained from DESeq2 (v 1.24.0) [220].

Data Analyses: Scatter dot plots depict the mean. Statistical analyses were performed with Prism 7.0 (Graphpad Software). Unpaired t tests (two-tailed) was used. P values % 0.05 were considered significant (*p < 0.05; **p < 0.01; ***p <0.001); p values > 0.05 were non-significant (ns).

CD4 T cell help sustains distinct subpopulations in functional and dysfunctional CD8 T cell responses.

Table 1. tDrop-seq and tSCBR-seq primer sequences.

| Primer | Primer full name | Primer sequence | Producer | Purity | Note |
|------------------|--|---|-----------------------------|------------------------------------|---|
| DS-BEADS | ChemGenes Barcoded Oligo dT primer ON Beads | 5'-Bead-Linker--TTTTTTTAAAGCAGTGGTATCAACGCAGATACJJJJJJJJJJJJNNNNNNTTTTTTTTTTTTTTTTTTTTTTTTTTT--3' | ChemGenes Corporation | - | J denotes a nucleic acid part of the cellular barcode, which is identical in all primers attached to one bead; N denotes a random nucleic acid part of the unique molecular identifier, which is a unique sequence in each primer attached to one bead. |
| DS-TSO | Drop-seq Template Switching Oligo | AAGCAGTGGTATCAACGCAGAGTGAATrGrG | Eurogentec | HPLC | rG denotes a riboguanine |
| DS-TSO-LNA | Drop-seq Template Switching Oligo with Locked Nucleic Acid | AAGCAGTGGTATCAACGCAGAGTGAATrGrG+G | Eurogentec | HPLC | rG denotes a riboguanine; +G denotes a locked nucleic acid guanine |
| DS-SMART PCR | Drop-seq SMART PCR Primer | AAGCAGTGGTATCAACGCAGAGT | Integrated DNA Technologies | HPLC | |
| DS-P5 | Drop-seq N5 primer | AATGATACGGGACCACCGAGATCTACACGGCTGTCCGGGGAAGCAGTGGTATCAACGCAGAGT*A'C | Integrated DNA Technologies | HPLC | * denotes a phosphorothioate bond |
| DS-CR1 | Drop-seq Custom Read 1 Primer | GCCTGTCCCGGGAAGCAGTGGTATCAACGCAGAGTAC | Integrated DNA Technologies | HPLC | |
| SCRB-dT plate v1 | tSCRB Barcoded Oligo-dT Primer Plate v1 | /5Biosg/ACACTCTTCCCTACACGACGCTCTCCGATCTJ(6)N(10)T(30)VN | Integrated DNA Technologies | Ultramer Plate; Standard desalting | /5Biosg/ denotes a 5' biotin; J denotes a nucleic acid part of the cellular barcode; N denotes a random nucleic acid part of the unique molecular identifier; V denotes A or C or G |
| SCRB-dT plate v2 | tSCRB Barcoded Oligo-dT Primer Plate v2 and v3 | /5Biosg/ACACTCTTCCCTACACGACGCTCTCCGATCTJ(7)N(9)T(30)VN | Integrated DNA Technologies | Ultramer Plate; Standard desalting | /5Biosg/ denotes a 5' biotin; J denotes a nucleic acid part of the cellular barcode; N denotes a random nucleic acid part of the unique molecular identifier; V denotes A or C or G |
| SCRB-TSO | tSCRB-seq Template Switching Oligo | iC-iG-iCACACTCTTCCCTACACGACGGrGrG | Eurogentec | HPLC | iC denotes a iso-dC; iG denotes a iso-dG; rG denotes a riboguanine |
| SCRB-TSO-LNA | SCRB-seq Template Switching Oligo with Locked Nucleic Acid | iC-iG-iCACACTCTTCCCTACACGACGGrGrG+G | Eurogentec | HPLC | iC denotes a iso-dC; iG denotes a iso-dG; rG denotes a riboguanine; +G denotes a locked nucleic acid guanine |
| SCRB-SMART-PCR | SCRB-seq SMART PCR Primer | /5Biosg/ACACTCTTCCCTACACGACGCGC | Integrated DNA Technologies | HPLC | /5Biosg/ denotes a 5' biotin |
| SMART-P5 | SCRB-seq N5 primer | AATGATACGGGACCACCGAGATCTACACTCTTCCCTACACGACGCTTCCTCCG*A*T*C*T* | Integrated DNA Technologies | HPLC | * denotes a phosphorothioate bond |
| SCRB-CR1 | SCRB-seq Custom Read 1 Primer | TCTTCCCTACACGACGCTCTCCGATCT | Integrated DNA Technologies | HPLC | |

6. Results

6.1. Tailoring the resolution of single-cell RNA sequencing to meet the challenges of primary cytotoxic T cells.

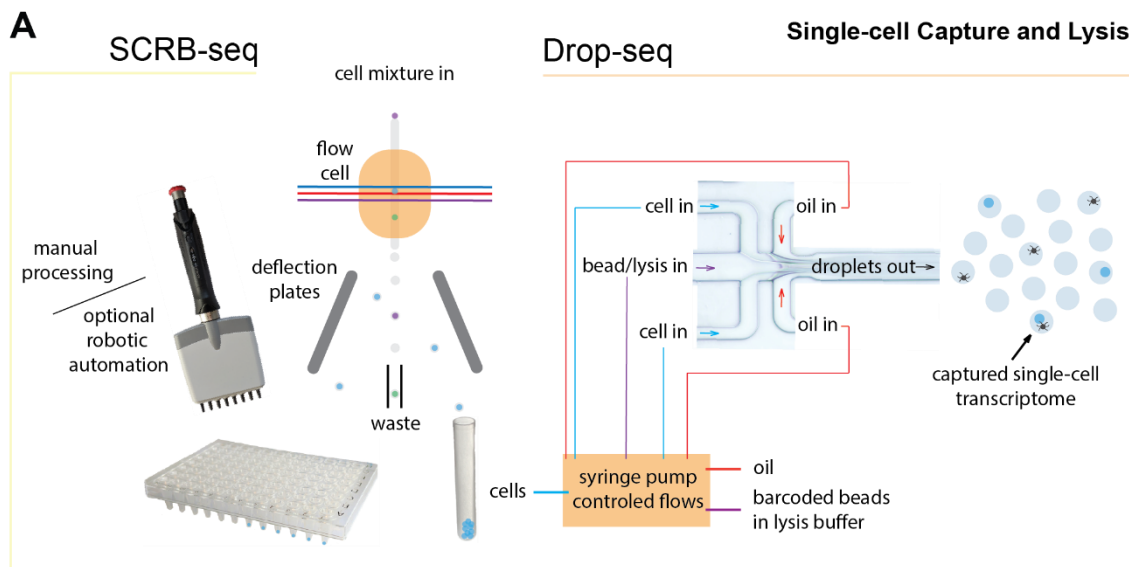


Figure 2. Schematic representation of the workflow of SCRIB-seq and Drop-seq [2].

(A) Illustrates the difference in the single-cell capturing strategy between SCRIB-seq and Drop-seq. While SCRIB-seq relies on sorting single-cells into individual wells of a PCR plate, Drop-seq relies on encapsulating single-cell with uniquely barcoded beads in individual droplets. (B) SCRIB-seq and Drop-seq utilize a common strategy for reverse transcription, cDNA amplification and library preparation. Abbreviations: PCR, polymerase chain reaction; UCI, unique cellular identifier; UMI, unique molecular identifier.

CD4 T cell help sustains distinct subpopulations in functional and dysfunctional CD8 T cell responses.

Primary CD8 T cells are particularly challenging for single-cell transcriptome profiling, as they bear only minute amount of messenger RNA, which critically impacts transcript capturing efficacy. In early 2016, as a starting point in our search for single-cell RNA sequencing solution for profiling of primary CD8 T cells, we used the study by Ziegenhain et al., who performed a comparative analysis of the prominent at that time single-cell RNA sequencing protocols for their strengths and limitations with the use of cultured mouse embryonic stem cells (ESCs) [221]. Out of all protocols tested, we decided to assess the performance of Drop-seq (droplet sequencing) and SCRB-seq (single-cell RNA barcoding and sequencing) for profiling of primary CD8 T cells (**Figure 2A**). Drop-seq appeared to be the most cost-efficient protocol, while SCRB-seq the one with the highest power to detect differentially expressed genes. From methodological perspective, both Drop-seq and SCRB-seq have sacrificed full-length coverage in order to incorporate early in reverse transcription unique cellular identifiers (UCIs) and unique molecular identifiers (UMIs; **Figure 2B**). The advantage of UMI-based over non-UMI-based protocols is that the former effectively eliminate the bias introduced by PCR, thus allowing for absolute quantification of gene expression. In order to assess and later on optimize both protocols for primary CD8 T cells, we used

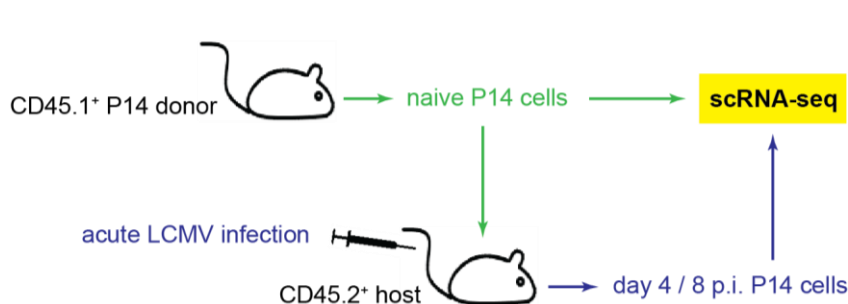


Figure 3. P14 T cell receptor (TCR) transgenic CD8 T cells as a versatile tool to assess various aspects of single-cell RNA sequencing protocol performance [2].

Naïve P14 CD8 T cells are isolated from CD45.1+ donor. They are either sequenced or transferred in CD45.2+ C57BL/6 host mice, followed by infection with LCMV Armstrong. The antigen experienced P14 CD8 T cells are isolated on day 4 or 8 post infection and subjected to single-cell RNA sequencing. Abbreviations: scRNA-seq, single-cell RNA sequencing; LCMV, lymphocytic choriomeningitis virus.

naïve or recovered from the active phase of an acute infection P14 TCR-transgenic CD8 T cells (**Figure 3**). Before encountering their cognate epitope, the unstimulated P14 T cells are biologically and transcriptionally homogeneous, a state useful to assess the technical performance between the two

protocols and their modification. When stimulated with their cognate antigen upon acute LCMV infection, the P14 T cells develop a polyfunctional effector phenotype, a state useful to assess the detection efficacy for key immune genes necessary for T cell function among the protocols and their optimizations. Thus, the P14 infection model represents a multifaceted tool for assessing various performance aspects of the different single-cell RNA sequencing techniques.

6.1.1. Drop-seq has low mRNA capturing efficacy for primary CD8 T cells and modifications of its chemistry only moderately improve sensitivity.

Drop-seq is a microdroplet technique which relies on encapsulating single-cells with uniquely barcoded beads into tiny droplets, which represent aqueous compartments formed by precisely combining aqueous and oil flows into a microfluidic device (**Figure 2A**) [194]. The aim is to have no more than one cell and one barcoded bead into one droplet in order to maintain single-cell resolution. We verified that the basic Drop-seq protocol published by Macosko et al. is correctly set up in our laboratory by performing the recommended mixing experiment with the use of primary human and mouse lymphocytes. We were able to successfully distinguish mouse from human lymphocytes, where the doublet rate indicating droplets which contained both mouse and human cell was zero (**Figure 4A**). Thus, at this bead and cell concentrations the single-cell resolution of Drop-seq was comparable to protocols based on single-cell sorting into individual wells of a PCR plate (e.g. SCR-seq), where the cell doublets are eliminated by the gating strategy. To assess the sensitivity of the basic Drop-seq protocol, we generated single-cell transcriptomes from naïve P14 T cells. Each single-cell was characterized with a median of 1607 genes and 2235 transcripts (UMIs), resulting with an average of 1.4 capture transcripts per gene (**Figure 4B**). Next, we sought to improve the mRNA capturing by modifying cell lysis and mRNA hybridization conditions. Three of the modifications modestly improved the mRNA capturing efficacy as indicated by the increased UMIs/gene ratio - 1) replacing the originally used for lysis Sarkosyl detergent with 0.1% Igepal CA-630; 2) supplementing the lysis buffer with 0.5

CD4 T cell help sustains distinct subpopulations in functional and dysfunctional CD8 T cell responses.

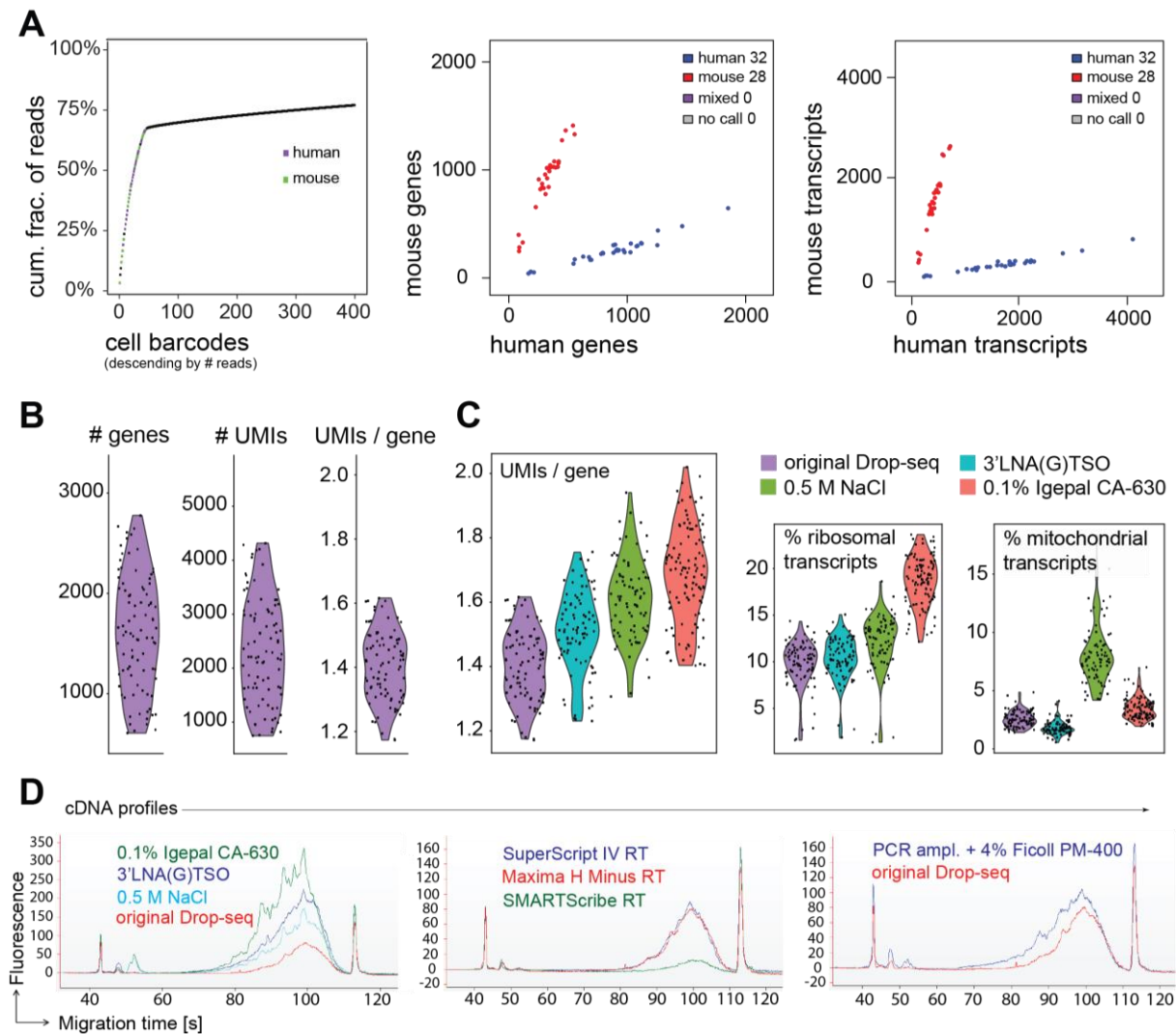


Figure 4. Modifying the chemistry of Drop-seq moderately increases its sensitivity for primary CD8 T cells [2].

(A) Analysis of Drop-seq generated single-cell transcriptomes from human and mouse lymphocytes. The knee plot represents the cumulative fraction of reads attributed to real cell and empty barcodes. (B and C) Analysis of Drop-seq generated single-cell transcriptomes from naïve P14 T cells. Each dot represents individual cell. (B) Number of detected genes, transcripts (UMIs – unique molecular identifiers) and transcripts per gene by the basic Drop-seq protocol (also referred in the text and figures as “original”). (C) Selected chemical modification improving the Drop-seq sensitivity. The indicated percentage of ribosomal and mitochondrial transcripts are out of total transcripts per cell. (D) Bioanalyzer electropherograms comparing the amplified cDNA yield between the basic and modified versions of Drop-seq. Abbreviations: cum. frac., cumulative fraction; #, number; UMI, unique molecular identifier.

M NaCl for increased hybridization; 3) replacing the 3' most rG in the template

switching oligo (TSO) with a locked nucleic acid base (3'LNA) to stabilize the TSO-cDNA dimer (**Figure 4C**). A gene was detected on average with 1.5 (use of Igepal CA-630), 1.6 (NaCl supplementation) and 1.7 (use of 3'LNA TSO) transcripts. This gain of transcripts was also accompanied by increased cDNA yields following PCR amplification (**Figure 4D**). Additionally, we tested three different reverse transcriptases (RTs) and PCR amplification in presence of 4% Ficoll PM-400 as a macromolecular crowding agent. From the three reverse transcriptases tested, Maxima H Minus RT (ThermoFisher) and SuperScript IV RT (ThermoFisher) performed similarly well in terms of cDNA yield following PCA amplification (**Figure 4D**). Supplementing the PCR amplification mix with Ficoll PM-400 also increased the cDNA yield (**Figure 4D**). Thus, we adopted a T cell tailored Drop-seq protocol (tDrop-seq) incorporating all above mentioned successful modification (Igepal CA-630; increased NaCl; 3'LNA TSO; Maxima H Minus RT and Ficoll PM-400).

6.1.2. SCBR-seq is an optimization flexible solution for profiling of primary CD8 T cells.

SCRB-seq is a plate-based protocol for single-cell RNA sequencing [204]. This protocol uses FACS (fluorescent-activated cell sorting) to sort single-cells into individual wells of a PCR plate (**Figure 2A**). In order to set up the basic SCBR-seq protocol published by Soumillon et al., we sorted naïve P14 CD8 T cells and attempted to generate cDNA. We failed to detect successful amplification using Bioanalyzer (**Figure 5A**), which we attributed to the low mRNA content of primary T cells combined with the use of silica-based spin columns for post reverse transcription pooling of the barcoded single-cell transcriptomes. Additionally, we considered that the thermal inactivation of Proteinase K might be insufficient, therefore this could affect the performance of the reverse transcriptase. Thus, we introduced a step of RNA purification before reverse transcription with the use of 2.2x Agencourt RNAClean XP magnetic beads (Beckman Coulter) and a step of purification after reverse transcription with the use of 0.6x Agencourt AMPure XP beads (Beckman Coulter). Although this strategy yielded cDNA, we noticed that a significant amount of captured and reverse transcribed mRNA molecules is lost during the second purification step (**Figure 5B**

CD4 T cell help sustains distinct subpopulations in functional and dysfunctional CD8 T cell responses.

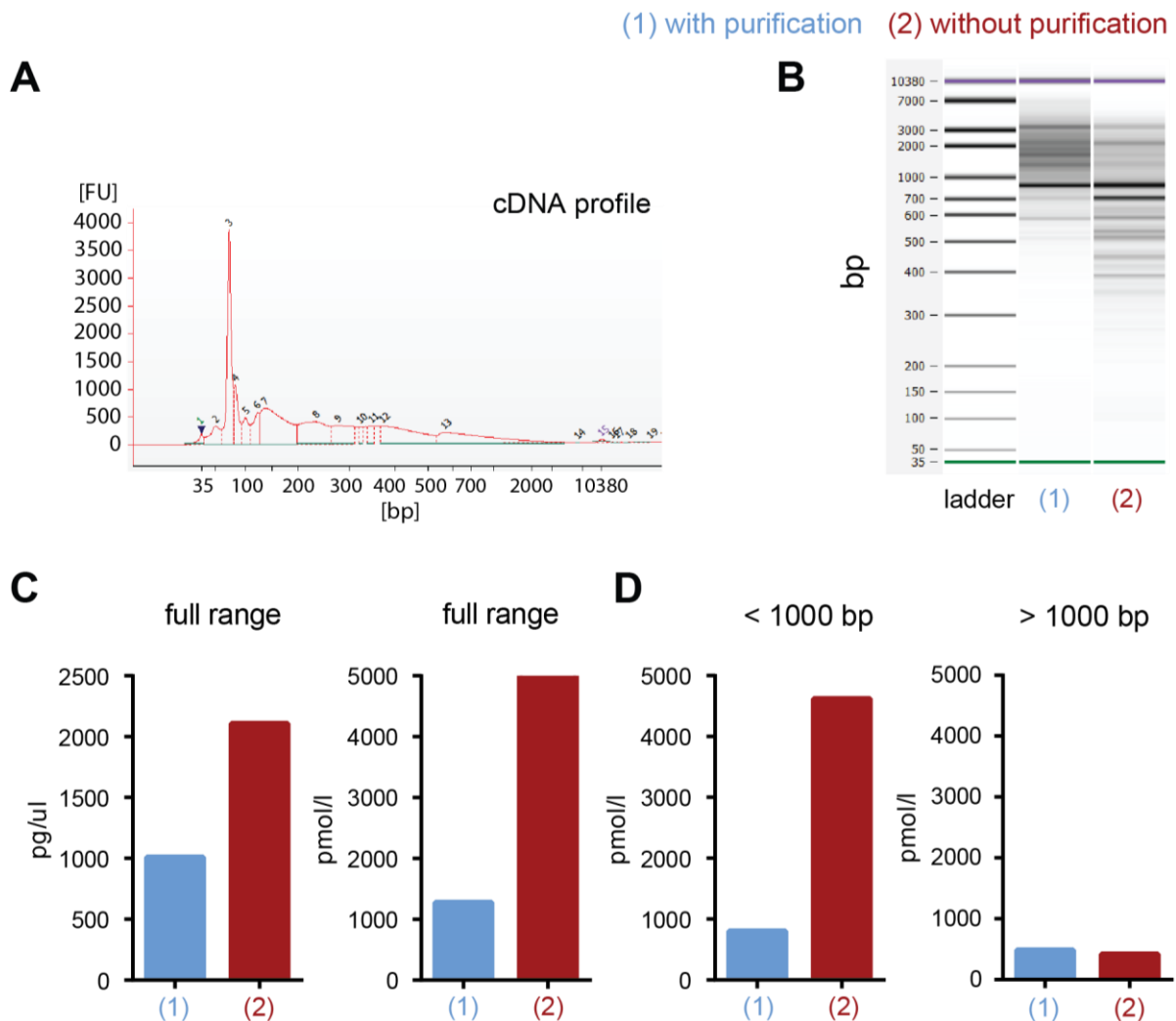


Figure 5. A purification step post-reverse transcription preferentially recovers long fragments, while transcripts smaller than 1000 bp are selectively lost [2].

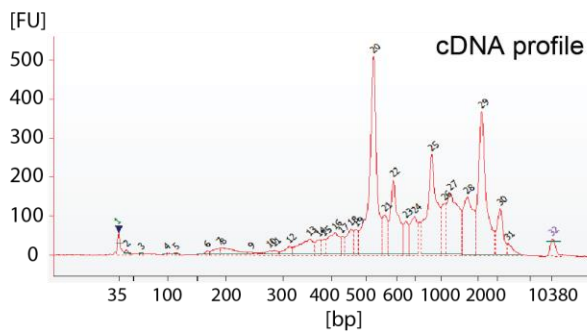
(A) Bioanalyzer electropherogram of the amplified cDNA profile of naïve P14 T cells processed with the basic SCRB-seq protocol (also referred in the text and the figures as “original”). (B-D) Bioanalyzer-based comparative analysis of the cDNA profiles of P14 T cells recovered from the early phase of acute LCMV Armstrong infection. (B) Gel-like image depicting cDNA size-distribution between the two protocols. (C) Plots depicting cDNA yield between the two protocols (D) Plots depicting cDNA yield of transcripts longer or shorter than 1000 bp between the two protocols. Abbreviations: FU, fluorescence; bp, base pairs.

and C). Moreover, as the bead-based purification preferentially recovers longer fragments, those smaller than 1000 bp were preferentially lost (Figure 5D). Their molar concentration declined 5-fold. In order to safeguard the breadth of captured transcripts,

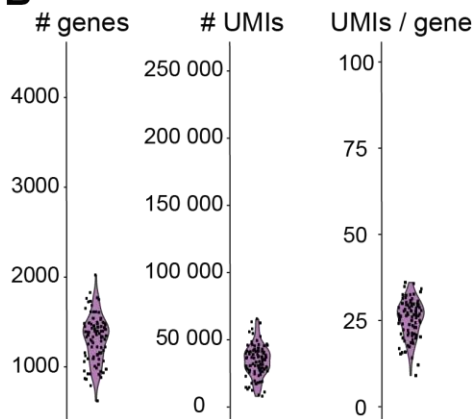
CD4 T cell help sustains distinct subpopulations in functional and dysfunctional CD8 T cell responses.

we decided to proceed directly to cDNA amplification without purification in the following experiments (**Figure 6A**). After library preparation and sequencing, SCRB-seq detected higher number of transcripts per gene in comparison to Drop-seq (**Figure 6B and 4B**). As introducing a step of RNA purification before reverse transcription

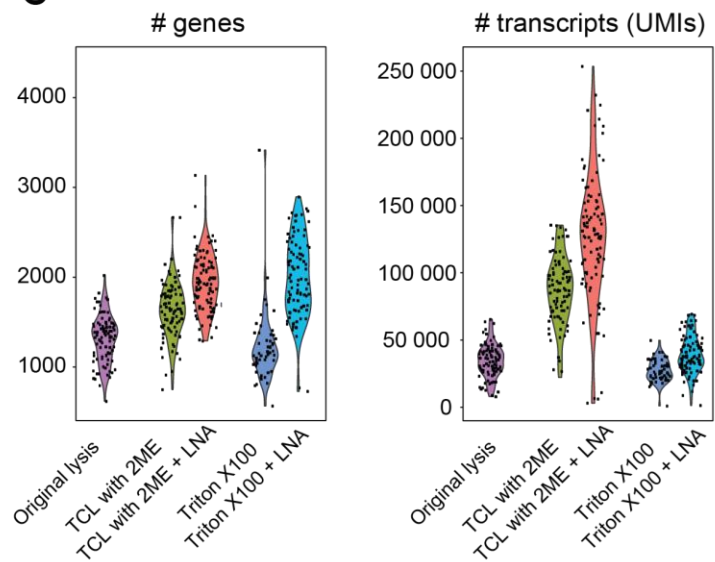
A



B



C



D

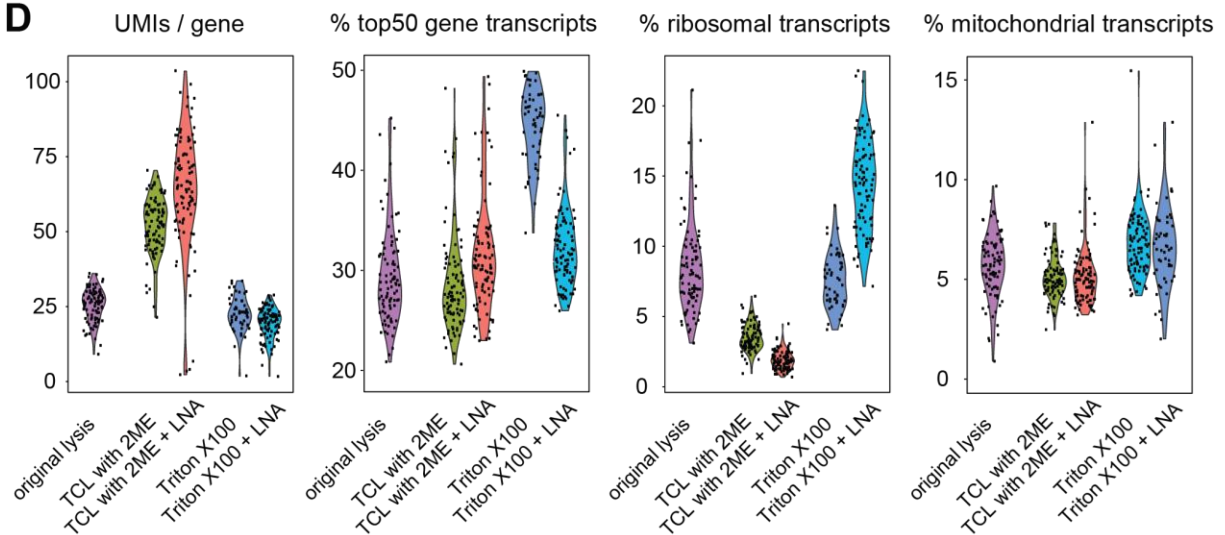


Figure 6. SCBR-seq is an optimization flexible solution for profiling of primary CD8 T cells [2].

(A-D) Analysis of SCRB-seq generated single-cell transcriptomes from naïve P14 T cells. (A) Bioanalyzer electropherogram of the amplified cDNA profile of a modified SCRB-seq version utilizing bead-based RNA purification before reverse transcription. (B-D) Each dot represents individual cell. (B) Single-cell transcriptomes generated with the bead-based SCRB-seq version. (C and D) Selected chemical modifications additionally improving the sensitivity of the bead-based SCRB-seq protocol. The indicated percentage of top50 gene, ribosomal and mitochondrial transcripts are out of total transcripts per cell. Abbreviations: #, number; UMI, unique molecular identifier.

allows for the use of harsher lysis condition, we decided to explore this opportunity. Thus, we exchanged the originally used milder lysis composition (1:500 dilution of Phusion HF buffer supplemented with Proteinase K) with a more stringent one containing either 0.2% Triton X-100 detergent or TCL buffer (Qiagen) supplemented with 1% β -mercaptoethanol. Out of the three lysis conditions tested, the use of Qiagen TCL buffer supplemented with 1% β -mercaptoethanol displayed the highest mRNA capturing efficacy, which was further increased when 3'LNA template switching oligo was used (**Figure 6C**). This led to increased UMIs/gene ratio, as well as decreased reads coming from non-informative ribosomal transcripts (**Figure 6D**). Thus, we adopted a T cell tailored SCRB-seq protocol (tSCRB-seq) incorporating all above mentioned successful modification (magnetic bead-based purification of RNA before RT; TCL buffer supplemented 1% β -mercaptoethanol and 3'LNA TSO). Due to improved performance, we selected tSCBR-seq over tDrop-seq for our subsequent studies on T cell biology, namely **the mechanism of teriflunomide-independence of the early memory-like CD8 T cell subpopulations formed in acute infection (Section 6.2) and the role of CD4 help for the progenitors and their progeny in functional versus exhausted CD8 T cell responses (Section 6.3).**

In 2021, following the generation of the single-cell data presented in section 6.2 and 6.3, we became aware that omitting the purification step before PCR amplification in order to preserve short transcripts could come at the expense of reducing the precision of the unique molecular identifier (UMI)-based enumeration of captured transcripts. This can arise as unpurified barcoded oligo-dT primer is still present during the PCR amplifications step. Although we ensured that the concentration of all reverse

CD4 T cell help sustains distinct subpopulations in functional and dysfunctional CD8 T cell responses.

(1) with purification (2) without purification
(3) with purification + oligo-dT primer

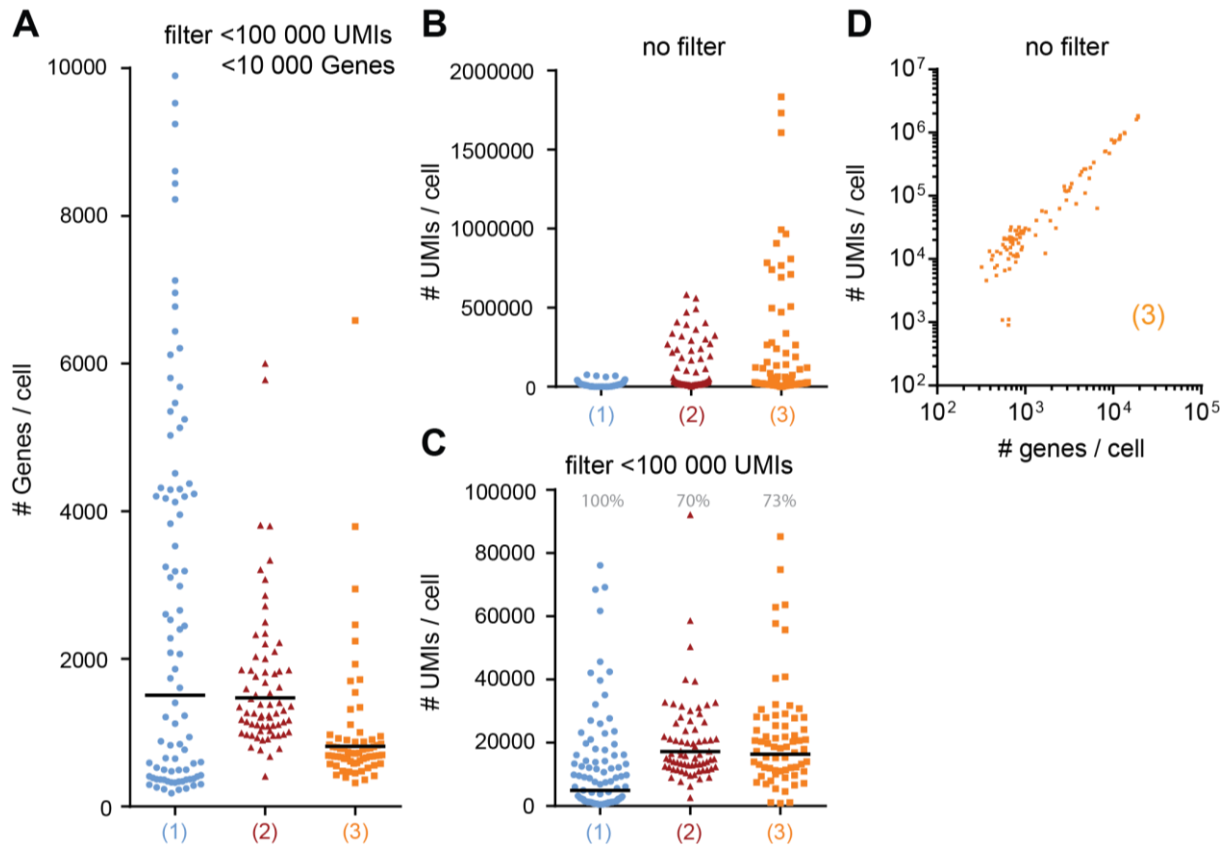


Figure 7. Omitting the purification step post reverse transcription preserves transcripts at the cost of certain degree of UMI inflation.

Comparative analysis of single-cell P14 T cell transcriptomes obtained in the acute phase of LCMV Armstrong infection. Three consecutively sorted plates of P14 T cells from the same animal were used. The libraries were generated using tSCBR-seq with purification (blue), without purification (red) and with purification plus spiking in the same amount of oligo-dT primer in the PCR master mix found in the unpurified sample (orange). The dots in all plots represent single-cells, while the horizontal lines the geometric mean. (A) Number of detected genes per cell among the three protocols after filtering for cells with no more than 100 000 UMIs and 10 000 genes. The gene filter is applied to display the effect of the protocols on the main body of cells. (B) Number of detected UMIs per cell among the three protocols before quality control filtering. (C) Number of detected UMIs per cell among the three protocols after filtering for cells with no more than 100 000 UMIs. The percentage represents the portion of retained cells. Abbreviations: #, number; UMI, unique molecular identifier.

transcription components is 3.5-fold diluted in the transition to PCR amplification, the

CD4 T cell help sustains distinct subpopulations in functional and dysfunctional CD8 T cell responses.

residual oligo-dT primer can still act as an alternative PCR primer and potentially introduce new UMIs, a phenomenon referred to as UMI inflation. Therefore, we performed series of test aimed at assessing both the gain in sensitivity versus the level

P14 cells recovered on day 8 post acute infection

| GENE | tDROP-seq | tSCRB-seq | 10xChrom. (Chen et al.) |
|-----------------------------|------------|------------|----------------------------|
| Gzma | 87% | 95% | 42% |
| Gzmb | 81% | 89% | 90% |
| Prf1 | 55% | 64% | 11% |
| Fasl | 12% | 10% | 21% |
| Klrg1 | 67% | 56% | 55% |
| Id2 | 80% | 76% | 95% |
| Tbx21 | 38% | 56% | 47% |
| Klf2 | 72% | 85% | 43% |
| Klf3 | 46% | 70% | 54% |
| S1pr1 | 38% | 41% | 58% |
| S1pr4 | 40% | 53% | 92% |
| S1pr5 | 37% | 42% | 21% |
| | | | |
| Tcf7 | 10% | 9% | 24% |
| Slamf6 | 14% | 12% | 45% |
| Ii7r | 9% | 6% | 10% |
| Eomes | 23% | 6% | 22% |
| Id3 | 0% | 1% | 5% |
| Bcl2 | 7% | 9% | 29% |
| | | | |
| Mki67 | 61% | 31% | 13% |
| Ezh2 | 35% | 38% | 29% |
| | | | |
| Cumulative detection | 41% | 42% | 40% |

Table 4. Fraction of cell positive for selected key immune genes among methods [2].

Analysis of libraries generated with tDrop-seq and tSCRB-seq from P14 T cells recovered on day 8 post-acute LCMV Armstrong infection, compared to a published 10xChromium dataset with matching experimental setup [5]. Comparison of the fraction of cell detected to express key immune genes among three methods.

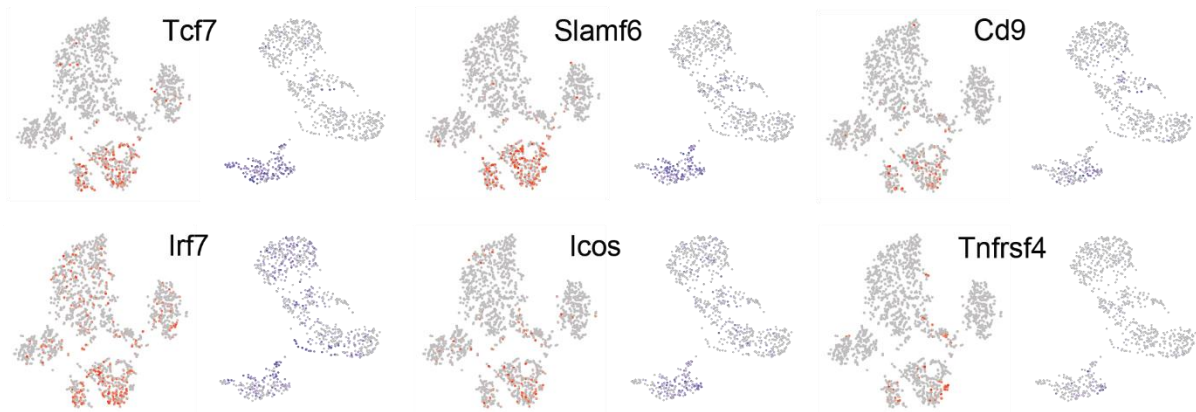
of new UMI incorporation in absence of a purification step before reverse transcription. For this purpose, we prepared libraries with purification, without purification and with purification plus spiking in the same amount of oligo-dT primer found in the non-purified samples. We observed that when the purification step was omitted, in result of transcript rescue, the minimum number of genes detected per cell was significantly increased in comparison to the purified sample (**Figure 7A**). This difference was not well described by the geometric mean, as the purification increased the data spread of the number of detected genes per cell. Alongside increased sensitivity, the absence of a purification step resulted in increased UMI counts caused by the residual oligo-dT primer (**Figure 7B**). Similar effect was

CD4 T cell help sustains distinct subpopulations in functional and dysfunctional CD8 T cell responses.

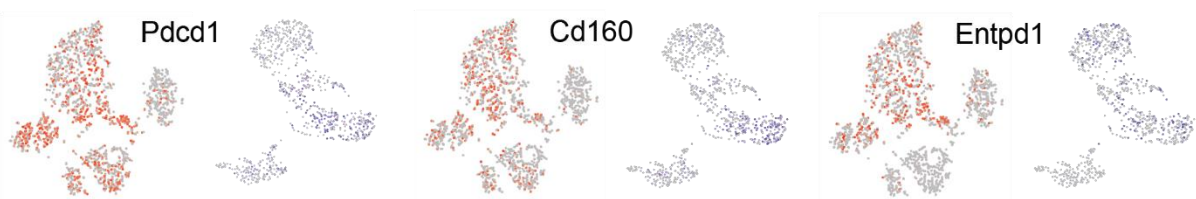
observed, when the oligo-dT primer was spiked in the PCR master mix following purification. Thus, the oligo-dT primer can indeed act as an alternative PCR primer. Next, we used loose filtering criteria to select cells having no more than 100 000 UMIs (stricter filtering criteria was used in the original analysis, were cell with more than 2-fold the median number of UMIs were excluded). After filtering, we observed that the presence of the barcoded oligo-dT primer during PCR amplification increased the UMI

tSCRB-seq 10xChromium

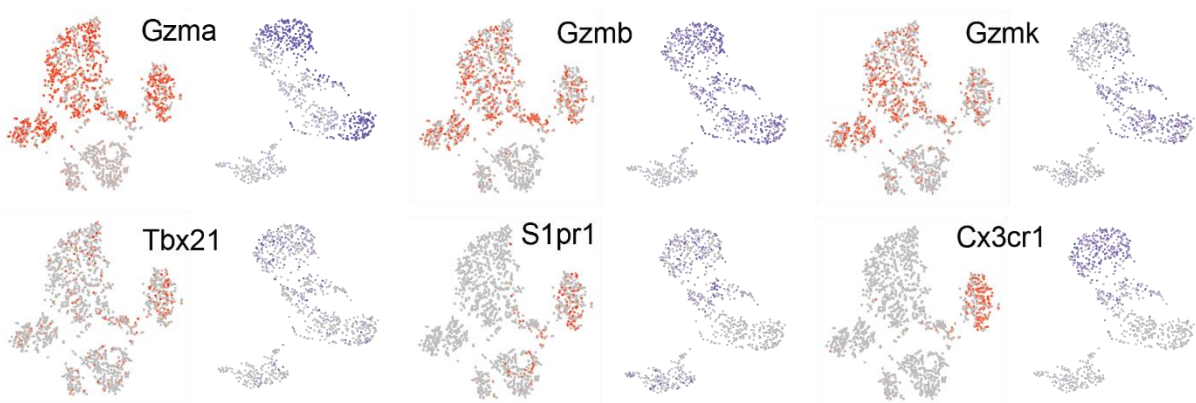
Progenitor markers



Exhaustion markers



Effector markers



CD4 T cell help sustains distinct subpopulations in functional and dysfunctional CD8 T cell responses.

Figure 8. In chronic infection, tSCRB-seq identifies T cell subpopulations and their gene markers in consensus with 10xChromium.

Comparative analysis of single-cell P14 T cell transcriptomes generated with tSCRB-seq[3] or 10xChromium[4] and recovered from established LCMV clone-13 infections (on day 40 and day 30 respectively). Each circle represents a single-cell. The plots represent the expression of key for CD8 T cell differentiation and function immune genes and regulatory receptors depicted over tSNE. The expression level is illustrated using the red scale in plots based on the tSCRB-seq data and violet scale in plots using the 10xChromium data.

count in the majority of cells about 2 to 3-folds (**Figure 7C**). Nevertheless, the number of UMIs detected per cells always correlated linearly with the number of genes detected per cells (**Figure 7D**). Next, we questioned how significant is this *de novo* UMI incorporation for data structure and results. Therefore, we compared the tSCRB-seq generated data with published 10xGenomics datasets with identical experimental set up. Firstly, tSCRB-seq and 10xChromium displayed equivalent cumulative detection of key immune genes in cells recovered on day 8 post-acute LCMV infection (**Table 4**). The differences in detection of individual genes between tSCRB-seq and 10xChromium was caused by interlaboratory variation. This is supported by the detection consensus between tSCRB-seq and tDrop-seq (includes purification before PCR amplification), both performed in our laboratory. Secondly, both tSCRB-seq and 10xChromium resolved key T cell subpopulations and their specific gene markers four weeks post-chronic LCMV infection in consensus (**Figure 8**). We concluded that while our method preserves unique transcripts resulting in the detection of more genes, the absence of a purification causes a certain degree of *de novo* UMI incorporation. Judged in the context of 18 to 20 cycles of PCR amplification, this 2 to 3-fold increase in UMI counts is still a rare event. Nevertheless, more efficiently amplified transcripts might potentially have slightly higher *de novo* UMI incorporation than less efficiently amplified sequences. This could potentially impact the quantitative assessment among different genes in the same cell (not used in any of analysis included in this thesis), but not between the same gene among different cells as it would be similarly scaled (at the basis of cluster and biomarker identification; both used for the analysis presented in this work). The unaffected clustering and marker gene expression are further

CD4 T cell help sustains distinct subpopulations in functional and dysfunctional CD8 T cell responses.

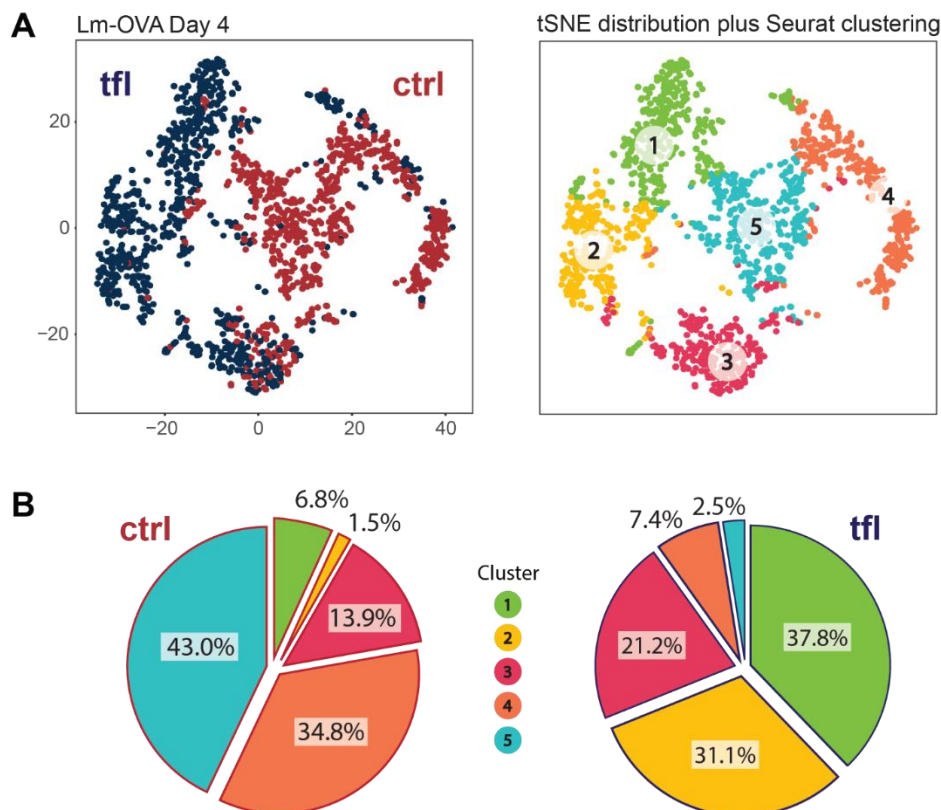
demonstrated by the fact, that tSCBR-seq identifies the T cell subpopulations found in our chronic dataset in consensus with a published 10xChromium dataset.

6.2. Higher DHODH expression and general capacity for *de novo* biosynthesis of pyrimidine nucleotides as a potential mechanism of leflunomide resistance in early memory-committed cells.

CD8 T cell differentiation and function requires tight regulation, the disruption of which is often associated failed protection or immunopathology. Therefore, developing strategies for dealing with these conditions is of utmost importance. Recently, we got interested in the mechanism of action of the prodrug leflunomide (bio-transformed to its active form teriflunomide), which since 1998 is routinely used for the treatment of rheumatoid arthritis (RA) due to its potent anti-inflammatory and immunosuppressive activity [222]. Leflunomide suppresses T cell proliferation via reverse inhibition of DHODH, an enzyme with a key role in the pathway for *de novo* biosynthesis of pyrimidine nucleotides [223, 224]. In a work performed by Stefanie Sarah Scherer, we observed that leflunomide selectively impacts the formation of terminally differentiated effector cells (KLRG^{hi}CD127^{lo}), but not the formation of memory-like progenitors (KLRG^{lo}CD127^{hi}; **Supplementary Figure 1B** – Appendix, page 105). Moreover, leflunomide did not affect the formation of memory in terms of numbers (**Supplementary Figure 1A**) and phenotype (**Supplementary Figure 1C**). Interestingly, leflunomide acts early following T cell activation, as its later application (after day 4 post infection) does not affect the development of a differentiated effector compartment. Taking into account that leflunomide was reported to suppress T cell proliferation via inhibition of DHODH, we hypothesized a differential requirement for the pathway for *de novo* biosynthesis of pyrimidine nucleotides between effector and progenitor T cells early following T cell activation. We considered that effector T cells which are subjected to more intense proliferation than progenitors would require higher amounts of pyrimidine nucleotides, which would render them more sensitive to DHODH inhibition. Major challenges in addressing this hypothesis is the limited knowledge and the lack of suitable markers to identify effector-like and memory-like subpopulations formed during early T cell expansion. Therefore, we addressed this question with the use of single-cell RNA sequencing.

6.2.1. DHODH inhibition prevents the formation of subpopulations with effector but not memory-like signature as early as day 4 post infection.

We generated a dataset of about 1700 single-cell OT-1 T cell transcriptomes recovered on day 4 post Lm-OVA infection, one half of which from control and one from teriflunomide treated hosts. After quality control, we jointly projected the single-cell transcriptomes from control and teriflunomide treated OT-1 T cells using tSNE (**Figure 9A**). In this way, we were able to visualize the shared or unique subpopulations between the two conditions. We used Seurat to predict clusters based on the euclidean distance in PCA space (cell color), which we visualized over the tSNE distribution. We identified 5 clusters in total, with differential enrichment for control and treated OT-1 T cells (**Figure 9B**). Based on their gene expression signatures, we assigned cluster 2 and 3 as memory-like and cluster 4 and 5 as effector-like (**Figure 10A and B**).



CD4 T cell help sustains distinct subpopulations in functional and dysfunctional CD8 T cell responses.

Figure 9. scRNA-seq of control and teriflunomide treated OT-1 cells recovered on day 4 post Lm-OVA infection.

Single-cell RNA sequencing analysis of OT-1 T cells recovered on day 4 post infection with recombinant OVA-expressing *Listeria monocytogenes* (Lm-OVA) from control (carboxymethylcellulose) and treated hosts (teriflunomide). Each condition is represented by cells from three individual mice. **(A)** Each circle represents a single-cell. Left plot, tSNE distribution of control and treated OT-1 T cells. Right plot, Seurat clustering (cell colour) overlaid on the tSNE cell distribution (cell location). **(B)** Cluster distribution of control and treated OT-1 T cells. Abbreviations: ctrl, control; tfl, teriflunomide; tSNE, t-distributed stochastic neighbor embedding.

Interestingly, cluster 1 expressed genes associated with both memory (expression of *Tcf7*, *Slamf6*, *Bcl2*, *Id3* and *Ccr7*) and effector (expression of *Id2* and *Gzmb*) T cell differentiation. Most importantly, teriflunomide treatment selectively inhibited the formation of the effector-like clusters 5 and 4, which size was reduced 182- and 50-fold respectively (**Figure 10C**). The treatment had only a modest effect over the size of the memory-like clusters, with cluster 3 undergoing 7-fold decline in size.

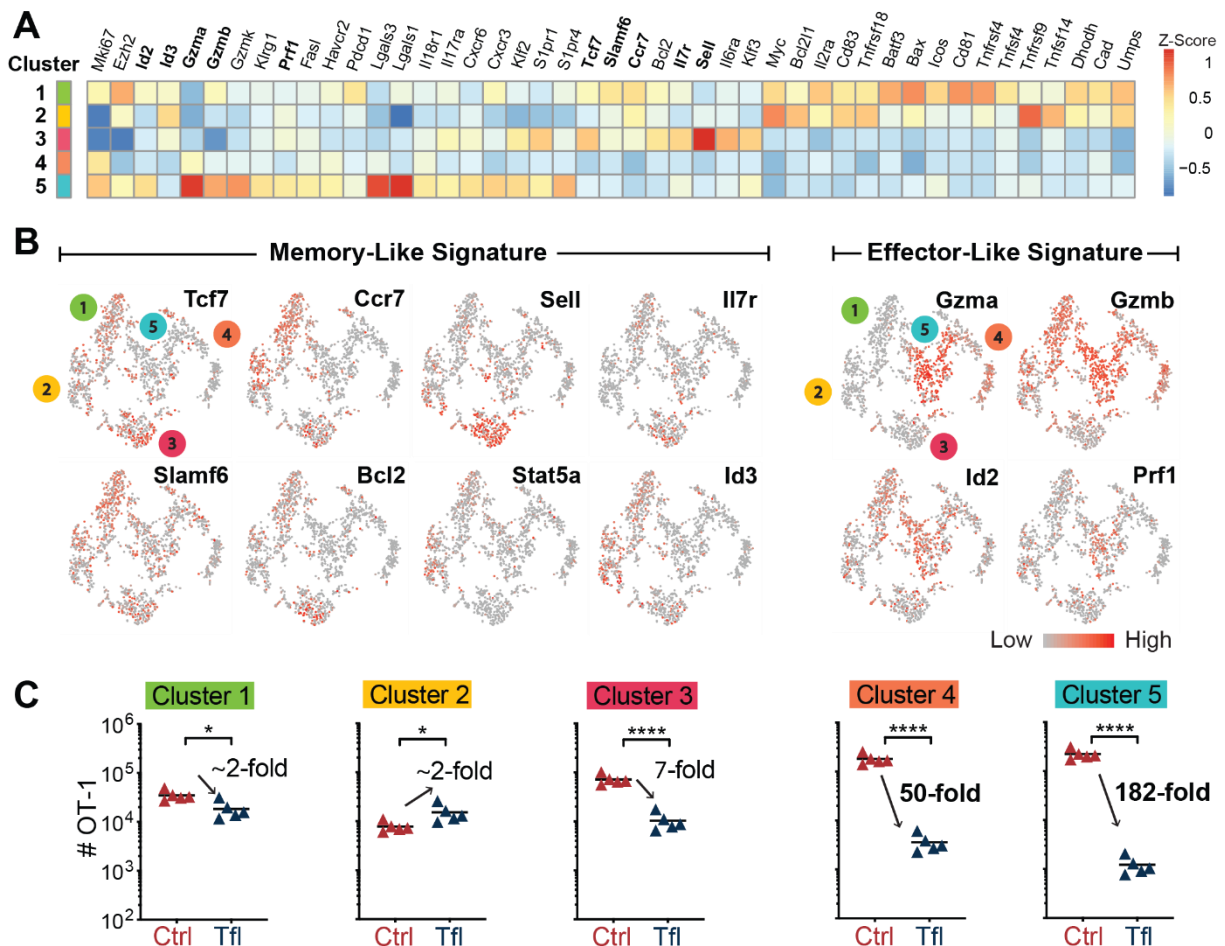


Figure 10. Teriflunomide prevents the formation of subpopulations with effector but not memory-like signature as early as day 4 post infection.

Single-cell RNA sequencing analysis of OT-1 T cells recovered on day 4 post infection with recombinant OVA-expressing *Listeria monocytogenes* (Lm-OVA) from control (carboxymethylcellulose) and treated hosts (teriflunomide). Each condition is represented by cells from three individual mice. **(A)** Heatmap depicting the differential expression of key immune genes among the predicted clusters. **(B)** tSNE plots with overlaid expression of selected genes involved in memory or effector CD8 differentiation and function. Each circle represents a single-cell. **(C)** Scatter plots with calculated absolute numbers of splenic OT-1 from control and Teriflunomide treated mice corresponding to each of the identified clusters. The calculation is based on the percentage wise representation of each cluster among total OT-1 as explained in the methods section. Symbols in data plots represent individual mice, small horizontal lines indicate the mean. *** $p < 0.001$; ** $p < 0.01$; * $p < 0.05$ based on unpaired t test. Abbreviations: ctrl, control; tfl, teriflunomide.

6.2.2. The teriflunomide-resistant memory-like clusters are marked by higher expression of DHODH and general capacity for *de novo* biosynthesis of pyrimidine nucleotides than their effector counterpart.

We noticed that the teriflunomide-resistant cluster 1 and 2 displayed significantly increased expression of *Myc* (**Figure 11A and B**), a key transcriptional regulator of metabolic reprogramming following T cell activation [225]. Moreover, the elevated expression of *Myc* resulted in enrichment for *Myc*-regulated gene networks in those clusters (**Figure 11C**). Therefore, we hypothesized that the teriflunomide-resistance observed in the shared signature cluster 1 and memory-like cluster 2 could be a result from a *Myc*-induced metabolic reprogramming, rather than just lower proliferation turnover in comparison to the effector-like clusters. In support of this notion is the fact that both the leflunomide-resistant shared signature cluster 1 and the leflunomide-sensitive effector-like clusters 5 display similarly high expression of *Mki67* (the gene coding *Ki67*, a nuclear protein associated with cellular proliferation) and enrichment for DNA replication and cell proliferation (**Figure 12A and B**). Interestingly, we observed that in both teriflunomide-resistant clusters (1 and 2), the increased *Myc* expression coincided with increased *DHODH* expression (**Figure 12A**). Moreover, both cluster 1 and 2 displayed a general enrichment for genes involved in the pathway

CD4 T cell help sustains distinct subpopulations in functional and dysfunctional CD8 T cell responses.

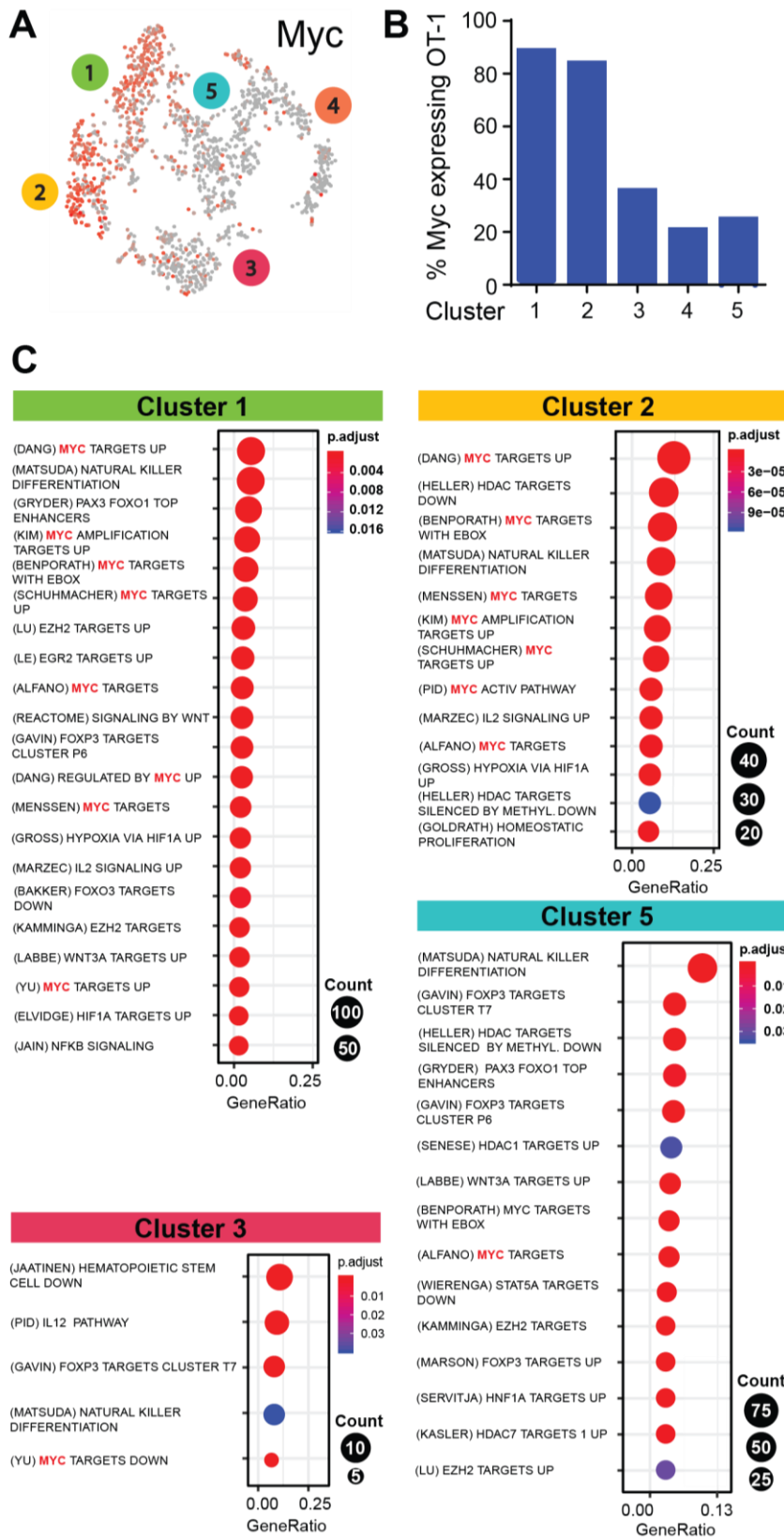


Figure 11. Transcriptional factor Myc and its networks are highly enriched in leflunomide-resistant subpopulations.

Single-cell RNA sequencing analysis of OT-1 T cells recovered on day 4 post infection with recombinant OVA-expressing *Listeria monocytogenes* (Lm-OVA) form control (carboxymethylcellulose) and treated hosts (teriflunomide). Each condition is represented by cells from three individual mice. (A) tSNE plot with overlaid expression of Myc. Each dot represents a cell. (B) Bar graph showing the percent of cells expressing Myc in each predicted cluster. (C) Cluster-resolved gene set enrichment analysis (GSEA).

for *de novo* biosynthesis of pyrimidine nucleotides (Figure 12C). Therefore, we concluded that the teriflunomide-resistance of the shared signature cluster 1 and memory-like cluster 2 is likely a

result of their higher spare capacity to produce pyrimidine nucleotides. Conversely, the

CD4 T cell help sustains distinct subpopulations in functional and dysfunctional CD8 T cell responses.

observed pronounced teriflunomide-sensitivity of the effector-like cluster 4 and 5 could be a consequence of their lower DHODH expression levels.

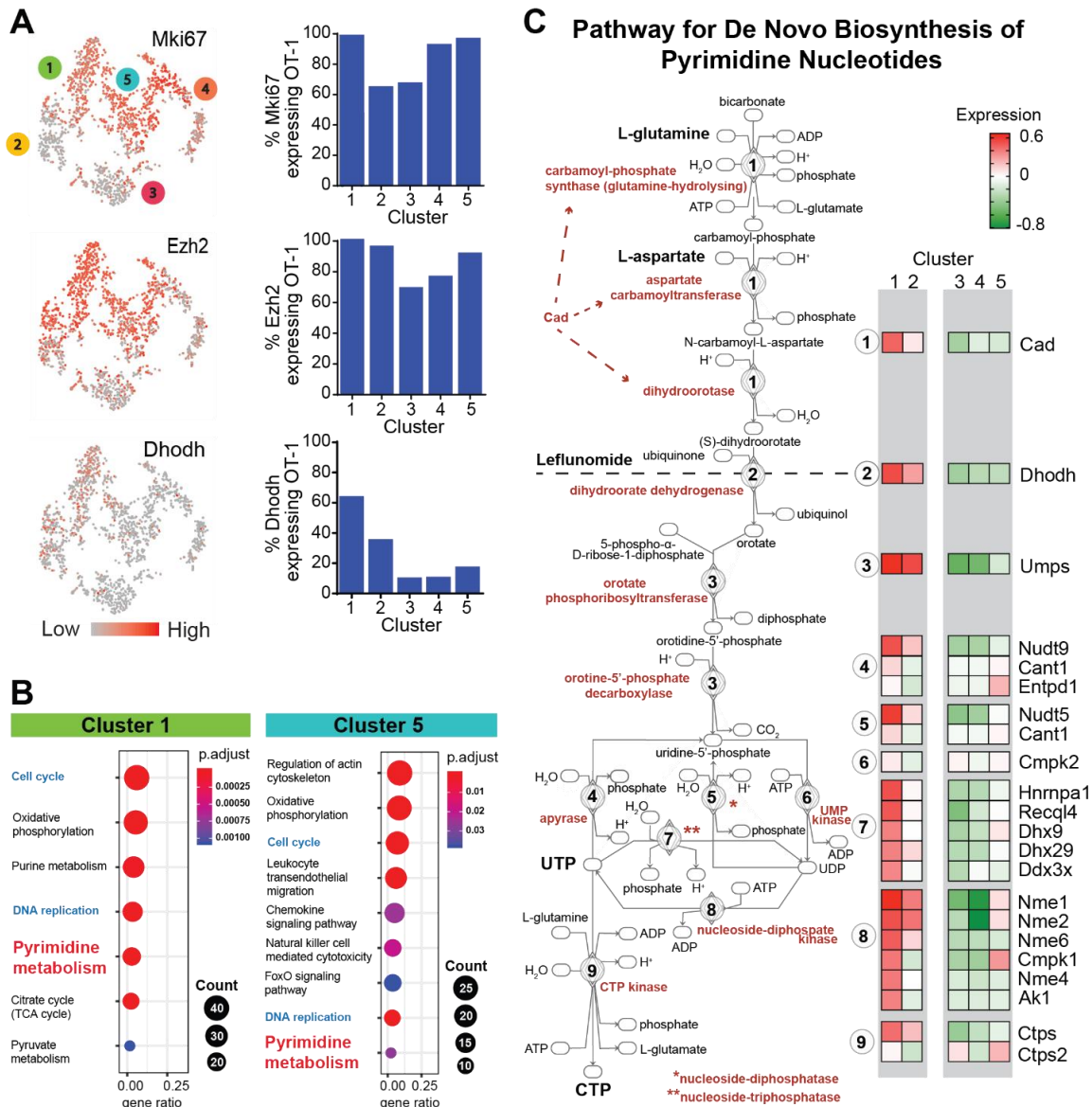


Figure 12. The teriflunomide-resistant memory-like clusters are marked by higher expression of DHODH and general capacity for *de novo* biosynthesis of pyrimidine nucleotides.

Single-cell RNA sequencing analysis of OT-1 T cells recovered on day 4 post infection with recombinant OVA-expressing *Listeria monocytogenes* (Lm-OVA) from control (carboxymethylcellulose) and treated hosts (teriflunomide). Each condition is represented by cells from three individual mice. (A) tSNE plots with overlaid expression of Mki67, Ezh2 and Dhodh. Bar graphs showing the percent of cells expressing Mki67, Ezh2 and Dhodh in each predicted cluster. (B) Cluster-resolved gene set enrichment analysis (GSEA) for metabolic processes. (C) Cluster-resolved expression analysis of genes involved in the *de novo* biosynthesis of pyrimidine ribonucleotides.

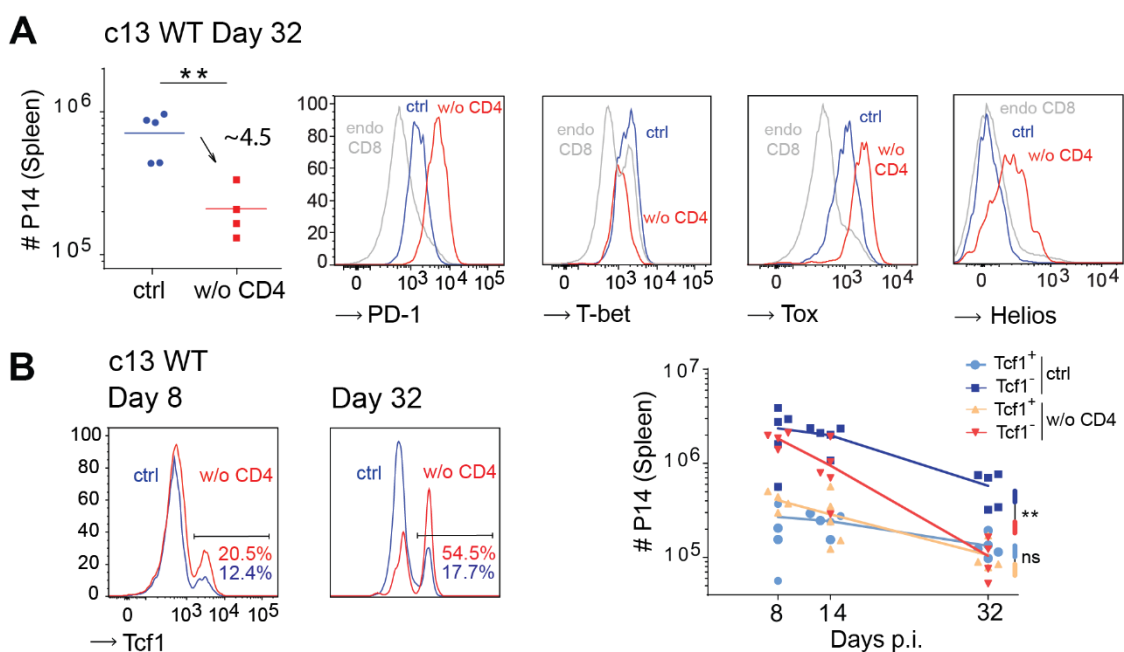
CD4 T cell help sustains distinct subpopulations in functional and dysfunctional CD8 T cell responses.

6.3. Terminally differentiated but not proliferation competent CD8 T cells require CD4 help in chronic infection.

As discussed in the introduction, the absence of cognate CD4 help in chronic infection is associated with progressive functional and numerical decline of the antigen-specific CD8 T cell response as well as decreased viral control, the reasons for which are still unclear. In this part of the study, we investigate the role of CD4 help in the formation and maintenance of the Tcf1⁺ progenitors and their Tcf1⁻ effector progeny. The Tcf1⁺ stem-like progenitors in chronic infection share features with the Tcf1⁺ progenitors in acute infection, which participate in the formation of the memory pool following infection resolution. Given the critical role of CD4 help for the generation of long-lasting and functional memory in acute infection, we hypothesized that absence of CD4 help in chronic infection initially affects the maintenance and function of the progenitors, which later translates in reduced output of newly generated terminally differentiated effector cells and ultimately response erosion.

Absence of CD4 help leads to selective loss of Tcf1⁻ but not Tcf1⁺ P14 T cells with dysfunctional phenotype in chronic infection.

To explore how CD4 help affects the transition and survival of the Tcf1⁺ progenitors and their terminally differentiated Tcf1⁻ effector progeny, we transferred

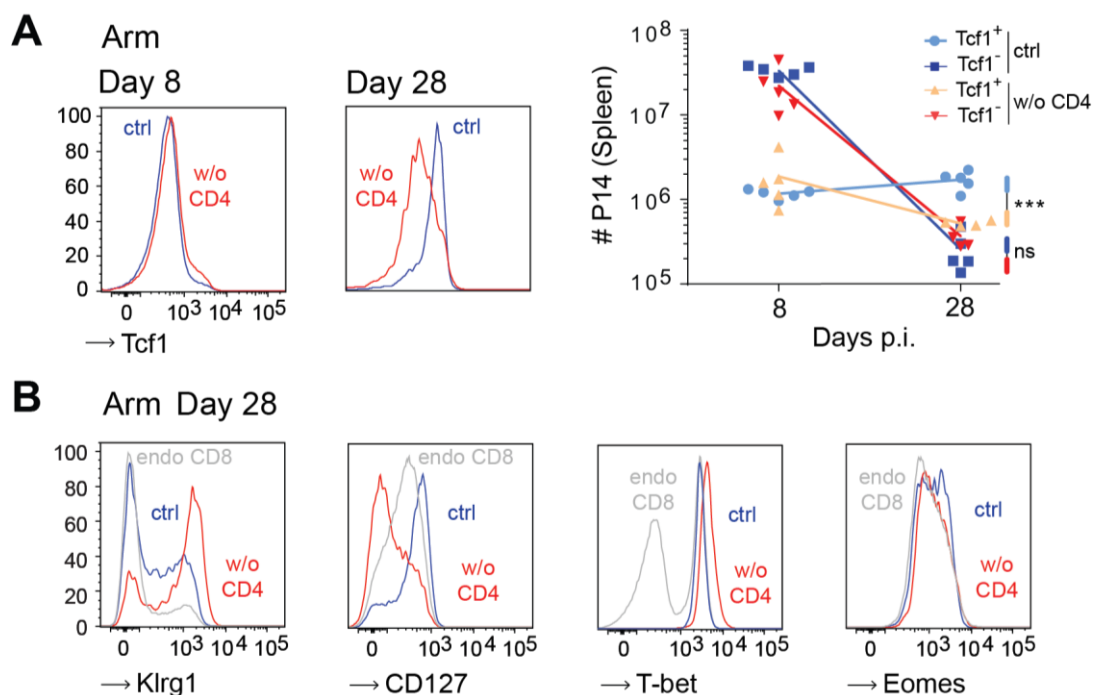


CD4 T cell help sustains distinct subpopulations in functional and dysfunctional CD8 T cell responses.

Figure 13. Absence of CD4 help leads to selective loss of Tcf1⁻ but not Tcf1⁺ P14 T cells with dysfunctional phenotype in chronic infection [3].

C57BL/6 mice (CD45.2⁺) were engrafted with transgenic gp33-specific P14 T cells (CD45.1⁺) prior to infection with LCMV c13 WT. CD4 depletion was performed as described in materials and methods. **(A and B)** Representative CD8⁺CD45.1⁺ gated flow cytometry plots and corresponding data graphs are shown. **(A)** P14 T cell numbers in spleens were determined 4 weeks after infection and stained for the indicated markers. **(B)** The numbers of P14 Tcf1⁺ and Tcf1⁻ cells in spleens were determined 8 days, 14 days and 4 weeks after infection. Symbols in data plots represent individual mice, small horizontal lines indicate the mean. ***p < 0.001; **p < 0.01; *p < 0.05 based on unpaired t test. Abbreviations: ctrl, control; w/o CD4, CD4 depleted; endo CD8, endogenous CD8 T cells; #, number.

transgenic P14 T cells in control and CD4 depleted hosts followed by LCMV c13 WT infection. As anticipated, the absence of CD4 help resulted in pronounced numerical reduction and aggravated P14 T cell exhaustion at 4 weeks post infection (**Figure 13A**). Contrary to our initial hypothesis, the absence of CD4 help did not affect the maintenance of the Tcf1⁺ progenitors over time (**Figure 13B**), but only caused selective numerical decline of their terminally differentiated Tcf1⁻ progeny. This was observed as early as 14 days post infection, but it was more pronounced at later time points. Of note, the absence of CD4 help in acute infection led to pronounced decline in the Tcf1⁺ memory compartment (**Figure 14A and B**). Next, we hypothesized that



CD4 T cell help sustains distinct subpopulations in functional and dysfunctional CD8 T cell responses.

Figure 14. In contrast to dysfunctional responses, the maintenance of the Tcf1+ progenitors following an acute infection strictly requires CD4 presence [3].

C57BL/6 mice (CD45.2+) were engrafted with transgenic gp33-specific P14 T cells (CD45.1+) prior to infection with LCMV Armstrong. CD4 depletion was performed as described in materials and methods. Representative CD8+CD45.1+ gated flow cytometry plots and corresponding data graphs are shown. (A) The numbers of P14 Tcf1+ and Tcf1- cells in spleens were determined 8 days and 28 days post infection. (B) Staining for selected effector and memory T cell markers. Symbols in data plots represent individual mice. ***p < 0.001; **p < 0.01; *p < 0.05 based on unpaired t test. Abbreviations: ctrl, control; w/o CD4, CD4 depleted; endo CD8, endogenous CD8T cells; #, number.

the differential requirement for CD4 help between the progenitors formed in chronic infection and those formed in acute infection might be a result of alternative differentiation programs. In support of this idea is the recent discovery that the transcription factor TOX directs the transcriptional and epigenetic reprogramming of the progenitors of exhausted T cell responses in chronic infection and cancer, an alteration which is later transferred to their exhausted progeny [177-181]. This or

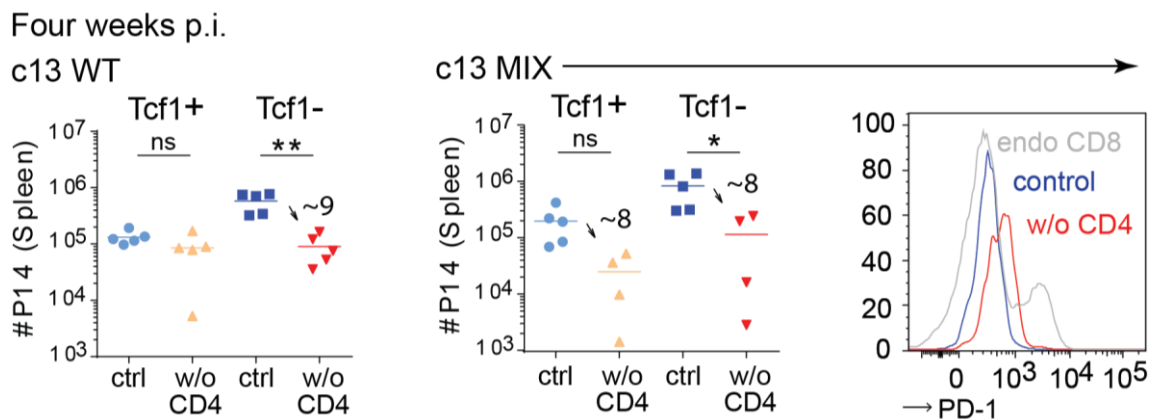


Figure 15. In contrast to dysfunctional responses, the acute-like progenitors formed in LCMV c13 MIX infection show similar to memory cells help dependence [3].

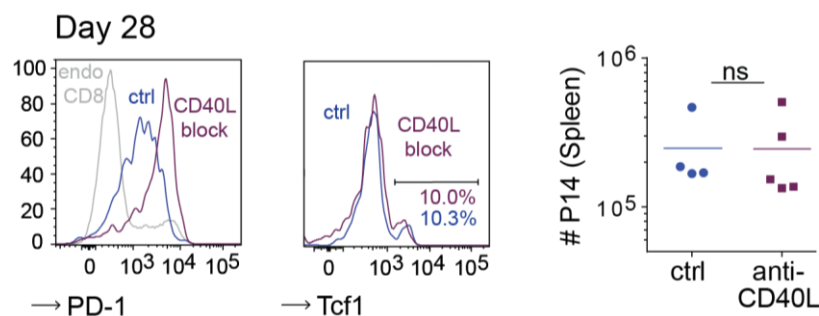
C57BL/6 mice (CD45.2+) were engrafted with transgenic gp33-specific P14 T cells (CD45.1+) prior to infection with LCMV c13 WT or c13 MIX. CD4 depletion was performed as described in materials and methods. The numbers of P14 Tcf1+ and Tcf1- cells in spleens were determined 4 weeks after infection. Representative CD8+CD45.1+ gated PD-1 expression is shown. Symbols in data plots represent individual mice, small horizontal lines indicate the mean. ***p < 0.001; **p < 0.01; *p < 0.05 based on unpaired t test. Abbreviations: p.i., post infection; ctrl, control; w/o CD4, CD4 depleted; endo CD8, endogenous CD8 T cells; #, number.

CD4 T cell help sustains distinct subpopulations in functional and dysfunctional CD8 T cell responses.

similar mechanisms could render the progenitors of exhausted T cell response independent of CD4 help. To address this hypothesis, we took advantage of a well-established clone-13-based experimental system, in which wild-type clone-13 virus is mixed with a mutant version bearing a point mutation in the gp33 peptide, making it incompetent to bind H-2Db [156]. In result, the endogenous gp33-specific CD8 T cells and the TCR transgenic P14 T cells are exposed to reduced amount of antigen, which prevents their exhaustion. As the total viral load is the same, the clone-13 MIX infection is as chronic as the clone-13 pure infection. Moreover, as only the presentation of the gp33-epitope is affected in the MIX infection model, all CD8 T cells with other antigen-specificities remain unaffected. Similar to acute infection and in contrast to clone-13 PURE infection, the maintenance of the progenitors formed in clone-13 MIX infection was clearly CD4 help dependent (**Figure 15**). The absence of CD4 help reduced the size of the progenitor population with 8-fold. Therefore, we concluded that the CD4 help independence of the progenitors only applies to dysfunctional CD8 T cell population, but not to CD8 T cells with non-dysfunctional phenotype in otherwise chronic infection.

Absence of CD40 ligation only partially explains the phenotype observed upon CD4 depletion.

Next, as CD40L-CD40 signaling is known as the one of the main mechanisms of CD4 help provision to CD8 T cells [45], we tested whether employing CD40L blockade would recapitulate the phenotype observed upon CD4 depletion in chronic infection. Interestingly, blocking CD40L-CD40 signaling increased PD-1 expression to levels similar to the observed upon CD4 depletion, but did not affect the CD8 T cell



CD4 T cell help sustains distinct subpopulations in functional and dysfunctional CD8 T cell responses.

Figure 16. Absence of CD40L-CD40 signaling in chronic infection exacerbates exhaustion, but does not cause numerical decline in the terminally differentiated effector compartment [3].

C57BL/6 mice (CD45.2+) were engrafted with transgenic gp33-specific P14 T cells (CD45.1+) prior to infection with LCMV c13 WT. CD40L blockade was performed as described in materials and methods. Representative CD8+CD45.1+ gated flow cytometry plots and corresponding data graphs are shown. P14 T cell numbers in spleens were determined 28 days post infection. Symbols in data plots represent individual mice, small horizontal lines indicate the mean. *** $p < 0.001$; ** $p < 0.01$; * $p < 0.05$ based on unpaired t test. Abbreviations: ns, not significant ($p > 0.05$) based unpaired t test; ctrl, control; CD40L block, CD40L blockade; endo CD8, endogenous CD8 T cells; #, number.

response numerically (**Figure 16**). Thus, absence of CD40L-CD40 signaling only partially explains the observed phenotype.

Absence of CD4 help leads to a major subset distribution shift in the terminally differentiated effector compartment.

We considered that the help provided to the terminally differentiated CD8 T cell effector compartment by CD4 T cells could be either direct or indirect via the progenitors. In the latter case, we reasoned that despite being maintained at comparable numbers, the progenitors' phenotype could be altered resulting in impaired ability to produce newly generated effector cells. To address this question, as well as to define the range of CD8 T cell effector states in presence and absence of CD4 help, we employed single-cell RNA sequencing. We generated a dataset of about 1700 single-cell P14 T cell transcriptomes recovered on day 40 post clone-13 WT infection, one half of which from control and one from CD4 depleted hosts. After quality control, we jointly projected the single-cell transcriptomes from control and unhelped P14 T cells using tSNE (**Figure 17A**). In this way, we were able to visualize the shared or unique subpopulations between the two conditions (**Figure 17B**). We used Seurat to predict clusters based on the euclidean distance in PCA space (cell color), which we visualized over the tSNE distribution (**Figure 17A**). We identified 5 clusters in total, four of which represented subset of differentiated effector cells as indicated by the expression of effector molecules such as *Gzma*, *Gzmb*, *Gzmk* and *Fasl*. In contrast, cluster 1 expressed *Tcf7* (the gene coding *Tcf1*) and represented the less differentiated progenitor compartment shared between the conditions. We found that control P14 T

CD4 T cell help sustains distinct subpopulations in functional and dysfunctional CD8 T cell responses.

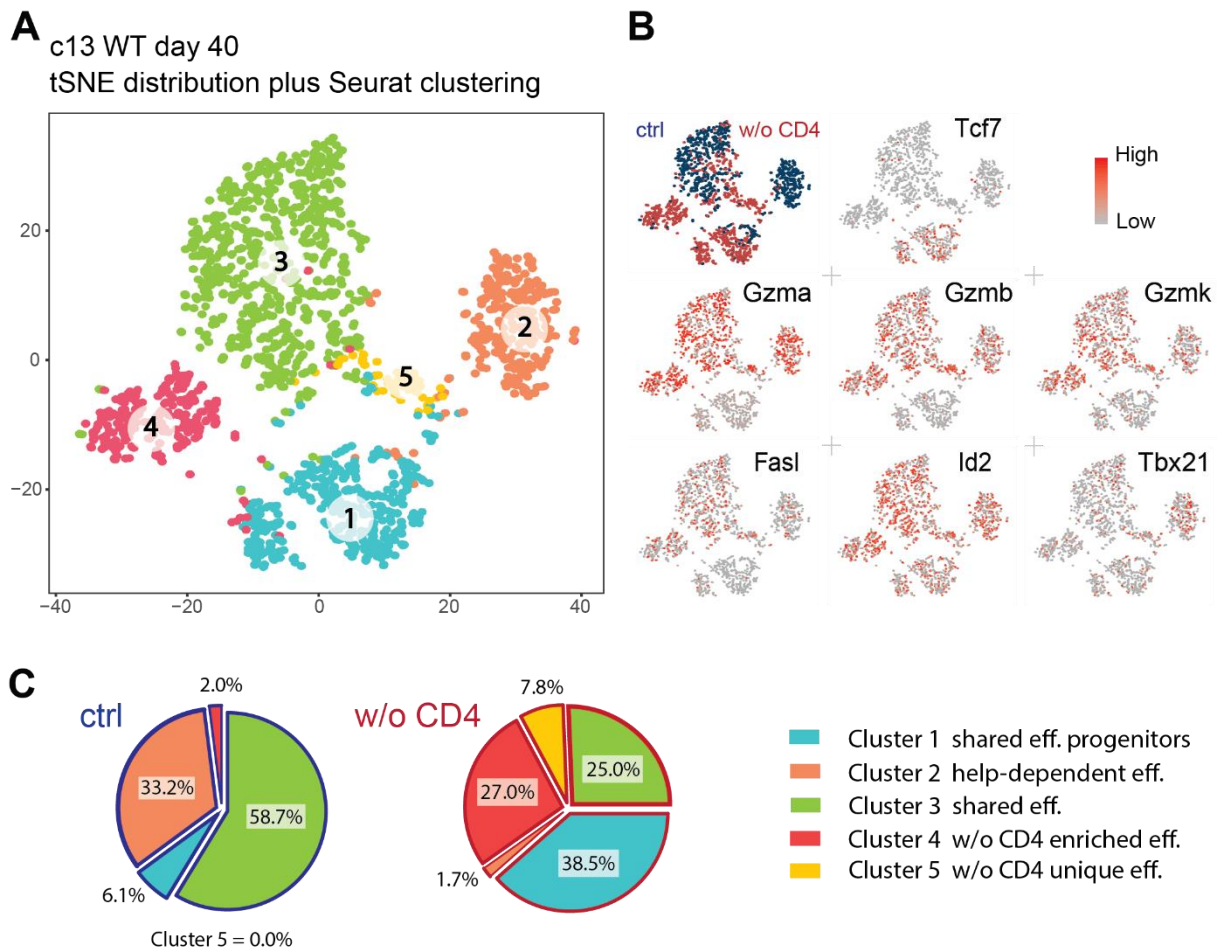


Figure 17. Absence of CD4 help leads to a major subset distribution shift in the terminally differentiated effector compartment [3].

Single-cell RNA sequencing analysis of P14 T cells recovered on day 40 post LCMV c13 WT infection from control and CD4 depleted hosts. Each condition is represented by cells from three individual mice. **(A and B)** Each circle represents a single-cell. **(A)** Seurat clustering (cell colour) overlaid on the tSNE cell distribution (cell location). **(B)** tSNE distribution of control and unhelped P14 cells. tSNE plots with overlaid expression of key genes involved in CD8 T cell function and differentiation. **(C)** Cluster distribution of control and unhelped P14 cells. Abbreviations: ctrl, control; w/o CD4, CD4 depleted; eff., effector; tSNE, t-distributed stochastic neighbor embedding.

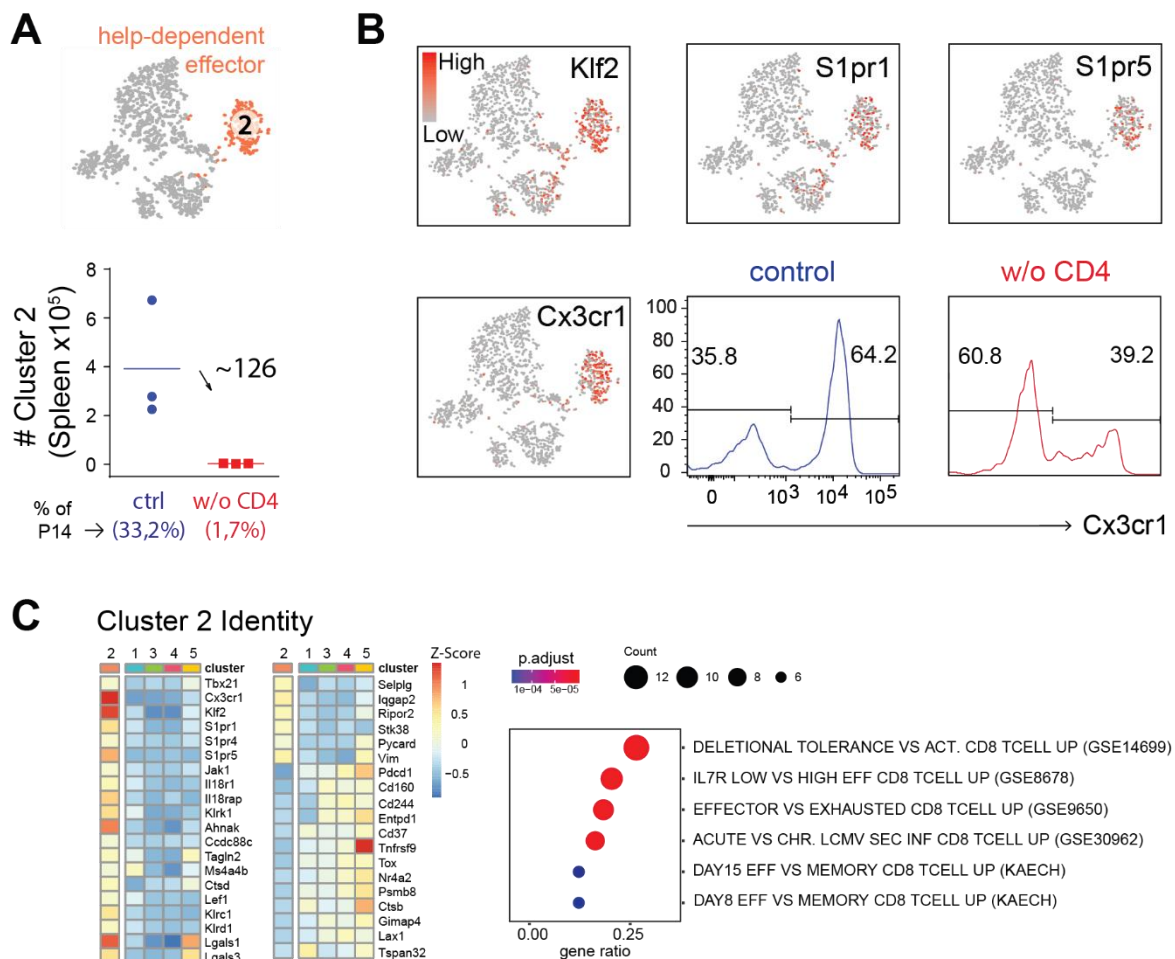
cells preferentially distributed in terminally differentiated effector clusters 2 and 3, while unhelped P14 T cells in clusters 3, 4 and 5 (**Figure 17C**). Therefore, we assigned cluster 2 as help-dependent effector, 3 as shared effector, 4 and 5 as preferentially enriched and unique in absence of CD4 help. It is important to note that the higher percentage-wise representation of unhelped P14 T cells in the progenitor cluster 1 is

CD4 T cell help sustains distinct subpopulations in functional and dysfunctional CD8 T cell responses.

a result of the reduced number of terminally differentiated effector cells in absence of CD4 help, leading to increased sampling of progenitor cells. In fact, the absolute numbers of Tcf1+ progenitors per mouse remained unchanged (**Figure 13B and 20B**). Based on these observations, we concluded that the absence of CD4 help triggers a major shift in the percentage wise representation of cells in the differentiated effector compartment. Moreover, the general capacity to form cells from all clusters found in control animals was not affected.

Cx3cr1+ T cells with pronounced effector phenotype and without apparent signature of exhaustion are mainly affected by absence of CD4 help.

The help dependent effector cluster 2 comprising 1/3 of all P14s found in control animals, showed the most dramatic 126-fold decline in size in absence of CD4 help (**Figure 18A**). Interestingly, this cluster was associated with unique expression of a set of migration associated molecules among which Cx3cr1, S1pr1 and S1pr5



CD4 T cell help sustains distinct subpopulations in functional and dysfunctional CD8 T cell responses.

Figure 18. Cx3cr1+ T cells with pronounced effector phenotype and without apparent signature of exhaustion are mainly affected by absence of CD4 help [3].

Single-cell RNA sequencing analysis of P14 T cells recovered on day 40 post LCMV c13 WT infection from control and CD4 depleted hosts. Each condition is represented by cells from three individual mice. **(A)** Upper plot, Seurat predicted cluster 2 highlighted in tSNE. Lower scatter plot, calculated absolute numbers of splenic P14 cells in control and CD4 depleted animals that are similar to the cells in cluster 2. The calculation is based on the percentage wise representation of cluster 2 among total P14 T cells as explained in the methods section, each symbol in the plot represent individual mouse and the bar the mean. **(B)** tSNE plots, gene expression of key and unique cluster 2 genes. Histograms, P14 T cells were isolated from control or CD4 depleted C57BL/6 host mice 5 weeks post infection and stained for Cx3cr1. Representative CD8+CD45.1+ gated flow cytometry histograms are shown, numbers indicate the fraction of cells with the specified expression intensity. **(C)** Differential gene expression analysis (DGEA) and gene set enrichment analysis (GSEA) of cluster 2. Abbreviations: ctrl, control; w/o CD4, CD4 depleted; #, number.

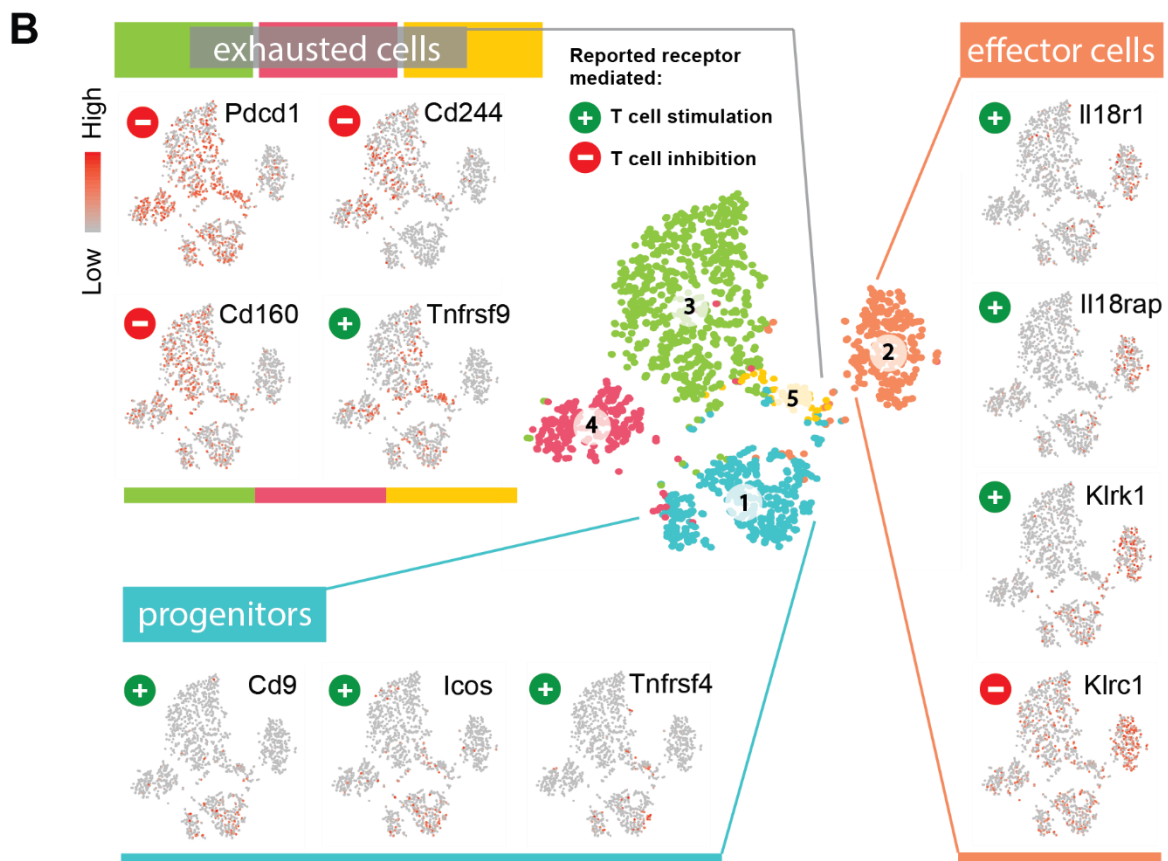
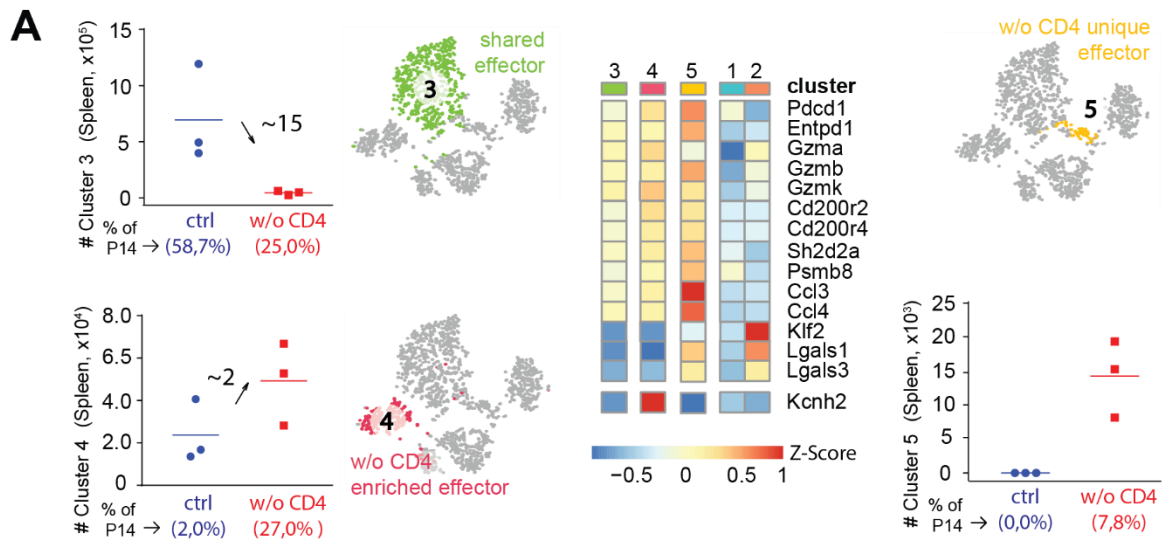
(Figure 18B). S1pr1 which expression is controlled by the zinc-finger transcription factor Klf2 (also upregulated in this cluster), promotes lymphocyte egress from the lymphoid organs [226, 227]. Increased expression of Cx3cr1 correlates with cytotoxic function and decreased inhibitory receptor expression in tumor models [228]. Moreover, differential gene expression (DGEA) and gene set enrichment analysis (GSEA) suggested a superior effector phenotype of this cluster **(Figure 18C)**. It is marked by increased expression of Tbx21 (the gene coding T-bet) and decreased expression of exhaustion-associated molecules such as Pdcd1, Cd160 and Cd244. Taking into account the phenotypic profile, we concluded that the main consequence in absence of cognate CD4 help is the loss of the phenotypically non-exhausted Cx3cr1+ effector subpopulation.

Absence of CD4 help shifts effector T cell distribution toward subpopulations with more pronounced exhaustion phenotype.

In contrast to cluster 2 which did not show phenotypic signs of exhaustion, the other three clusters (3, 4 and 5) displayed progressively elevated expression of inhibitory receptors such as PD-1, CD160 and CD244 **(Figure 19A and B)**. Interestingly, while the size of the less exhausted cluster 3 declined in absence of CD4 help, the size of the more exhausted cluster 4 increased, although not in the same

CD4 T cell help sustains distinct subpopulations in functional and dysfunctional CD8 T cell responses.

magnitude (**Figure 19A**). Moreover, the phenotypically most exhausted cluster 5 selectively appeared in absence of CD4 help. Cells with cluster-5-like phenotype were not found in control mice. Therefore, absence of CD4 help does not simply cause loss of phenotypically non-exhausted and accumulation of exhausted cells. It rather induces shift of effector T cell distribution towards subpopulations with more pronounced



CD4 T cell help sustains distinct subpopulations in functional and dysfunctional CD8 T cell responses.

Figure 19. Absence of CD4 help shifts effector T cell distribution toward subpopulations with more pronounced exhaustion phenotype [3].

Single-cell RNA sequencing analysis of P14 T cells recovered on day 40 post LCMV c13 WT infection from control and CD4 depleted hosts. Each condition is represented by cells from three individual mice. **(A)** tSNE plots - highlight the Seurat predicted cluster 3, 4 and 5 for illustrative purpose. Scatter plots - calculated absolute numbers of splenic P14 cells in control and CD4 depleted animals that are similar to the cells in cluster 3, 4 and 5. The calculation is based on the percentage wise representation of cluster 3, 4 and 5 among total P14 T cells as explained in the methods section, each symbol in the plot represent individual mouse and the bar the mean. **(B)** tSNE plots with overlaid compartment specific expression of selected surface receptor with previously reported T cell modulatory function [6-16]. Abbreviations: ctrl, control; w/o CD4, CD4 depleted; #, number.

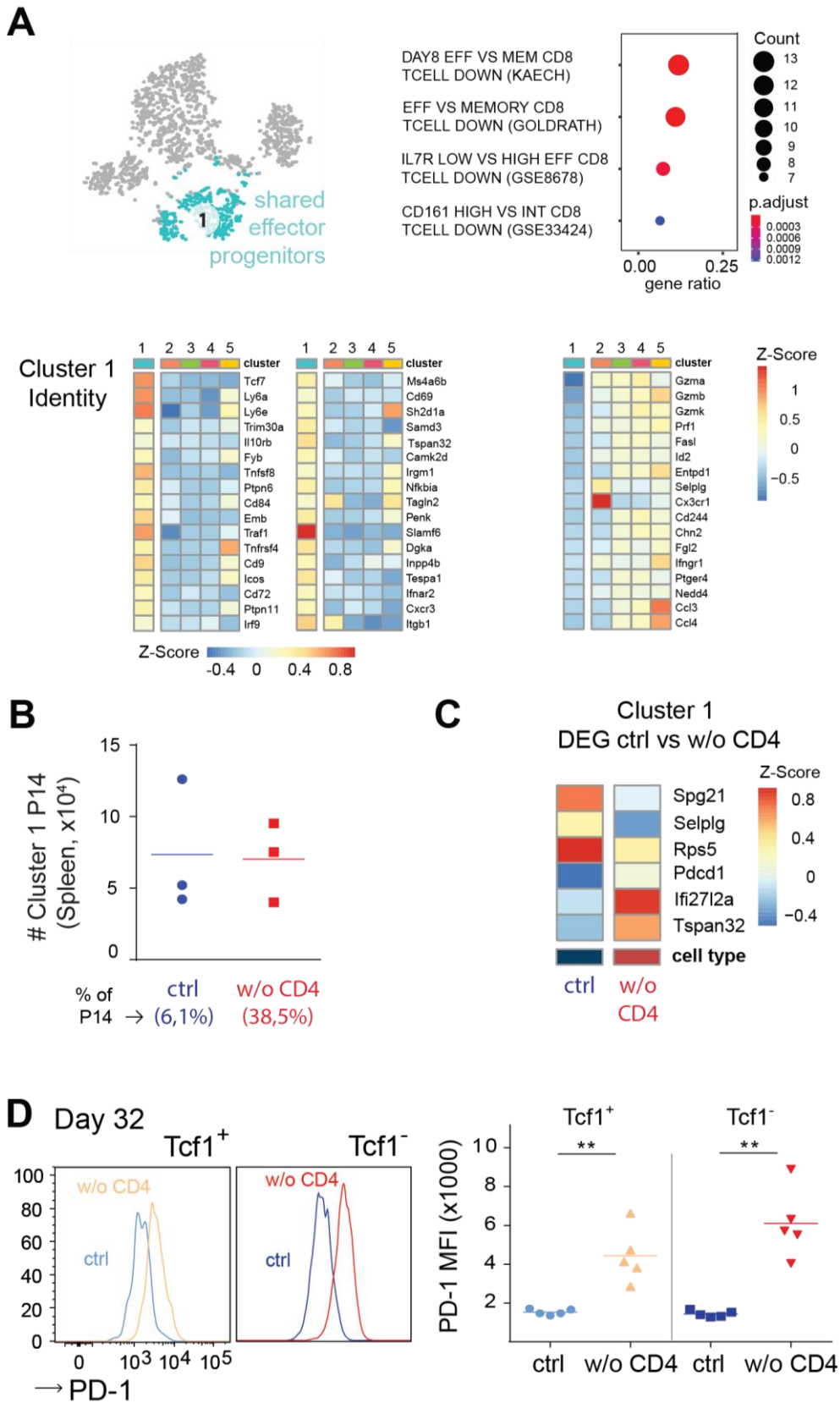
exhaustion phenotype. As this single-cell dataset models the range of CD8 T cell states found in chronic infection (**Figure 19B**), we were able to identify regulatory receptors with potential application for selective targeting of progenitor (Cd9, Icos and Tnfrsf4), functional (Il18r, Klrc1, Klrd1 and Klrk1) and dysfunctional (Cd244 and Tnfrsf9) subpopulations.

The progenitor's phenotype is unaltered in absence of CD4 help and proliferative capacity can be restored by subsequent provision of antigen-specific CD4 T cells.

The progenitor identity of cluster 1 was verified by DGEA and GSEA (**Figure 20A**). In agreement with the FACS data (**Figure 12B**), similar numbers of cluste-1-like P14 T cells were observed in control and treated mice (**Figure 20B**). To test the hypothesis that despite being maintained at comparable numbers, the progenitors' phenotype could be altered in absence of CD4 help, we compared the genetic programs of the progenitors formed in presence and absence of CD4 help (**Figure 20C**). We observed only minor differences, including slightly elevated PD-1 expression, which was confirmed on protein level (**Figure 20D**). Thus, the progenitors seemed largely spared from being phenotypically impacted in absence of CD4 help. To provide direct evidence and test their functionality, next we reinstalled a LCMV-specific CD4 T cell compartment. For that purpose, CD4 depletion was discontinued on day 15 post infection, followed by transgenic SMARTA CD4 T cell transfer on day

CD4 T cell help sustains distinct subpopulations in functional and dysfunctional CD8 T cell responses.

25 post infection. The readout was performed 10 days later. The restored endogenous



CD4 T cell help sustains distinct subpopulations in functional and dysfunctional CD8 T cell responses.

Figure 20. The progenitor's phenotype is unaltered in absence of CD4 help [3].

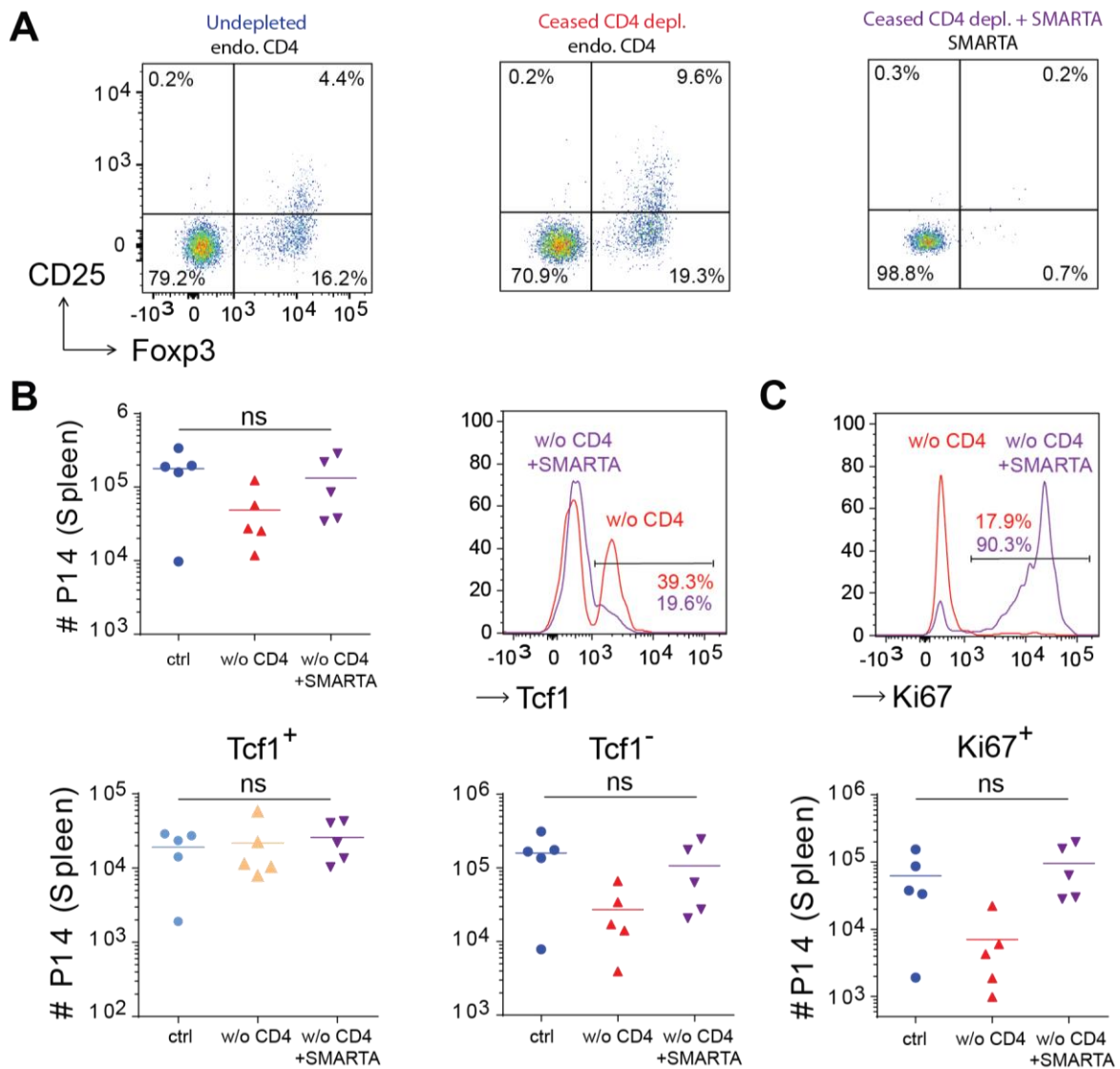
Single-cell RNA sequencing analysis of P14 T cells recovered on day 40 post LCMV c13 WT infection from control and CD4 depleted hosts. Each condition is represented by cells from three individual mice. **(A)** tSNE plot highlighting the Seurat predicted cluster 1 for illustrative purpose. Differential gene expression analysis (DGEA) and gene set enrichment analysis (GSEA) of cluster 1. **(B)** Scatter plot with calculated absolute numbers of splenic P14 cells in control and CD4 depleted animals that are similar to the cells in cluster 1. The calculation is based on the percentage wise representation of cluster 1 among total P14 T cells as explained in the methods section, each symbol in the plot represent individual mouse and the bar the mean. **(C)** Differential gene expression between control and unhelped P14s co-localizing in cluster 1. **(D)** Representative CD8+CD45.1+Tcf1+ or CD8+CD45.1+Tcf1- gated flow cytometry plots and corresponding data graphs are shown. Symbols in data plots represent individual mice, small horizontal lines indicate the mean. ***p < 0.001; **p < 0.01; *p < 0.05 based on unpaired t test. Abbreviations: ctrl, control; w/o CD4, CD4 depleted; #, number; DEG, differentially expressed genes.

CD4 T cell compartment which included normal frequencies of regulatory T cells **(Figure 21A)**, was unable to reinvigorate the P14 T cell response alone **(Figure 21B)**. This is probably a result of the absence of antigen-specific CD4 T cells due to thymic tolerance in LCMV infected hosts. In contrast, the transferred antigen-specific SMARTA T cells which acquired helper phenotype **(Figure 21A)**, were able to boost the P14 T cell response **(Figure 21B)**. The increase in total P14 numbers was a result of gains in the differentiated effector compartment. The number of progenitor cells remained unchanged. Moreover, the SMARTA transfer increased the portion of Ki67+

Figure 21. The progenitor's proliferative capacity can be restored by subsequent provision of antigen-specific CD4 T cells [3].

C57BL/6 mice (CD45.2+) were engrafted with transgenic gp33-specific P14 T cells (CD45.1+) prior to infection with LCMV c13 WT. Transgenic SMARTA CD4 T cells were transferred on day 25 post infection. Data were collected 35 days post infection. **(A)** Representative CD4+CD45.2+ (endogenous CD4) and CD4+CD45.1+ (SMARTA CD4) gated flow cytometry plots. **(B)** Representative CD8+CD45.1+ gated flow cytometry plots and corresponding data graphs for all mice. Lower two graphs, P14 T cells were subdivided by Tcf1 expression and absolute numbers for all mice are shown. **(C)** Up, CD8+CD45.1+ gated flow cytometry plot. Down, enumeration of Ki-67 positive P14 T cells. ***p < 0.001; **p < 0.01; *p < 0.05 based on unpaired t test. Abbreviations: ns, not significant (p > 0.05) based unpaired t test; ctrl, control; w/o CD4, CD4 depleted; endo CD4, endogenous CD4 T cells; #, number.

CD4 T cell help sustains distinct subpopulations in functional and dysfunctional CD8 T cell responses.



P14 cells from about 17 to 90% (**Figure 21C**). In result, control and reconstituted mice displayed similar number of total Ki67⁺ P14 cells in spleen. Of note, the addition of SMARTA cells aggravated immunopathology limiting the length of the possible observation period. Thus, the experiments were terminated before the full restoration of the P14 compartment. We concluded that the proliferative capacity of the progenitors remains unchanged in absence of CD4 help.

7. Discussion

As a **first immunological question** in this study, we addressed **how teriflunomide (the biologically active form of the prodrug leflunomide) affects T cell differentiation and subpopulation formation as early as day 4 following T cell activation**. In agreement with the pre-existing data from our laboratory on day 7 and day 28, the teriflunomide treatment caused selective decline in size of the subpopulations with a clear effector-like phenotype (cluster 4 and 5), but those with memory-like (cluster 2 and 3) or mixed (cluster 1) phenotype remained virtually unaffected. As teriflunomide is a reversible inhibitor of DHODH, an enzyme with a key role in the pathway for *de novo* biosynthesis of pyrimidine nucleotides, teriflunomide is assumed to preferentially impact cells with high biosynthetic needs, such as the actively proliferating cells. When compared side-by-side, the teriflunomide-resistant cluster 1 displayed similarly high enrichment for cell cycle processes and Mki67 expression as the teriflunomide most sensitive effector-like cluster 5 that was lost upon teriflunomide treatment. Therefore, the increased proliferation activity alone cannot explain why certain clusters are sensitive to teriflunomide treatment, while others are not. Interestingly, the teriflunomide-resistant cluster 1 displayed higher DHODH expression in comparison to the teriflunomide-sensitive cluster 5. Along with this, the teriflunomide-resistant cluster 1 had generally higher expression of multiple enzymes involved in the pathway for *de novo* biosynthesis of pyrimidine nucleotides. Therefore, we favor the hypothesis that differential capacity to produce pyrimidine nucleotides combined with proliferation activity renders some T cells resistant to leflunomide treatment, while others not. The actively proliferating cluster 1, which displays features of both effector and memory phenotype, is teriflunomide-resistant due to its comparatively higher expression of enzymes involved in the pathway for *de novo* biosynthesis of pyrimidine nucleotides, which provides enough spare capacity for pyrimidine production at this drug concentration. Conversely, the comparatively lower expression of enzymes involved in the pathway for *de novo* biosynthesis of pyrimidine nucleotides combined with high biosynthetic demands due to active proliferation, renders the effector-like cluster 4 and 5 sensitive to teriflunomide treatment, resulting

in their pronounced numerical decline. Lastly, the memory-like clusters 2 and 3 are resistant to teriflunomide treatment despite their low expression of the enzymes involved in the pathway for *de novo* biosynthesis of pyrimidine nucleotides due to their low proliferation rate.

Intriguingly, we observed that the expression level of DHODH and the other enzymes involved in the pathway for *de novo* biosynthesis of pyrimidine nucleotides positively correlated with the expression of Myc. Myc is a well know transcriptional regulator of variety of T cell processes, among which T cell metabolism [229]. Upregulated shortly after T cell activation, Myc promotes the transition from fatty acid oxidation and mitochondrial-dependent oxidative phosphorylation (OXPHOS) to robust aerobic glycolysis and glutaminolysis [225]. Currently, the full scale of Myc-driven T cell metabolic reprogramming remains underexplored. We suspect that Myc could potentially serve as a positive regulator of the pathway for *de novo* biosynthesis of pyrimidine nucleotides in T cells, a notion which would be critical to address in subsequent studies.

From a clinical perspective, the observed blockade of effector, but not memory T cell differentiation upon inhibition of the pathway for *de novo* biosynthesis of pyrimidine nucleotides offers interesting insights in the context of prophylactic vaccine development. Here the generation of effector T cells can be viewed as an unnecessary byproduct given that only memory cells are needed for subsequent protection. In fact, effector cells and their cytokine production capacity might only contribute to vaccine induced adverse effects and tissues pathology. Due to its safety profile including drug-induced liver injury, the direct use of leflunomide in healthy patients is unlikely and hard to be justified in the context of vaccination. Nevertheless, the mechanistic insights gained using leflunomide inhibition of DHODH early following T cell activation can inform the design of other inhibitors that target the same or related mechanisms.

Aside from the potential translational applications, this study identifies teriflunomide as a tool enriching for memory-like subpopulations as early as 4 days following T cell activation. This is of particular importance, as memory-like T cells are numerically underrepresented at this timepoint and markers for their isolation are currently not well defined. Thus, by using teriflunomide one can reduce the number of

CD4 T cell help sustains distinct subpopulations in functional and dysfunctional CD8 T cell responses.

cells required for reliable single-cell analysis of the memory-like compartment. This is of relevance even when cost is not under consideration, as bioinformatical analysis could prove challenging given the tendency of clustering algorithms to underperform when subpopulations with too big difference in size are present (such as the difference between the effector and the memory compartment) [230].

As a **second immunological question**, we addressed **the role of CD4 help for the maintenance and function of the Tcf1+ progenitors and their Tcf1-progeny in exhausted and functional immune responses**. To our surprise, we discovered that the progenitors of exhausted CD8 T cell responses are maintained independently of CD4 help. This was in sharp contrast to the critical role of CD4 help for the generation of long-lasting and functional memory in acute infection. Instead, in exhausted CD8 T cells responses, the CD4 help is only critical for the maintenance and phenotype of the terminally differentiated effector CD8 T cell compartment. In absence of CD4 help, a shift of effector T cell distribution towards subpopulations with more pronounced exhaustion phenotype is induced. Nevertheless, the general capacity to form cells from all clusters found in control animals is not affected.

We observed an interesting correlation between the phenotype of the progenitors formed in chronic infection and their independence on CD4 help. As explained in the results section, the clone-13 MIX infection results in a situation where the progenitors and their progeny retain a non-exhausted phenotype. Interestingly, these non-exhausted progenitors remained dependent on CD4 help, as they underwent 8-fold size reduction in absence of CD4 T cells. We observed similar CD4 help dependence in acute infection, where the maintenance of the Tcf1+ CD8 memory cells was compromised in absence of CD4 help. Therefore, we considered that the observed differential requirement of CD4 help between exhausted and non-exhausted progenitors formed in chronic infection could be a result from an alternative differentiation program.

An interesting and yet unresolved question is what leads to this differential sensitivity to CD4 help. In the past our laboratory has studied mechanisms that guide the differentiation of progenitors and their progeny in chronic versus acute infection. Hereby we and others have identified TOX as an exhaustion specific transcriptional

CD4 T cell help sustains distinct subpopulations in functional and dysfunctional CD8 T cell responses.

factor, which primarily drives transcriptional and epigenetic changes in the progenitors in early infection, which are later transferred to their exhausted progeny [177-181]. By imposing the state of exhaustion first on progenitors and in result to their progeny, TOX attunes the CD8 T cell responses to be sustained in context of persistent stimulation. This is demonstrated by the fact that although TOX-deficiency prevents exhaustion and increases viral control, over time this results in progenitor loss and subsequent response erosion [177]. We reasoned that the transcriptional and epigenetic changes induced by TOX or similar exhaustion-specific transcriptional regulators can release the progenitors of exhausted CD8 T cell responses from their dependence on CD4 help, thus equipping them with the means to survive the progressively declining levels of CD4 support during the course of a chronic infection. Identifying the exact transcriptional regulators and mechanisms of action would be a key question to be addressed in subsequent studies.

In both clone-13 PURE and MIX infection, the absence of CD4 help led to a similar reduction in the size of the terminally differentiated effector compartment. Nevertheless, this could be a result from two distinct mechanisms.

In clone-13 PURE infection, the absence of CD4 help might prevent the formation or maintenance of newly generated effector CD8 T cells. Therefore, the effector compartment declines in terms of number and phenotype with time. This goes along with our observation that absence of CD4 help leads to loss of Cx3cr1+ effector cells, which lack the classical signs of exhaustion such as high inhibitory receptor expression, at the expense of accumulation of cells with more pronounced exhaustion phenotype. In a parallel study addressing the differentiation relationships among the CD8 T cell subpopulations found in chronic infection using cell transfer experiments, Hudson and colleagues demonstrated that the Cx3cr1+ effector cells are likely the recent progeny of the Tcf1+ progenitors and can further differentiate to cell with dysfunctional phenotype [231]. Moreover, Zander and colleagues showed that a diphtheria toxin receptor (DTR) induced ablation of the Cx3cr1+ effector subpopulation leads to increased viral load [4], demonstrating the important role of these cells in viral control. In our study, the Cx3cr1+ effector subpopulation also uniquely expressed the receptors promoting systemic circulation - S1pr1 and S1pr5, as well as their

CD4 T cell help sustains distinct subpopulations in functional and dysfunctional CD8 T cell responses.

transcriptional regulator Klf2. In a parallel study using parabiosis to compare the migration abilities of acutely and chronically stimulated antigen-specific CD8 T cells, Im and colleagues demonstrated that in comparison to acutely stimulated CD8 T cells, the chronically stimulated CD8 T cells displayed more resident phenotype and were less capable to systemic circulation [232]. Moreover, among the chronically stimulated antigen-specific CD8 T cells, the Cx3cr1⁺ effector cells displayed the highest capability for systemic circulation. It remains of interest whether enforcing KLF2 expression in the phenotypically more exhausted Cx3cr1⁻ effector cells could lead to therapeutic benefit, by partially reversing their exhausted phenotype or improving their capability for systemic circulation. Although purely speculative (especially taking into account the understudied role of the rest of the observed effector subpopulations in viral control), enriching for the Cx3cr1⁺ phenotype might be therapeutically beneficial. This is highlighted by the fact, that PD-1 blockade particularly boosts the production of Cx3cr1⁺ effector cells [231]. Altogether, the loss of Cx3cr1⁺ effector cells in absence of CD4 help can at least in part explain the deteriorating viral control, without depreciating the role of diminished humoral immunity.

In clone-13 MIX infection, we suspected a rather different mechanism of CD8 T cell effector compartment erosion in absence of CD4 help. Given the CD4 help dependence of the progenitors in this set up as well as the progenitor-progeny relationship, we reasoned that the observed decline in the effector compartment size is a direct consequence of the size reduction in the progenitor compartment, rather than deficiencies in mechanisms of effector cell formation or maintenance. In support of this notion is the fact that both, the progenitor and the effector compartment declined 8-fold in size. Additionally, in the clone-13 MIX setting, the absence of CD4 help was unable to induce a pronounced phenotypic change in the effector compartment, such as sensibly increased PD-1 expression as seen in clone-13 PURE infection. Therefore, we hypothesized that CD4 help likely has different mechanisms of action in functional and phenotypically exhausted CD8 T cell responses.

Currently, the form of CD4 help to functional and phenotypically exhausted CD8 T cell responses remains unclear. CD40L-CD40 signaling between antigen-specific CD4 T cells and APCs is known as an important mechanism of indirect CD4 help to

CD4 T cell help sustains distinct subpopulations in functional and dysfunctional CD8 T cell responses.

CD8 T cell responses [45]. In this study, we demonstrated that blocking CD40L signaling only partially recapitulates the phenotype observed in absence of CD4 help. Although the expression of PD-1 increased to levels similar to that observed upon CD4 depletion, this treatment did not affect the size of the P14 T cell population. The partial effect of the CD40L blockade could be explained with an observation from a parallel study by Zander and colleagues, who demonstrated that the formation or maintenance of the Cx3cr1⁺ effector cells depend on IL-21 produced by CD4 T cells [4]. To highlight both the role of IL-21 and Cx3cr1⁺ effector cells, it is well known that in absence of IL-21 the CD8 T cell responses are severely impaired and viral control is undermined [233-235]. Therefore, we favor a hypothesis in which CD4 T cells provide help to CD8 T cell responses via multiple mechanisms, two of which are CD40L-CD40 and IL-21 signaling. We foresee that further discoveries in this respect will be made in the near future.

The new insights about role of CD4 help in CD8 T cells responses with different level of exhaustion are of clinical relevance.

Firstly, the expression of Cx3cr1 by effector CD8 T cells might potentially serve as a surrogate biomarker indicating the state of the response in chronic infection and cancer. It was recently reported that increased frequency of circulatory Cx3cr1⁺ CD8 T cells positively correlates with response and survival following anti-PD1 blockade in patients with non-small cell lung cancer [236].

Secondly, the differential CD4 help requirement of the progenitors of functional and those of exhausted CD8 T cell responses could have ramifications for human conditions associated with progressive CD4 T cell loss, such as AIDS (acquired immunodeficiency syndrome). In this scenario, disease progression could cause the erosion of the progenitors of ongoing non-exhausted CD8 T cell responses, but would preserve the progenitors of the phenotypically exhausted ones. This could potentially affect not only the response to HIV, but also the response to the opportunistic infections accompanying AIDS.

Thirdly, understanding the role of the distinct CD8 T cell subpopulation formed in persistent stimulation combined with their specific expression of regulatory receptors, can inform new therapeutic strategies aimed at harnessing the full

CD4 T cell help sustains distinct subpopulations in functional and dysfunctional CD8 T cell responses.

therapeutic potential of CD8 T cells. Currently, it is widely recognized that PD-1 blockade only transiently boosts the production by the progenitors of newly generated effector cells which soon after become exhausted [85]. Therefore, combining PD-1 blockade with a secondary treatment aimed at promoting progenitor health or preventing effector T cell exhaustion could prove beneficial. For instance, we noticed that in our study the phenotypically non-exhausted Cx3cr1⁺ effector subpopulation uniquely expressed the receptor for IL-18 (subunits Il18r1 and Il18rap). IL18 is known to limit activation-induced cell death, promote proliferation as well as IFN γ secretion in CD8 T cells [14, 237]. Taking into account these effects, as well as the compartment-specific expression of its receptor, we consider IL-18 supplementation as a potentially promising mechanism to promote effector T cell health and function. In a recent study, Zhou and colleagues designed a decoy resistant IL-18, which maintains signaling potential but cannot be inhibited by its soluble inhibitor known as IL-18BP [238]. Using this decoy resistant IL-18 in mouse tumor models, Zhou and colleagues showed that IL-18 supplementation promotes the formation of effector CD8 T cells with poly-functional phenotype and decreases the prevalence of those with exhausted phenotype, thus demonstrating the benefit of this treatment. The clinical effectiveness of IL-18 supplementation alone or in combination with other treatments remains to be demonstrated in human patients.

8. Abbreviations

| | |
|----------|--|
| 4-1BB | TNF Receptor Superfamily Member 9 |
| ADP | Adenosindiphosphat |
| AIDS | acquired immunodeficiency syndrome |
| AP-1 | Activator Protein 1 |
| APC | antigen-presenting cell |
| ATP | Adenosintriphosphat |
| BATF | Basic Leucine Zipper ATF-Like Transcription Factor |
| Bcl6 | B-Cell Lymphoma 6 Protein |
| BCR | B-cell receptor |
| Blimp-1 | B-Lymphocyte-Induced Maturation Protein 1 |
| CAR | chimeric antigen receptor |
| Ccr7 | C-C Motif Chemokine Receptor 7 |
| CD | Cluster of Differentiation |
| CD127 | Interleukin 7 Receptor |
| CD27 | TNF Receptor Superfamily Member 7 |
| CD62L | Selectin L, also known as SELL |
| CEACAM1 | Carcinoembryonic Antigen-Related Cell Adhesion Molecule 1 |
| CFU | colony-forming unit |
| CRS | cytokine release syndrome |
| CTL | cytotoxic T lymphocyte |
| CTLA4 | Cytotoxic T-Lymphocyte Associated Protein 4 |
| ctrl | control |
| Cxcr3 | C-X-C Motif Chemokine Receptor 3 |
| Cxcr5 | C-X-C Motif Chemokine Receptor 5 |
| DC | dendritic cell |
| DGEA | differential gene expression analysis |
| DHODH | dihydroorotate dehydrogenase |
| Drop-seq | droplet sequencing |
| EDTA | ethylenediaminetetraacetic |
| ENTPD1 | Ectonucleoside Triphosphate Diphosphohydrolase 1, also known as CD39 |
| Eomes | Eomesodermin |
| ERK | Extracellular Signal-Regulated Kinase, also known as MAPK1 |
| Ezh2 | Enhancer Of Zeste 2 Polycomb Repressive Complex 2 Subunit |
| FACS | fluorescent-activated cell sorting |
| Fas | TNF Receptor Superfamily Member 6 |
| FasL | TNF Ligand Superfamily Member 6 |
| FCS | fetal calf serum |
| FDA | United States Food and Drug Administration |
| Foxo1 | Forkhead Box Protein O1 |
| GATA-3 | GATA Binding Protein 3 |

CD4 T cell help sustains distinct subpopulations in functional and dysfunctional CD8 T cell responses.

| | |
|---------------|--|
| GITR | TNF Receptor Superfamily Member 18 |
| GSEA | gene set enrichment analysis |
| Gzma | Granzyme A |
| Gzmb | Granzyme B |
| HBV | hepatitis B virus |
| HCV | hepatitis C virus |
| HEPES | 2-[4-(2-hydroxyethyl)piperazin-1-yl]ethanesulfonic acid |
| hi | high |
| HIV | human immunodeficiency virus |
| HLA | human leukocyte antigen |
| ID2 | Inhibitor of Differentiation 2 |
| ID3 | Inhibitor of Differentiation 3 |
| IFN- α | Interferon Alpha |
| IFN- β | Interferon Beta |
| IFN- γ | Interferon Gamma |
| Ig | immunoglobulin |
| IL | Interleukin |
| IRF4 | Interferon Regulatory Factor 4 |
| ITIM | Immunoreceptor tyrosine-based inhibitory motif |
| KLRG-1 | Killer Cell Lectin Like Receptor G1 |
| KNN | k-nearest neighbor |
| Lag-3 | Lymphocyte-Activation Gene 3 |
| LCMV | lymphocytic choriomeningitis virus |
| LCMV Arm | lymphocytic choriomeningitis virus strain Armstrong, causes acute infection |
| LCMV c13 | lymphocytic choriomeningitis virus strain clone-13, causes chronic infection |
| LCMV WE | lymphocytic choriomeningitis virus strain WE, causes either acute or chronic infection depending on the infection dose |
| lefl | leflunomide |
| Lm-OVA | rocombinant Listeria monocytogenes expressing OVA containing the SIINFEKL (N4) epitope |
| lo | low |
| LPS | lipopolysaccharide |
| MAPK | Mitogen-Activated Protein Kinase |
| Mki67 | Marker Of Proliferation Ki-67 |
| md. # mito | median number of mitochondrial transcripts per cell |
| md. # ribo | median number of ribosomal transcripts per cell |
| md. % mito | median portion of mitochondrial transcripts out of the total transcripts per cell |
| md. % ribo | median portion of ribosomal transcripts out of the total transcripts per cell |
| md. genes | median number of captured genes per cell |

CD4 T cell help sustains distinct subpopulations in functional and dysfunctional CD8 T cell responses.

| | |
|----------------------|---|
| md. top50 | median portion of transcripts attributed to the top 50 most highly expressed genes per cell |
| md. transcripts | median number of captured transcripts per cell |
| md. transcripts/gene | median number of transcripts detected per gene |
| MEK | Mitogen-Activated Protein Kinase |
| MHC | major histocompatibility complex |
| mTOR | Mechanistic Target of Rapamycin Kinase |
| NFATc1 | Nuclear Factor of Activated T Cells 1 |
| NK | natural killer cell |
| Nr4a2 | Nuclear Receptor Subfamily 4 Group A Member 2 |
| OX40 | TNF Receptor Superfamily Member 4 |
| OXPPOS | mitochondrial-dependent oxidative phosphorylation of glucose |
| PAMP | pathogen-associated molecular pattern |
| PBMC | peripheral blood mononuclear cells |
| PCR | polymerase chain reaction |
| PD-1 | Programmed Cell Death 1 |
| PD-L1 | Programmed Cell Death 1 Ligand 1 |
| PDMS | polydimethylsiloxane |
| PFU | plaque-forming unit |
| PI-3K | Phosphoinositide-3-Kinase |
| Prf1 | |
| PRR | pattern recognition receptor |
| RA | rheumatoid arthritis |
| RORyt | RAR Related Orphan Receptor C |
| RT | room temperature |
| RT | reverse transcription |
| RTse | reverse transcriptase |
| scGEP | single-cell resolved gene expression profile |
| sc-qPCR | single-cell quantitative PCR |
| SCRB-seq | single-cell RNA barcoding and sequencing |
| scRNA-seq | single-cell RNA sequencing |
| Sell | Selectin L, also known as CD62L |
| SHP-2 | Protein Tyrosine Phosphatase Non-Receptor Type 11 |
| SIV | simian immunodeficiency virus |
| SMAD | Sma- And Mad-Related Protein Family |
| STAT-3 | Signal Transducer and Activator Of Transcription 3 |
| STAT5 | Signal Transducer and Activator Of Transcription 5A |
| T-bet | T-Box Transcription Factor 21 |
| Tcf1 | T-Cell-Specific Transcription Factor 1 |
| Tcf7 | T-Cell-Specific Transcription Factor 1, coding gene |
| Tcm | central memory T cell |
| TCR | T cell receptor |

CD4 T cell help sustains distinct subpopulations in functional and dysfunctional CD8 T cell responses.

| | |
|--------------|--|
| tDrop-seq | primary T cell tailored droplet sequencing |
| Tem | effector memory T cell |
| TF | transcription factor |
| Tfh | follicular helper T cell |
| tfl | teriflunomide |
| TGF- β | Transforming Growth Factor Beta |
| Th | helper T cell |
| TIGIT | T Cell Immunoreceptor With Ig And ITIM Domains |
| TIL | tumor-infiltrating lymphocyte |
| Tim-3 | T cell Immunoglobulin Mucin Family Member 3 |
| TNF | Tumor Necrosis Factor |
| TOX | Thymocyte Selection Associated High Mobility Group Box |
| Treg | regulatory T cell |
| Trm | tissue resident memory T cell |
| tSCRB-seq | primary T cell tailored single-cell RNA barcoding and sequencing |
| TSO | template switching oligo |
| UCI | unique cellular identifier |
| UMI | unique molecular identifier |
| WT | wild type |

9. Literature

1. Williams, M.A. and M.J. Bevan, *Effector and memory CTL differentiation*. Annu Rev Immunol, 2007. **25**: p. 171-92.
2. Kanev, K., et al., *Tailoring the resolution of single-cell RNA sequencing for primary cytotoxic T cells*. Nature Communications, 2021. **12**(1): p. 569.
3. Kanev, K., et al., *Proliferation-competent Tcf1+ CD8 T cells in dysfunctional populations are CD4 T cell help independent*. Proceedings of the National Academy of Sciences, 2019. **116**(40): p. 20070-20076.
4. Zander, R., et al., *CD4(+) T Cell Help Is Required for the Formation of a Cytolytic CD8(+) T Cell Subset that Protects against Chronic Infection and Cancer*. Immunity, 2019. **51**(6): p. 1028-1042.e4.
5. Chen, Z., et al., *TCF-1-Centered Transcriptional Network Drives an Effector versus Exhausted CD8 T Cell-Fate Decision*. Immunity, 2019. **51**(5): p. 840-855 e5.
6. Sheppard, K.A., et al., *PD-1 inhibits T-cell receptor induced phosphorylation of the ZAP70/CD3zeta signalosome and downstream signaling to PKCtheta*. FEBS Lett, 2004. **574**(1-3): p. 37-41.
7. Agresta, L., K.H.N. Hoebe, and E.M. Janssen, *The Emerging Role of CD244 Signaling in Immune Cells of the Tumor Microenvironment*. Frontiers in Immunology, 2018. **9**: p. 2809.
8. Viganò, S., et al., *CD160-associated CD8 T-cell functional impairment is independent of PD-1 expression*. PLoS Pathog, 2014. **10**(9): p. e1004380.
9. Long, A.H., et al., *4-1BB costimulation ameliorates T cell exhaustion induced by tonic signaling of chimeric antigen receptors*. Nature Medicine, 2015. **21**(6): p. 581-590.
10. Tai, X.G., et al., *A role for CD9 molecules in T cell activation*. J Exp Med, 1996. **184**(2): p. 753-8.
11. Dong, C., et al., *ICOS co-stimulatory receptor is essential for T-cell activation and function*. Nature, 2001. **409**(6816): p. 97-101.
12. Redmond, W.L., C.E. Ruby, and A.D. Weinberg, *The role of OX40-mediated co-stimulation in T-cell activation and survival*. Crit Rev Immunol, 2009. **29**(3): p. 187-201.
13. Zhou, T., et al., *IL-18BP is a secreted immune checkpoint and barrier to IL-18 immunotherapy*. Nature, 2020.

CD4 T cell help sustains distinct subpopulations in functional and dysfunctional CD8 T cell responses.

14. Li, W., et al., *Protection of CD8+ T cells from activation-induced cell death by IL-18*. J Leukoc Biol, 2007. **82**(1): p. 142-51.
15. Rapaport, A.S., et al., *The Inhibitory Receptor NKG2A Sustains Virus-Specific CD8+ T Cells in Response to a Lethal Poxvirus Infection*. Immunity, 2015. **43**(6): p. 1112-24.
16. Wensveen, F.M., V. Jelenčić, and B. Polić, *NKG2D: A Master Regulator of Immune Cell Responsiveness*. Frontiers in Immunology, 2018. **9**: p. 441.
17. Hornef, M.W., et al., *Bacterial strategies for overcoming host innate and adaptive immune responses*. Nat Immunol, 2002. **3**(11): p. 1033-40.
18. Turvey, S.E. and D.H. Broide, *Innate immunity*. J Allergy Clin Immunol, 2010. **125**(2 Suppl 2): p. S24-32.
19. Janeway, C.A., Jr. and R. Medzhitov, *Innate immune recognition*. Annu Rev Immunol, 2002. **20**: p. 197-216.
20. Cooper, M.D. and M.N. Alder, *The evolution of adaptive immune systems*. Cell, 2006. **124**(4): p. 815-22.
21. Hedrick, S.M., *Thymus lineage commitment: a single switch*. Immunity, 2008. **28**(3): p. 297-9.
22. Bonilla, F.A. and H.C. Oettgen, *Adaptive immunity*. J Allergy Clin Immunol, 2010. **125**(2 Suppl 2): p. S33-40.
23. Yoon, H., T.S. Kim, and T.J. Braciale, *The cell cycle time of CD8+ T cells responding in vivo is controlled by the type of antigenic stimulus*. PLoS One, 2010. **5**(11): p. e15423.
24. Mescher, M.F., et al., *Signals required for programming effector and memory development by CD8+ T cells*. Immunol Rev, 2006. **211**: p. 81-92.
25. Parish, I.A. and S.M. Kaech, *Diversity in CD8(+) T cell differentiation*. Curr Opin Immunol, 2009. **21**(3): p. 291-7.
26. Gerlach, C., et al., *One naive T cell, multiple fates in CD8+ T cell differentiation*. J Exp Med, 2010. **207**(6): p. 1235-46.
27. Zhou, X., et al., *Differentiation and persistence of memory CD8(+) T cells depend on T cell factor 1*. Immunity, 2010. **33**(2): p. 229-40.
28. Jeannet, G., et al., *Essential role of the Wnt pathway effector Tcf-1 for the establishment of functional CD8 T cell memory*. Proc Natl Acad Sci U S A, 2010. **107**(21): p. 9777-82.

29. Watts, T.H., *TNF/TNFR family members in costimulation of T cell responses*. Annu Rev Immunol, 2005. **23**: p. 23-68.
30. Zhang, N. and M.J. Bevan, *CD8(+) T cells: foot soldiers of the immune system*. Immunity, 2011. **35**(2): p. 161-8.
31. Pearce, E.L. and H. Shen, *Generation of CD8 T cell memory is regulated by IL-12*. J Immunol, 2007. **179**(4): p. 2074-81.
32. Michalek, R.D. and J.C. Rathmell, *The metabolic life and times of a T-cell*. Immunol Rev, 2010. **236**: p. 190-202.
33. Groom, J.R. and A.D. Luster, *CXCR3 ligands: redundant, collaborative and antagonistic functions*. Immunol Cell Biol, 2011. **89**(2): p. 207-15.
34. Tan, J.T., et al., *Interleukin (IL)-15 and IL-7 jointly regulate homeostatic proliferation of memory phenotype CD8+ cells but are not required for memory phenotype CD4+ cells*. J Exp Med, 2002. **195**(12): p. 1523-32.
35. Martin, M.D. and V.P. Badovinac, *Defining Memory CD8 T Cell*. Frontiers in Immunology, 2018. **9**: p. 2692.
36. Wherry, E.J., et al., *Lineage relationship and protective immunity of memory CD8 T cell subsets*. Nature Immunology, 2003. **4**(3): p. 225-234.
37. Sallusto, F., et al., *Two subsets of memory T lymphocytes with distinct homing potentials and effector functions*. Nature, 1999. **401**(6754): p. 708-12.
38. Sathaliyawala, T., et al., *Distribution and compartmentalization of human circulating and tissue-resident memory T cell subsets*. Immunity, 2013. **38**(1): p. 187-97.
39. Schenkel, J.M., et al., *Sensing and alarm function of resident memory CD8+ T cells*. Nature Immunology, 2013. **14**(5): p. 509-513.
40. Jiang, X., et al., *Skin infection generates non-migratory memory CD8+ TRM cells providing global skin immunity*. Nature, 2012. **483**(7388): p. 227-231.
41. Walton, S., S. Mandaric, and A. Oxenius, *CD4 T cell responses in latent and chronic viral infections*. Front Immunol, 2013. **4**: p. 105.
42. Constant, S.L. and K. Bottomly, *Introduction of Th1 and Th2 CD4+ T cell responses: The Alternative Approaches*. Annual Review of Immunology, 1997. **15**(1): p. 297-322.
43. Laidlaw, B.J., J.E. Craft, and S.M. Kaech, *The multifaceted role of CD4+ T cells in CD8+ T cell memory*. Nature Reviews Immunology, 2016. **16**(2): p. 102-111.

CD4 T cell help sustains distinct subpopulations in functional and dysfunctional CD8 T cell responses.

44. Wiesel, M. and A. Oxenius, *From crucial to negligible: functional CD8⁺ T-cell responses and their dependence on CD4⁺ T-cell help*. Eur J Immunol, 2012. **42**(5): p. 1080-8.
45. Schoenberger, S.P., et al., *T-cell help for cytotoxic T lymphocytes is mediated by CD40-CD40L interactions*. Nature, 1998. **393**(6684): p. 480-3.
46. Shedlock, D.J. and H. Shen, *Requirement for CD4 T cell help in generating functional CD8 T cell memory*. Science, 2003. **300**(5617): p. 337-9.
47. Sun, J.C., M.A. Williams, and M.J. Bevan, *CD4⁺ T cells are required for the maintenance, not programming, of memory CD8⁺ T cells after acute infection*. Nat Immunol, 2004. **5**(9): p. 927-33.
48. Janssen, E.M., et al., *CD4⁺ T cells are required for secondary expansion and memory in CD8⁺ T lymphocytes*. Nature, 2003. **421**(6925): p. 852-6.
49. Murali-Krishna, K., et al., *Counting antigen-specific CD8 T cells: a reevaluation of bystander activation during viral infection*. Immunity, 1998. **8**(2): p. 177-87.
50. Badovinac, V.P., J.S. Haring, and J.T. Harty, *Initial T cell receptor transgenic cell precursor frequency dictates critical aspects of the CD8(+) T cell response to infection*. Immunity, 2007. **26**(6): p. 827-41.
51. Miller, J.D., et al., *Human effector and memory CD8⁺ T cell responses to smallpox and yellow fever vaccines*. Immunity, 2008. **28**(5): p. 710-22.
52. Arens, R. and S.P. Schoenberger, *Plasticity in programming of effector and memory CD8 T-cell formation*. Immunol Rev, 2010. **235**(1): p. 190-205.
53. Harari, A., et al., *Functional signatures of protective antiviral T-cell immunity in human virus infections*. Immunol Rev, 2006. **211**: p. 236-54.
54. Wherry, E.J., *T cell exhaustion*. Nat Immunol, 2011. **12**(6): p. 492-9.
55. Moskophidis, D., et al., *Virus persistence in acutely infected immunocompetent mice by exhaustion of antiviral cytotoxic effector T cells*. Nature, 1993. **362**(6422): p. 758-761.
56. Zajac, A.J., et al., *Viral immune evasion due to persistence of activated T cells without effector function*. J Exp Med, 1998. **188**(12): p. 2205-13.
57. Gallimore, A., et al., *Induction and exhaustion of lymphocytic choriomeningitis virus-specific cytotoxic T lymphocytes visualized using soluble tetrameric major histocompatibility complex class I-peptide complexes*. J Exp Med, 1998. **187**(9): p. 1383-93.

CD4 T cell help sustains distinct subpopulations in functional and dysfunctional CD8 T cell responses.

58. Goepfert, P.A., et al., *A significant number of human immunodeficiency virus epitope-specific cytotoxic T lymphocytes detected by tetramer binding do not produce gamma interferon*. J Virol, 2000. **74**(21): p. 10249-55.
59. Shankar, P., et al., *Impaired function of circulating HIV-specific CD8(+) T cells in chronic human immunodeficiency virus infection*. Blood, 2000. **96**(9): p. 3094-101.
60. Kostense, S., et al., *High viral burden in the presence of major HIV-specific CD8(+) T cell expansions: evidence for impaired CTL effector function*. European journal of immunology, 2001. **31**(3): p. 677-686.
61. Day, C.L., et al., *PD-1 expression on HIV-specific T cells is associated with T-cell exhaustion and disease progression*. Nature, 2006. **443**(7109): p. 350-4.
62. Lechner, F., et al., *Analysis of successful immune responses in persons infected with hepatitis C virus*. J Exp Med, 2000. **191**(9): p. 1499-512.
63. Gruener, N.H., et al., *Sustained dysfunction of antiviral CD8+ T lymphocytes after infection with hepatitis C virus*. J Virol, 2001. **75**(12): p. 5550-8.
64. Ye, B., et al., *T-cell exhaustion in chronic hepatitis B infection: current knowledge and clinical significance*. Cell Death Dis, 2015. **6**(3): p. e1694.
65. Mumprecht, S., et al., *Programmed death 1 signaling on chronic myeloid leukemia-specific T cells results in T-cell exhaustion and disease progression*. Blood, 2009. **114**(8): p. 1528-36.
66. Baitsch, L., et al., *Exhaustion of tumor-specific CD8+ T cells in metastases from melanoma patients*. J Clin Invest, 2011. **121**(6): p. 2350-60.
67. Lee, P.P., et al., *Characterization of circulating T cells specific for tumor-associated antigens in melanoma patients*. Nat Med, 1999. **5**(6): p. 677-85.
68. Matsuzaki, J., et al., *Tumor-infiltrating NY-ESO-1-specific CD8+ T cells are negatively regulated by LAG-3 and PD-1 in human ovarian cancer*. Proc Natl Acad Sci U S A, 2010. **107**(17): p. 7875-80.
69. Zhang, Y., et al., *Programmed death-1 upregulation is correlated with dysfunction of tumor-infiltrating CD8+ T lymphocytes in human non-small cell lung cancer*. Cell Mol Immunol, 2010. **7**(5): p. 389-95.
70. Gandhi, M.K., et al., *Expression of LAG-3 by tumor-infiltrating lymphocytes is coincident with the suppression of latent membrane antigen-specific CD8+ T-cell function in Hodgkin lymphoma patients*. Blood, 2006. **108**(7): p. 2280-9.
71. Riches, J.C., et al., *T cells from CLL patients exhibit features of T-cell exhaustion but retain capacity for cytokine production*. Blood, 2013. **121**(9): p. 1612-21.

72. Speiser, D.E., et al., *T cell differentiation in chronic infection and cancer: functional adaptation or exhaustion?* Nat Rev Immunol, 2014. **14**(11): p. 768-74.
73. Virgin, H.W., E.J. Wherry, and R. Ahmed, *Redefining chronic viral infection.* Cell, 2009. **138**(1): p. 30-50.
74. Freel, S.A., K.O. Saunders, and G.D. Tomaras, *CD8+T-cell-mediated control of HIV-1 and SIV infection.* Immunologic Research, 2011. **49**(1): p. 135-146.
75. Schmitz, J.E., et al., *Control of viremia in simian immunodeficiency virus infection by CD8+ lymphocytes.* Science, 1999. **283**(5403): p. 857-60.
76. Jin, X., et al., *Dramatic rise in plasma viremia after CD8(+) T cell depletion in simian immunodeficiency virus-infected macaques.* J Exp Med, 1999. **189**(6): p. 991-8.
77. Price, D.A., et al., *T cell receptor recognition motifs govern immune escape patterns in acute SIV infection.* Immunity, 2004. **21**(6): p. 793-803.
78. Walker, B. and A. McMichael, *The T-cell response to HIV.* Cold Spring Harb Perspect Med, 2012. **2**(11).
79. Fridman, W.H., et al., *The immune contexture in human tumours: impact on clinical outcome.* Nature Reviews Cancer, 2012. **12**(4): p. 298-306.
80. Barber, D.L., et al., *Restoring function in exhausted CD8 T cells during chronic viral infection.* Nature, 2006. **439**(7077): p. 682-7.
81. West, E.E., et al., *PD-L1 blockade synergizes with IL-2 therapy in reinvigorating exhausted T cells.* J Clin Invest, 2013. **123**(6): p. 2604-15.
82. Hirano, F., et al., *Blockade of B7-H1 and PD-1 by monoclonal antibodies potentiates cancer therapeutic immunity.* Cancer Res, 2005. **65**(3): p. 1089-96.
83. Iwai, Y., S. Terawaki, and T. Honjo, *PD-1 blockade inhibits hematogenous spread of poorly immunogenic tumor cells by enhanced recruitment of effector T cells.* Int Immunol, 2005. **17**(2): p. 133-44.
84. Keir, M.E., et al., *PD-1 and its ligands in tolerance and immunity.* Annu Rev Immunol, 2008. **26**: p. 677-704.
85. Pauken, K.E., et al., *Epigenetic stability of exhausted T cells limits durability of reinvigoration by PD-1 blockade.* Science, 2016. **354**(6316): p. 1160-1165.
86. Rehermann, B., *Hepatitis C virus versus innate and adaptive immune responses: a tale of coevolution and coexistence.* J Clin Invest, 2009. **119**(7): p. 1745-54.

CD4 T cell help sustains distinct subpopulations in functional and dysfunctional CD8 T cell responses.

87. Bowen, D.G. and C.M. Walker, *Adaptive immune responses in acute and chronic hepatitis C virus infection*. *Nature*, 2005. **436**(7053): p. 946-52.
88. Doering, T.A., et al., *Network analysis reveals centrally connected genes and pathways involved in CD8+ T cell exhaustion versus memory*. *Immunity*, 2012. **37**(6): p. 1130-44.
89. Schietinger, A. and P.D. Greenberg, *Tolerance and exhaustion: defining mechanisms of T cell dysfunction*. *Trends Immunol*, 2014. **35**(2): p. 51-60.
90. Wherry, E.J. and M. Kurachi, *Molecular and cellular insights into T cell exhaustion*. *Nat Rev Immunol*, 2015. **15**(8): p. 486-99.
91. Ghoneim, H.E., et al., *De Novo Epigenetic Programs Inhibit PD-1 Blockade-Mediated T Cell Rejuvenation*. *Cell*, 2017. **170**(1): p. 142-157.e19.
92. Philip, M., et al., *Chromatin states define tumour-specific T cell dysfunction and reprogramming*. *Nature*, 2017. **545**(7655): p. 452-456.
93. Sen, D.R., et al., *The epigenetic landscape of T cell exhaustion*. *Science*, 2016. **354**(6316): p. 1165-1169.
94. Wherry, E.J., et al., *Molecular signature of CD8+ T cell exhaustion during chronic viral infection*. *Immunity*, 2007. **27**(4): p. 670-84.
95. McLane, L.M., M.S. Abdel-Hakeem, and E.J. Wherry, *CD8 T Cell Exhaustion During Chronic Viral Infection and Cancer*. *Annu Rev Immunol*, 2019. **37**: p. 457-495.
96. Wherry, E.J., et al., *Viral persistence alters CD8 T-cell immunodominance and tissue distribution and results in distinct stages of functional impairment*. *J Virol*, 2003. **77**(8): p. 4911-27.
97. Fuller, M.J., et al., *Maintenance, loss, and resurgence of T cell responses during acute, protracted, and chronic viral infections*. *J Immunol*, 2004. **172**(7): p. 4204-14.
98. Blackburn, S.D., et al., *Coregulation of CD8+ T cell exhaustion by multiple inhibitory receptors during chronic viral infection*. *Nat Immunol*, 2009. **10**(1): p. 29-37.
99. Topalian, S.L., C.G. Drake, and D.M. Pardoll, *Targeting the PD-1/B7-H1(PD-L1) pathway to activate anti-tumor immunity*. *Curr Opin Immunol*, 2012. **24**(2): p. 207-12.
100. Strome, S.E., et al., *B7-H1 blockade augments adoptive T-cell immunotherapy for squamous cell carcinoma*. *Cancer Res*, 2003. **63**(19): p. 6501-5.

CD4 T cell help sustains distinct subpopulations in functional and dysfunctional CD8 T cell responses.

101. Bengsch, B., et al., *Bioenergetic Insufficiencies Due to Metabolic Alterations Regulated by the Inhibitory Receptor PD-1 Are an Early Driver of CD8(+) T Cell Exhaustion*. *Immunity*, 2016. **45**(2): p. 358-73.
102. Patsoukis, N., et al., *PD-1 alters T-cell metabolic reprogramming by inhibiting glycolysis and promoting lipolysis and fatty acid oxidation*. *Nat Commun*, 2015. **6**: p. 6692.
103. Hui, E., et al., *T cell costimulatory receptor CD28 is a primary target for PD-1-mediated inhibition*. *Science*, 2017. **355**(6332): p. 1428-1433.
104. Utzschneider, D.T., et al., *T Cell Factor 1-Expressing Memory-like CD8(+) T Cells Sustain the Immune Response to Chronic Viral Infections*. *Immunity*, 2016. **45**(2): p. 415-27.
105. Wieland, D., et al., *TCF1(+) hepatitis C virus-specific CD8(+) T cells are maintained after cessation of chronic antigen stimulation*. *Nat Commun*, 2017. **8**: p. 15050.
106. Im, S.J., et al., *Defining CD8+ T cells that provide the proliferative burst after PD-1 therapy*. *Nature*, 2016. **537**(7620): p. 417-421.
107. Brummelman, J., et al., *High-dimensional single cell analysis identifies stem-like cytotoxic CD8⁺ T cells infiltrating human tumors*. *The Journal of Experimental Medicine*, 2018. **215**(10): p. 2520-2535.
108. Gullicksrud, J.A., et al., *Differential Requirements for Tcf1 Long Isoforms in CD8(+) and CD4(+) T Cell Responses to Acute Viral Infection*. *J Immunol*, 2017. **199**(3): p. 911-919.
109. He, R., et al., *Follicular CXCR5- expressing CD8(+) T cells curtail chronic viral infection*. *Nature*, 2016. **537**(7620): p. 412-428.
110. Leong, Y.A., et al., *CXCR5(+) follicular cytotoxic T cells control viral infection in B cell follicles*. *Nat Immunol*, 2016. **17**(10): p. 1187-96.
111. Wu, T., et al., *The TCF1-Bcl6 axis counteracts type I interferon to repress exhaustion and maintain T cell stemness*. *Science Immunology*, 2016. **1**(6): p. eaai8593.
112. Miller, B.C., et al., *Subsets of exhausted CD8(+) T cells differentially mediate tumor control and respond to checkpoint blockade*. *Nat Immunol*, 2019. **20**(3): p. 326-336.
113. Lee, J., et al., *Reinvigorating Exhausted T Cells by Blockade of the PD-1 Pathway*. *For Immunopathol Dis Therap*, 2015. **6**(1-2): p. 7-17.

CD4 T cell help sustains distinct subpopulations in functional and dysfunctional CD8 T cell responses.

114. Siddiqui, I., et al., *Intratumoral Tcf1(+)PD-1(+)CD8(+) T Cells with Stem-like Properties Promote Tumor Control in Response to Vaccination and Checkpoint Blockade Immunotherapy*. *Immunity*, 2019. **50**(1): p. 195-211.e10.
115. Brummelman, J., et al., *High-dimensional single cell analysis identifies stem-like cytotoxic CD8(+) T cells infiltrating human tumors*. *J Exp Med*, 2018. **215**(10): p. 2520-2535.
116. El-Far, M., et al., *T-cell exhaustion in HIV infection*. *Current HIV/AIDS Reports*, 2008. **5**(1): p. 13-19.
117. Brooks, D.G., D.B. McGavern, and M.B. Oldstone, *Reprogramming of antiviral T cells prevents inactivation and restores T cell activity during persistent viral infection*. *J Clin Invest*, 2006. **116**(6): p. 1675-85.
118. Angelosanto, J.M., et al., *Progressive loss of memory T cell potential and commitment to exhaustion during chronic viral infection*. *J Virol*, 2012. **86**(15): p. 8161-70.
119. Wilson, E.B. and D.G. Brooks, *The role of IL-10 in regulating immunity to persistent viral infections*. *Curr Top Microbiol Immunol*, 2011. **350**: p. 39-65.
120. Brooks, D.G., et al., *Interleukin-10 determines viral clearance or persistence in vivo*. *Nat Med*, 2006. **12**(11): p. 1301-9.
121. Brooks, D.G., et al., *IL-10 and PD-L1 operate through distinct pathways to suppress T-cell activity during persistent viral infection*. *Proceedings of the National Academy of Sciences*, 2008. **105**(51): p. 20428-20433.
122. Li, M.O., et al., *Transforming growth factor-beta regulation of immune responses*. *Annu Rev Immunol*, 2006. **24**: p. 99-146.
123. Bachmann, M.F., et al., *Differential role of IL-2R signaling for CD8+ T cell responses in acute and chronic viral infections*. *Eur J Immunol*, 2007. **37**(6): p. 1502-12.
124. Abrams, D., et al., *Interleukin-2 therapy in patients with HIV infection*. *N Engl J Med*, 2009. **361**(16): p. 1548-59.
125. Spolski, R. and W.J. Leonard, *Interleukin-21: basic biology and implications for cancer and autoimmunity*. *Annu Rev Immunol*, 2008. **26**: p. 57-79.
126. Fröhlich, A., et al., *IL-21R on T cells is critical for sustained functionality and control of chronic viral infection*. *Science*, 2009. **324**(5934): p. 1576-80.
127. McNab, F., et al., *Type I interferons in infectious disease*. *Nat Rev Immunol*, 2015. **15**(2): p. 87-103.

128. Iwai, Y., et al., *Involvement of PD-L1 on tumor cells in the escape from host immune system and tumor immunotherapy by PD-L1 blockade*. Proc Natl Acad Sci U S A, 2002. **99**(19): p. 12293-7.
129. Urbani, S., et al., *PD-1 expression in acute hepatitis C virus (HCV) infection is associated with HCV-specific CD8 exhaustion*. J Virol, 2006. **80**(22): p. 11398-403.
130. Patsoukis, N., et al., *Selective effects of PD-1 on Akt and Ras pathways regulate molecular components of the cell cycle and inhibit T cell proliferation*. Sci Signal, 2012. **5**(230): p. ra46.
131. Chemnitz, J.M., et al., *SHP-1 and SHP-2 associate with immunoreceptor tyrosine-based switch motif of programmed death 1 upon primary human T cell stimulation, but only receptor ligation prevents T cell activation*. J Immunol, 2004. **173**(2): p. 945-54.
132. Odorizzi, P.M., et al., *Genetic absence of PD-1 promotes accumulation of terminally differentiated exhausted CD8+ T cells*. J Exp Med, 2015. **212**(7): p. 1125-37.
133. Le, D.T., et al., *Mismatch repair deficiency predicts response of solid tumors to PD-1 blockade*. Science, 2017. **357**(6349): p. 409-413.
134. Lee, C.H., et al., *Update on Tumor Neoantigens and Their Utility: Why It Is Good to Be Different*. Trends Immunol, 2018. **39**(7): p. 536-548.
135. Johnston, R.J., et al., *The immunoreceptor TIGIT regulates antitumor and antiviral CD8(+) T cell effector function*. Cancer Cell, 2014. **26**(6): p. 923-937.
136. Yu, X., et al., *The surface protein TIGIT suppresses T cell activation by promoting the generation of mature immunoregulatory dendritic cells*. Nat Immunol, 2009. **10**(1): p. 48-57.
137. Workman, C.J., K.J. Dugger, and D.A. Vignali, *Cutting edge: molecular analysis of the negative regulatory function of lymphocyte activation gene-3*. J Immunol, 2002. **169**(10): p. 5392-5.
138. Kuchroo, V.K., et al., *New roles for TIM family members in immune regulation*. Nat Rev Immunol, 2008. **8**(8): p. 577-80.
139. Parry, R.V., et al., *CTLA-4 and PD-1 receptors inhibit T-cell activation by distinct mechanisms*. Mol Cell Biol, 2005. **25**(21): p. 9543-53.
140. Veiga-Parga, T., S. Sehrawat, and B.T. Rouse, *Role of regulatory T cells during virus infection*. Immunol Rev, 2013. **255**(1): p. 182-96.
141. Porichis, F. and D.E. Kaufmann, *HIV-specific CD4 T cells and immune control of viral replication*. Curr Opin HIV AIDS, 2011. **6**(3): p. 174-80.

142. Klenerman, P. and R. Thimme, *T cell responses in hepatitis C: the good, the bad and the unconventional*. Gut, 2012. **61**(8): p. 1226-34.
143. Battegay, M., et al., *Enhanced establishment of a virus carrier state in adult CD4+ T-cell-deficient mice*. J Virol, 1994. **68**(7): p. 4700-4.
144. Matloubian, M., R.J. Concepcion, and R. Ahmed, *CD4+ T cells are required to sustain CD8+ cytotoxic T-cell responses during chronic viral infection*. J Virol, 1994. **68**(12): p. 8056-63.
145. Waldman, A.D., J.M. Fritz, and M.J. Lenardo, *A guide to cancer immunotherapy: from T cell basic science to clinical practice*. Nature Reviews Immunology, 2020. **20**(11): p. 651-668.
146. Couzin-Frankel, J., *Breakthrough of the year 2013. Cancer immunotherapy*. Science, 2013. **342**(6165): p. 1432-3.
147. Leach, D.R., M.F. Krummel, and J.P. Allison, *Enhancement of antitumor immunity by CTLA-4 blockade*. Science, 1996. **271**(5256): p. 1734-6.
148. Kumar, V., et al., *Current Diagnosis and Management of Immune Related Adverse Events (irAEs) Induced by Immune Checkpoint Inhibitor Therapy*. Front Pharmacol, 2017. **8**: p. 49.
149. Rosenberg, S.A., et al., *Use of tumor-infiltrating lymphocytes and interleukin-2 in the immunotherapy of patients with metastatic melanoma. A preliminary report*. N Engl J Med, 1988. **319**(25): p. 1676-80.
150. Garrido, F., et al., *The urgent need to recover MHC class I in cancers for effective immunotherapy*. Curr Opin Immunol, 2016. **39**: p. 44-51.
151. Neelapu, S.S., et al., *Chimeric antigen receptor T-cell therapy - assessment and management of toxicities*. Nat Rev Clin Oncol, 2018. **15**(1): p. 47-62.
152. Utzschneider, D.T., et al., *T cells maintain an exhausted phenotype after antigen withdrawal and population reexpansion*. Nat Immunol, 2013. **14**(6): p. 603-10.
153. Monticelli, S. and G. Natoli, *Transcriptional determination and functional specificity of myeloid cells: making sense of diversity*. Nat Rev Immunol, 2017. **17**(10): p. 595-607.
154. Youngblood, B., et al., *Chronic virus infection enforces demethylation of the locus that encodes PD-1 in antigen-specific CD8(+) T cells*. Immunity, 2011. **35**(3): p. 400-12.
155. Zhang, F., et al., *Epigenetic manipulation restores functions of defective CD8+ T cells from chronic viral infection*. Mol Ther, 2014. **22**(9): p. 1698-706.

156. Utzschneider, D.T., et al., *High antigen levels induce an exhausted phenotype in a chronic infection without impairing T cell expansion and survival*. J Exp Med, 2016. **213**(9): p. 1819-34.
157. Intlekofer, A.M., et al., *Effector and memory CD8+ T cell fate coupled by T-bet and eomesodermin*. Nat Immunol, 2005. **6**(12): p. 1236-44.
158. Pearce, E.L., et al., *Control of effector CD8+ T cell function by the transcription factor Eomesodermin*. Science, 2003. **302**(5647): p. 1041-3.
159. Sullivan, B.M., et al., *Antigen-driven effector CD8 T cell function regulated by T-bet*. Proc Natl Acad Sci U S A, 2003. **100**(26): p. 15818-23.
160. Dominguez, C.X., et al., *The transcription factors ZEB2 and T-bet cooperate to program cytotoxic T cell terminal differentiation in response to LCMV viral infection*. J Exp Med, 2015. **212**(12): p. 2041-56.
161. Banerjee, A., et al., *Cutting edge: The transcription factor eomesodermin enables CD8+ T cells to compete for the memory cell niche*. J Immunol, 2010. **185**(9): p. 4988-92.
162. Paley, M.A., et al., *Progenitor and terminal subsets of CD8+ T cells cooperate to contain chronic viral infection*. Science, 2012. **338**(6111): p. 1220-5.
163. Masson, F., et al., *Id2-Mediated Inhibition of E2A Represses Memory CD8⁺ T Cell Differentiation*. The Journal of Immunology, 2013. **190**(9): p. 4585-4594.
164. Menner, A.J., et al., *Id3 Controls Cell Death of 2B4+ Virus-Specific CD8+ T Cells in Chronic Viral Infection*. The Journal of Immunology, 2015. **195**(5): p. 2103-2114.
165. Martinez, G.J., et al., *The transcription factor NFAT promotes exhaustion of activated CD8⁺ T cells*. Immunity, 2015. **42**(2): p. 265-278.
166. Quigley, M., et al., *Transcriptional analysis of HIV-specific CD8+ T cells shows that PD-1 inhibits T cell function by upregulating BATF*. Nat Med, 2010. **16**(10): p. 1147-51.
167. Oestreich, K.J., et al., *NFATc1 regulates PD-1 expression upon T cell activation*. J Immunol, 2008. **181**(7): p. 4832-9.
168. Rutishauser, R.L., et al., *Transcriptional repressor Blimp-1 promotes CD8(+) T cell terminal differentiation and represses the acquisition of central memory T cell properties*. Immunity, 2009. **31**(2): p. 296-308.
169. Kallies, A., et al., *Blimp-1 transcription factor is required for the differentiation of effector CD8(+) T cells and memory responses*. Immunity, 2009. **31**(2): p. 283-95.

CD4 T cell help sustains distinct subpopulations in functional and dysfunctional CD8 T cell responses.

170. Shin, H., et al., *A role for the transcriptional repressor Blimp-1 in CD8(+) T cell exhaustion during chronic viral infection.* Immunity, 2009. **31**(2): p. 309-20.
171. Man, K., et al., *The transcription factor IRF4 is essential for TCR affinity-mediated metabolic programming and clonal expansion of T cells.* Nature Immunology, 2013. **14**(11): p. 1155-1165.
172. Man, K., et al., *Transcription Factor IRF4 Promotes CD8(+) T Cell Exhaustion and Limits the Development of Memory-like T Cells during Chronic Infection.* Immunity, 2017. **47**(6): p. 1129-1141.e5.
173. Hess Michelini, R., et al., *Differentiation of CD8 memory T cells depends on Foxo1.* J Exp Med, 2013. **210**(6): p. 1189-200.
174. Staron, M.M., et al., *The transcription factor FoxO1 sustains expression of the inhibitory receptor PD-1 and survival of antiviral CD8(+) T cells during chronic infection.* Immunity, 2014. **41**(5): p. 802-14.
175. Delpoux, A., et al., *FOXO1 opposition of CD8+ T cell effector programming confers early memory properties and phenotypic diversity.* Proceedings of the National Academy of Sciences, 2017. **114**(42): p. E8865-E8874.
176. Kurachi, M., et al., *The transcription factor BATF operates as an essential differentiation checkpoint in early effector CD8+ T cells.* Nature Immunology, 2014. **15**(4): p. 373-383.
177. Alfei, F., et al., *TOX reinforces the phenotype and longevity of exhausted T cells in chronic viral infection.* Nature, 2019. **571**(7764): p. 265-269.
178. Khan, O., et al., *TOX transcriptionally and epigenetically programs CD8+ T cell exhaustion.* Nature, 2019. **571**(7764): p. 211-218.
179. Yao, C., et al., *Single-cell RNA-seq reveals TOX as a key regulator of CD8(+) T cell persistence in chronic infection.* Nat Immunol, 2019. **20**(7): p. 890-901.
180. Seo, H., et al., *TOX and TOX2 transcription factors cooperate with NR4A transcription factors to impose CD8⁺ T cell exhaustion.* Proceedings of the National Academy of Sciences, 2019. **116**(25): p. 12410-12415.
181. Chen, J., et al., *NR4A transcription factors limit CAR T cell function in solid tumours.* Nature, 2019. **567**(7749): p. 530-534.
182. Hwang, B., J.H. Lee, and D. Bang, *Single-cell RNA sequencing technologies and bioinformatics pipelines.* Experimental & Molecular Medicine, 2018. **50**(8): p. 96.
183. Spitzer, M.H. and G.P. Nolan, *Mass Cytometry: Single Cells, Many Features.* Cell, 2016. **165**(4): p. 780-91.

184. DiPiazza, A.T., et al., *OMIP-061: 20-Color Flow Cytometry Panel for High-Dimensional Characterization of Murine Antigen-Presenting Cells*. Cytometry A, 2019. **95**(12): p. 1226-1230.
185. Bengtsson, M., et al., *Quantification of mRNA in single cells and modelling of RT-qPCR induced noise*. BMC Mol Biol, 2008. **9**: p. 63.
186. Tang, F., et al., *RNA-Seq analysis to capture the transcriptome landscape of a single cell*. Nature Protocols, 2010. **5**(3): p. 516-535.
187. Ramsköld, D., et al., *Full-length mRNA-Seq from single-cell levels of RNA and individual circulating tumor cells*. Nature Biotechnology, 2012. **30**(8): p. 777-782.
188. Luecken, M.D. and F.J. Theis, *Current best practices in single-cell RNA-seq analysis: a tutorial*. Mol Syst Biol, 2019. **15**(6): p. e8746.
189. Stubbington, M.J.T., et al., *T cell fate and clonality inference from single-cell transcriptomes*. Nat Methods, 2016. **13**(4): p. 329-332.
190. Stoeckius, M., et al., *Simultaneous epitope and transcriptome measurement in single cells*. Nature Methods, 2017. **14**(9): p. 865-868.
191. Macaulay, I.C., et al., *G&T-seq: parallel sequencing of single-cell genomes and transcriptomes*. Nat Methods, 2015. **12**(6): p. 519-22.
192. Buenrostro, J.D., et al., *Single-cell chromatin accessibility reveals principles of regulatory variation*. Nature, 2015. **523**(7561): p. 486-490.
193. Papalexis, E. and R. Satija, *Single-cell RNA sequencing to explore immune cell heterogeneity*. Nat Rev Immunol, 2018. **18**(1): p. 35-45.
194. Macosko, E.Z., et al., *Highly Parallel Genome-wide Expression Profiling of Individual Cells Using Nanoliter Droplets*. Cell, 2015. **161**(5): p. 1202-1214.
195. Oldstone, M.B. and K.P. Campbell, *Decoding arenavirus pathogenesis: essential roles for alpha-dystroglycan-virus interactions and the immune response*. Virology, 2011. **411**(2): p. 170-9.
196. Ahmed, R., et al., *Selection of genetic variants of lymphocytic choriomeningitis virus in spleens of persistently infected mice. Role in suppression of cytotoxic T lymphocyte response and viral persistence*. J Exp Med, 1984. **160**(2): p. 521-40.
197. Zinkernagel, R.M., *Lymphocytic choriomeningitis virus and immunology*. Curr Top Microbiol Immunol, 2002. **263**: p. 1-5.
198. Salvato, M., et al., *Molecular basis of viral persistence: a single amino acid change in the glycoprotein of lymphocytic choriomeningitis virus is associated*

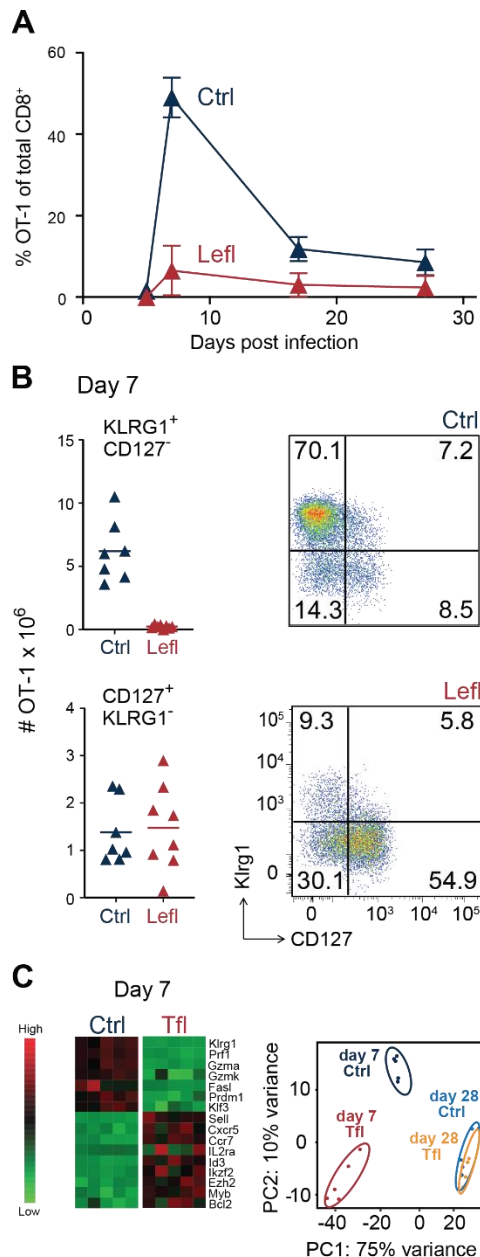
- with suppression of the antiviral cytotoxic T-lymphocyte response and establishment of persistence.* J Virol, 1991. **65**(4): p. 1863-9.
199. Matloubian, M., et al., *Molecular determinants of macrophage tropism and viral persistence: importance of single amino acid changes in the polymerase and glycoprotein of lymphocytic choriomeningitis virus.* J Virol, 1993. **67**(12): p. 7340-9.
200. Bergthaler, A., et al., *Viral replicative capacity is the primary determinant of lymphocytic choriomeningitis virus persistence and immunosuppression.* Proc Natl Acad Sci U S A, 2010. **107**(50): p. 21641-6.
201. Zenewicz, L.A. and H. Shen, *Innate and adaptive immune responses to Listeria monocytogenes: a short overview.* Microbes Infect, 2007. **9**(10): p. 1208-15.
202. Khan, S.H. and V.P. Badovinac, *Listeria monocytogenes: a model pathogen to study antigen-specific memory CD8 T cell responses.* Semin Immunopathol, 2015. **37**(3): p. 301-10.
203. Conlan, J.W., *Early pathogenesis of Listeria monocytogenes infection in the mouse spleen.* J Med Microbiol, 1996. **44**(4): p. 295-302.
204. Soumillon, M., et al., *Characterization of directed differentiation by high-throughput single-cell RNA-Seq.* bioRxiv, 2014: p. 003236.
205. Roelli, P., S. Mueller, and C. Girardot, *DropSeqPipe: v0.4.* GitHub, 2020.
206. Martin, M., *Cutadapt removes adapter sequences from high-throughput sequencing reads.* EMBnet.journal; Vol 17, No 1: Next Generation Sequencing Data AnalysisDO - 10.14806/ej.17.1.200, 2011.
207. Dobin, A., et al., *STAR: ultrafast universal RNA-seq aligner.* Bioinformatics, 2013. **29**(1): p. 15-21.
208. Satija, R., et al., *Spatial reconstruction of single-cell gene expression data.* Nature Biotechnology, 2015. **33**: p. 495.
209. Butler, A., et al., *Integrating single-cell transcriptomic data across different conditions, technologies, and species.* Nat Biotechnol, 2018. **36**(5): p. 411-420.
210. Yu, G., et al., *clusterProfiler: an R package for comparing biological themes among gene clusters.* Omics, 2012. **16**(5): p. 284-7.
211. Liberzon, A., et al., *The Molecular Signatures Database (MSigDB) hallmark gene set collection.* Cell Syst, 2015. **1**(6): p. 417-425.

212. Koster, J. and S. Rahmann, *Snakemake-a scalable bioinformatics workflow engine*. Bioinformatics, 2018. **34**(20): p. 3600.
213. Bolger, A.M., M. Lohse, and B. Usadel, *Trimmomatic: a flexible trimmer for Illumina sequence data*. Bioinformatics, 2014. **30**(15): p. 2114-20.
214. Anders, S., P.T. Pyl, and W. Huber, *HTSeq--a Python framework to work with high-throughput sequencing data*. Bioinformatics, 2015. **31**(2): p. 166-9.
215. Ewels, P., et al., *MultiQC: summarize analysis results for multiple tools and samples in a single report*. Bioinformatics, 2016. **32**(19): p. 3047-8.
216. Love, M.I., W. Huber, and S. Anders, *Moderated estimation of fold change and dispersion for RNA-seq data with DESeq2*. Genome Biol, 2014. **15**(12): p. 550.
217. Ritchie, M.E., et al., *limma powers differential expression analyses for RNA-sequencing and microarray studies*. Nucleic Acids Res, 2015. **43**(7): p. e47.
218. Wickham, H., *ggplot2: Elegant Graphics for Data Analysis*. 2016.
219. Kolde, R., *Pheatmap: Pretty Heatmaps*. 2019: p. Version 1.0.12.
220. Ludo Waltman, N.J.v.E., *A smart local moving algorithm for large-scale modularity-based community detection*. N.J. Eur. Phys. J. B, 2013.
221. Ziegenhain, C., et al., *Comparative Analysis of Single-Cell RNA Sequencing Methods*. Mol Cell, 2017. **65**(4): p. 631-643 e4.
222. Aly, L., B. Hemmer, and T. Korn, *From Leflunomide to Teriflunomide: Drug Development and Immunosuppressive Oral Drugs in the Treatment of Multiple Sclerosis*. Curr Neuropharmacol, 2017. **15**(6): p. 874-891.
223. Cherwinski, H.M., et al., *Leflunomide interferes with pyrimidine nucleotide biosynthesis*. Inflammation Research, 1995. **44**(8): p. 317-322.
224. Rückemann, K., et al., *Leflunomide inhibits pyrimidine de novo synthesis in mitogen-stimulated T-lymphocytes from healthy humans*. J Biol Chem, 1998. **273**(34): p. 21682-91.
225. Wang, R., et al., *The transcription factor Myc controls metabolic reprogramming upon T lymphocyte activation*. Immunity, 2011. **35**(6): p. 871-82.
226. Carlson, C.M., et al., *Kruppel-like factor 2 regulates thymocyte and T-cell migration*. Nature, 2006. **442**(7100): p. 299-302.

227. Matloubian, M., et al., *Lymphocyte egress from thymus and peripheral lymphoid organs is dependent on S1P receptor 1*. *Nature*, 2004. **427**(6972): p. 355-60.
228. Yamauchi, T., et al., *Identification of dysfunctional CD8+ T-cell subsets rescued by PD-L1 blockade in the tumor microenvironment*. *The Journal of Immunology*, 2018. **200**(1 Supplement): p. 58.3-58.3.
229. Gnanaprakasam, J.N. and R. Wang, *MYC in Regulating Immunity: Metabolism and Beyond*. *Genes (Basel)*, 2017. **8**(3).
230. Grün, D., et al., *Single-cell messenger RNA sequencing reveals rare intestinal cell types*. *Nature*, 2015. **525**(7568): p. 251-5.
231. Hudson, W.H., et al., *Proliferating Transitory T Cells with an Effector-like Transcriptional Signature Emerge from PD-1(+) Stem-like CD8(+) T Cells during Chronic Infection*. *Immunity*, 2019. **51**(6): p. 1043-1058.e4.
232. Im, S.J., et al., *PD-1+ stemlike CD8 T cells are resident in lymphoid tissues during persistent LCMV infection*. *Proceedings of the National Academy of Sciences*, 2020. **117**(8): p. 4292-4299.
233. Elsaesser, H., K. Sauer, and D.G. Brooks, *IL-21 is required to control chronic viral infection*. *Science*, 2009. **324**(5934): p. 1569-72.
234. Fröhlich, A., et al., *IL-21R on T Cells Is Critical for Sustained Functionality and Control of Chronic Viral Infection*. *Science*, 2009. **324**(5934): p. 1576-1580.
235. Yi, J.S., M. Du, and A.J. Zajac, *A Vital Role for Interleukin-21 in the Control of a Chronic Viral Infection*. *Science*, 2009. **324**(5934): p. 1572-1576.
236. Yamauchi, T., et al., *T-cell CX3CR1 expression as a dynamic blood-based biomarker of response to immune checkpoint inhibitors*. *Nat Commun*, 2021. **12**(1): p. 1402.
237. Okamura, H., et al., *Cloning of a new cytokine that induces IFN-gamma production by T cells*. *Nature*, 1995. **378**(6552): p. 88-91.
238. Zhou, T., et al., *IL-18BP is a secreted immune checkpoint and barrier to IL-18 immunotherapy*. *Nature*, 2020. **583**(7817): p. 609-614.

10. Appendix

10.1. Supplementary Figure 1



Leflunomide blocks effector but memory CD8 T cell differentiation.

(A-C) C57BL/6 mice (CD45.2+) were engrafted with transgenic ovalbumin-specific OT-1 T cells (CD45.1+) prior to infection with recombinant OVA-expressing *Listeria monocytogenes* (Lm-OVA). Animals were treated every second day with carboxymethylcellulose vehicle control (ctrl) or leflunomide (lefl) starting three days before the infection until day 7 post infection. Then animals were treated every third day until readout. (A and B) Data courtesy - Stefanie Sarah Scherer. (A) Expansion kinetics of ctrl and treated OT-1 T cells. (B) Representative CD8+CD45.1+ gated flow cytometry plots and corresponding data graphs obtained on day 7 post infection are shown. Symbols in data plots represent individual mice, small horizontal lines indicate the mean. (C) Bulk RNA sequencing of OT-1 cell recovered from control and treated mice at day 7 and day 28. The heatmap presents selected differentially expressed genes with effector or memory function. Abbreviations: ctrl, control; lefl, leflunomide.

10.2. Acknowledgements

First of all, I would like to thank to my supervisor Prof. Dr. Dietmar Zehn for the outstanding opportunity to make my PhD in his laboratory. I am very grateful for his openness for discussion, the scientific freedom I was provided and the unlimited support I received.

I would like to thank Patrick Roelli and Ming Wu, without whose bioinformatics expertise this work would not have been possible.

I would like to thank Tobias Herbinger, Waltraud Schmid, Brigitte Dötterböck, and Charline Amette for their technical assistance and animal husbandry.

I am extremely thankful to all lab mates for the great working and scientific atmosphere they created.

Furthermore, I would like to thank Assoc. Prof. Ivanka Tsacheva, who started my passion for immunology.

Special thanks for their unlimited support and patience goes to my family (Svetlana, Bozhidar, Aglika and Maya) and my wife Luiza, who were always next to me.

I dedicate this work to my lovely daughter Kristina.